Detailed Geochemical and Mineralogical Analyses of Naturally Occurring Arsenic in the Hawthorn Group

by

Olesya Lazareva

A thesis submitted in partial fulfillment
of the requirements for the degree of
Master of Science
Department of Geology
College of Arts and Sciences
University of South Florida

Major Professor: Thomas Pichler, Ph.D.
Thomas Scott, Ph.D.
Jonathan Arthur, Ph.D
Peter Harries, Ph.D.

Date of Approval:
November 2, 2004

Keywords: phosphate, mining, pyrite, aquifer, trace metal, florida

ACKNOWLEDGEMENTS

First and foremost, I would like to gratefully acknowledge the help, support and encouragement of my advisor Dr. Thomas Pichler, who presented me with this wonderful opportunity, and assisted me with developing the research topic and with completing and revising the paper. His contribution to my development as a geochemist cannot be underestimated. I am extremely thankful for his endless effort to provide invaluable assistance and inspired ideas. It was my luck to work with Dr. Thomas Pichler as my advisor.

I would like greatly appreciate Southwest Florida Water Management District (SWFWMD) and Mr. Greg Jones, Director of Resource and Conservation Development for SWFWMD, for financial support of this project

I would like to thank my Thesis Committee, Dr. Thomas Scott, Dr. Jonathan Arthur, and Dr. Peter Harries, for supporting me throughout my academic career, reviewing the manuscript and providing very valuable and helpful suggestions.

I am also grateful to Dr. Chuck Connor, Department of Geology Chair, for his support in my efforts to study statistics.

I want to express my gratitude to a great colleague and a good friend, Roy Price, for his incredible help during field work and throughout the entire academic period.

I would like to thank faculty, staff and students in the Department of Geology, University of South Florida for their support and guidance throughout this work.

Finally I am grateful to my family, my lovely boyfriend Dmitri Prokhorov, and his wonderful parents for their constant inspiration, advice, support, and wisdom. Without their help, patience, and love this work would never happen.

TABLE OF CONTENTS

LIST OF TABLES

LIST OF FIGURES

Detailed Geochemical and Mineralogical Analyses of Naturally Occurring Arsenic in the Hawthorn Group

Olesya Lazareva

ABSTRACT

In order to understand the mineralogical association and distribution of arsenic (As) in the Hawthorn Group in central Florida, I examined in detail the chemical and mineralogical composition of 361 samples that were collected from 16 cores.

Geochemical analyses were performed by hydride generation - atomic fluorescence spectrometry (HG-AFS) and inductively coupled plasma optical emission spectrometry (ICP-OES). The identification of discrete minerals was aided by scanning electron microscopy (SEM) and chemical compositions were obtained by electron-probe microanalyses (EMPA).

Arsenic concentrations for all Hawthorn samples vary from 0.1 to 69.0 ppm with a mean of 5.6 ppm. Average As concentrations for the individual units of the Hawthorn Group vary significantly from 9.0 ppm in the Peace River Formation to 3.0 ppm in the Tampa Member of the Arcadia Formation. This detailed mineralogical and geochemical study demonstrates that: (1) Arsenic in the Hawthorn Group varies from the formation to formation and is primarily concentrated in trace minerals, such as pyrite; (2) Concentrations of arsenic in pyrite crystals can vary drastically from a

minimum of 0 ppm to a maximum of 8260 ppm; (3) Pyrite occurs in framboidal and euhedral forms and is unevenly distributed throughout the Hawthorn Group; (4) Hydrous ferric oxides can contain up to 540 ppm of arsenic; (5) Phosphate and organic material, and clays contain lower arsenic concentrations that pyrite and hydrous ferric oxides; and (6) Arsenic, sulfur, and iron have lognormal distribution throughout the Hawthorn Group.

This study is important because phosphorous, arsenic and sulfur are chemically closely related, and thus they co-occur posing a potential problem for the phosphate industry.

Information about the concentration, distribution and mineralogical association of naturally occurring arsenic is essential to forecast its behavior during anthropogenically induced physico-chemical changes in the aquifer. Recently, aquifer storage and recovery (ASR) facilities in west-central Florida reported arsenic concentrations in excess of 100 µg/L (100 ppb) in recovered water. The ASR storage zone in this area is in the Suwannee Limestone, which directly underlies the Hawthorn sediments. It is crucial to the future of ASR in this area to understand the source, distribution, and cycling of arsenic in the overlying Hawthorn Group and the Florida Platform.

CHAPTER ONE

INTRODUCTION

The first discovery of phosphate rock in Florida was opened in 1879 near Hawthorne, Alachua County by Dr. C.A. Simmons (Blakey, 1973), who instigated mining operations there in 1883. The original find was a low-grade, phosphatic limestone, possibly from the Hawthorn Group. At the present time, Florida phosphate mining of the Hawthorn Group supplies about one-quarter of the world's and three-quarters of United States domestic phosphate needs. Most phosphate is used to produce feed supplements, soft drinks, vitamins, toothpaste and as fertilizers. In 2000, $1.13 billion dollars of fertilizer were sold overseas from the state of Florida (Hodges et al., 2001).

In addition to the phosphate mining industry there are several aquifer storage and recovery (ASR) facilities in Florida. Aquifer storage and recovery is the procedure of storing treated recharge water in a confined aquifer during rainy seasons with the subsequent recovery of that water during dry seasons. ASR is rapidly developing into substitute choice to withdrawing Florida aquifer groundwater due to growing water demands in highly populated areas of the Florida peninsula (Jones and Owen, 2001).

Problem Statement

The Environmental Protection Agency (EPA) approved a new standard for arsenic in drinking water of 10 µg/L beginning January 23, 2006 (www.epa.gov/safewater/arsenic.html). Recently, aquifer storage and recovery (ASR) facilities in central Florida reported arsenic concentrations in excess of 100 µg/L (100 ppb) in recovered water (Arthur et al., 2001; Arthur et al., 2002). The ASR storage zone in the study area is the Suwannee Limestone, which directly underlies the Hawthorn sediments. The ASR storage zones in other parts of Florida are the Avon Park Formation, Ocala Group, and a part of the Hawthorn Group. The arsenic in the Suwannee Limestone storage zone may have migrated from the Hawthorn Group (Price and Pichler, 2002). Therefore, information about its concentration, distribution, and mineralogical association is important, because this is a first step to forecast its behavior during anthropogenically induced physico-chemical changes in the aquifer.

Because phosphorous, arsenic and sulfur are chemically closely related, they co-occur in nature. In addition, the highly open crystal structure of francolite (carbonate fluorapatite) shows a tendency to accumulate such elements as As, Mo, Se, Y, Zn, and the REE during diagenesis, which poses a potential problem for the phosphate industry. There have been several occurrences of swine fatalities due to arsenic poisoning as a result of phosphate feed supplements (El Bahri et al., 1991).

The study area is located in the Southwest Florida Water Management District (SWFWMD) between Tampa and Fort Myers. The research area includes both, phosphate mining facilities and aquifer storage and recovery (ASR) projects.

Purpose of Research

This research was funded by the Southwest Florida Water Management District (SWFWMD) to determine the geographic and stratigraphic distribution of arsenic in the Hawthorn Group and to provide new information about the fate and cycling of arsenic throughout the Florida platform.

Therefore, the six main questions to be answered in this research are:

- What is the concentration of arsenic in the Hawthorn Group?
- How does concentration of arsenic vary from the Formation to Formation and from the Member to Member of the Hawthorn Group?
- What are the mineralogical associations and distribution of arsenic in the Hawthorn Group?
- What are the potential arsenic contamination problems for the phosphate mining industry?
- What is the predicted behavior of the arsenic in the Hawthorn Group during ASR?
- What is the spatial distribution of arsenic in the Hawthorn units?

Research Plan

A combination of petrographic and geochemical techniques was applied to evaluate the abundance and mineralogical associations of arsenic in 16 cores from the Hawthorn Group (Table 1a, 1b and Figure 1). The cores were initially collected as part of the Regional Observation Monitor Well Program (ROMP) by the SWFWMD. The cores were chosen on the basis of their proximity to the Central Florida Phosphate District. In addition, core selection was based on a previous study (Price, 2003) detailing the abundance and mineralogical association of arsenic in the Suwannee Limestone, which directly underlies the Hawthorn Group sediments. The cores are archived at the warehouse of the Florida Geological Survey (FGS) in Tallahassee and were accessible for sampling. Each core was sampled at evenly spaced distance to represent the entire Hawthorn Group interval. In addition, samples with possibly high arsenic concentrations were taken, where trace minerals, organic matter, or minor constituents were visible.

The samples were examined and described in detail using stereo microscopy, and polished thin sections of selected samples were studied using petrographic microscope for mineralogical determinations. Additionally, several samples were selected for a more focused mineralogical analysis using scanning electron microscopy (SEM).

To perform a bulk chemical composition of the Hawthorn Group samples, the following chemical elements were analyzed by inductively coupled plasma optical emission spectroscopy (ICP-OES): calcium (Ca), iron (Fe), magnesium (Mg),

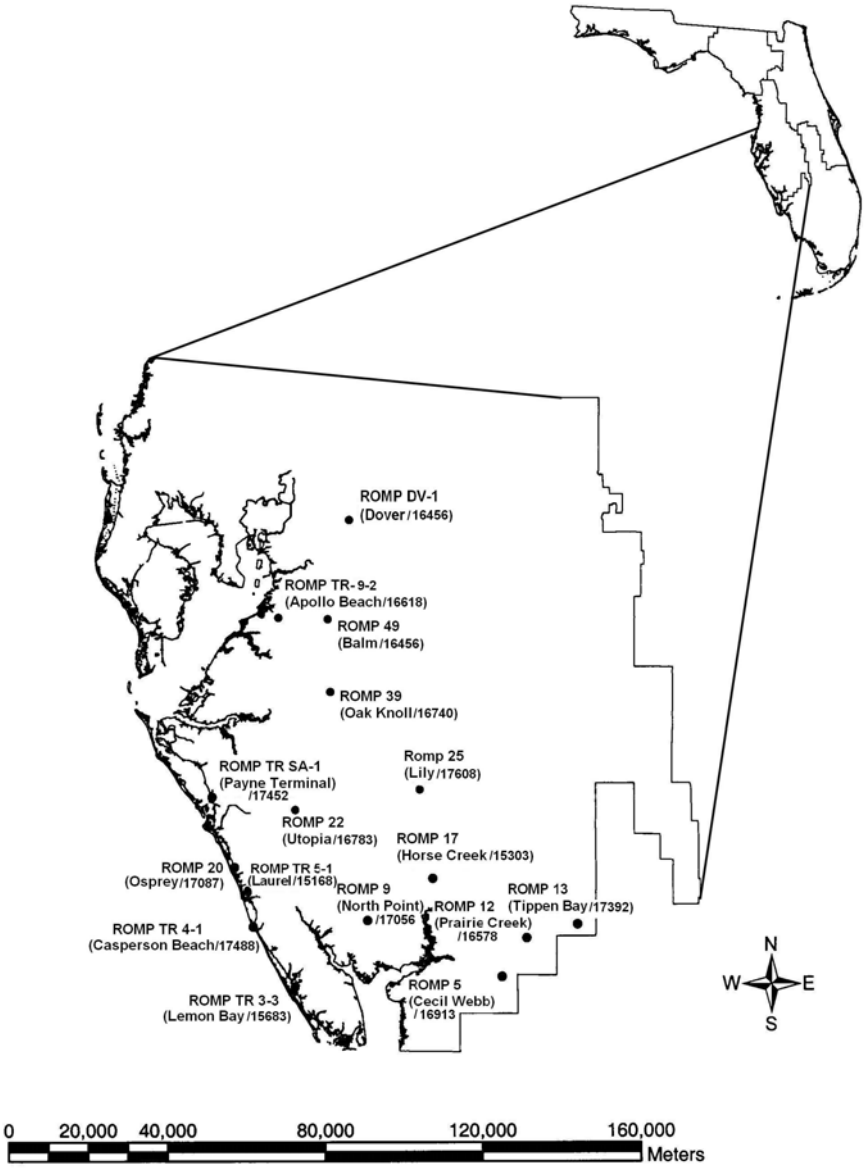

Figure 1. Map of the research area including the ROMP locations, numbers, names, and the FGS well numbers of the 16 cores that were sampled.

manganese (Mn), sulfur (S), phosphorous (P), silica (Si), and aluminum (Al). Bulk arsenic (As) concentrations were determined by hydride generation-atomic fluorescence spectrometry (HG-AFS) at the Center for Water Analysis, University of South Florida. These chemical elements were selected to determine mineralogical composition of the Hawthorn Group and to assess possible correlations with arsenic.

To better understand the mineral phases containing arsenic, several samples with high arsenic concentrations were selected for electron-probe microanalysis (EMPA) at the University of New Mexico.

Table.1a. List of 16 core wells chosen for this research (English units).

County	ROMP Number	ROMP Name	FGS well id	Hawthorn Interval (ft)	Monitor -top (ft bsl)	Monitor-bot (ft bsl)	Total (ft bsl)	Surface Elevation (ft bsl)
DESOTO	13	Tippen Bay	17392	19-704	282	592	310	61.5
DESOTO	17	Horse Creek	15303	26-439	100	470	370	22.6
DESOTO	12	Prairie Creek	16578	40-719	280	710	430	41.0
HILLSBOROUGH	49	Balm	16456	78-379	195	620	425	151.1
HILLSBOROUGH	DV-1	DV-1	16576	?-153	90	139	49	112.5
HILLSBOROUGH	TR 9-2	Apollo Beach	16618	36-268	118	148	30	10.6
MANATEE	39	Oak Knoll	16740	47-513	125	207	82	125.0
CHARLOTTE	TR 3-3	Lemon Bay	15683	56-686	155	410	255	5.8
CHARLOTTE	5	Cecil Webb	16913	69-711	130	600	470	40.1
SARASOTA	9	North Port	17056	27.5-545	40	320	280	25.0
SARASOTA	20	Osprey	17087	38.5-479	75	370	295	18.4
SARASOTA	TR 5-1	Laurel	15168	86-488	275	289	14	11.6
SARASOTA	22	Utopia	16783	18.6-373.5	95	290	195	34.5
SARASOTA	TR SA-1	Payne Terminal	17452	29-484	328	388	60	6.5
SARASOTA	TR 4-1	Casperson Beach	17488	26-599	30	645	615	10.0
HARDEE	25	Lily	17608	45-313	105	145	40	85

Table 1b. List of 16 cores chosen for this study (Metric units).

County	ROMP Number	ROMP Name	FGS well id	Hawthorn Interval (m)	Monitor -top (m bsl)	Monitor -bot (m bsl)	Total (m bsl)	Surface Elevation (m bsl)
DESOTO	13	Tippen Bay	17392	6-215	86	180	94	19
DESOTO	17	Horse Creek	15303	8-134	30	143	113	7
DESOTO	12	Prairie Creek	16578	12-219	85	216	131	12
HILLSBOROUGH	49	Balm	16456	24-116	59	189	130	46
HILLSBOROUGH	DV-1	DV-1	16576	2-47	27	42	15	34
HILLSBOROUGH	TR 9-2	Apollo Beach	16618	11-82	36	45	9	3
MANATEE	39	Oak Knoll	16740	14-156	38	63	25	38
CHARLOTTE	TR 3-3	Lemon Bay	15683	17-209	47	125	78	2
CHARLOTTE	5	Cecil Webb	16913	21-217	40	183	143	12
SARASOTA	9	North Port	17056	8-166	12	98	85	8
SARASOTA	20	Osprey	17087	12-146	23	113	90	6
SARASOTA	TR 5-1	Laurel	15168	26-149	84	88	4	4
SARASOTA	22	Utopia	16783	6-114	29	88	59	11
SARASOTA	TR SA-1	Payne Terminal	17452	9-148	100	118	18	2
SARASOTA	TR 4-1	Casperson Beach	17488	8-183	9	197	187	3
HARDEE	25	Lily	17608	14-95	32	44	12	26

CHAPTER TWO

GEOLOGY AND HYDROGEOLOGY

The stratigraphic unit for this study is the predominantly Miocene Hawthorn Group, which is subdivided into a lower section comprising the undifferentiated Arcadia Formation, Tampa and Nocatee Members of the Arcadia Formation and the upper section of the Peace River Formation (Scott, 1988).

The hydrogeologic framework of the southwestern part of Florida is composed of three discrete hydrogeologic units (Figure 2). The hydrogeologic units and their stratigraphic components include the Floridan aquifer system (FAS), the Intermediate aquifer system (IAS) or Intermediate confining unit, and the Surficial aquifer system (SAS) (Figure 2).

The Upper Pliocene to Pleistocene Surficial aquifer system (SAS) is generally comprised of unconsolidated to poorly indurated clastic deposits such as sands, sandy clays, phosphorite and some well-indurated carbonate rocks (Figure 2). The SAS is primarily unconfined with some semi-confined or locally confined sections (Gilboy, 1985).

The Upper Oligocene to Lower Pliocene Intermediate aquifer system (IAS) consists of layers of clays, sand beds, carbonate lenses, and phosphorite (Figure 2). The water-yielding beds of carbonate lenses lie between clayey confining units. As a

result, the water in the IAS is under principally confined conditions excluding local areas, where the upper confining unit is missing and the system is in direct hydraulic contact with the overlying SAS. Generally, water moves downward from the SAS and through the upper confining unit of the IAS and the majority of this water subsequently follows short flow paths and discharges to surface drainage area. On the other hand, some water penetrates downward through the lower confining unit of the IAS to recharge the underlying FAS (USGS, 1999).

The IAS is the major source of water supply in Charlotte and Sarasota Counties, where the underlying FAS is deeply buried and holds only brackish or saltwater (SWFWMD, 2000).

The FAS is a continuous sequence of carbonate rocks with generally high porosity and permeability. The confining unit separating the Upper and Lower Floridan aquifers consists of clay, dolomite with the pore spaces filled with anhydrite, or a very fine-grained (micritic) limestone (USGS, 1999).

The FAS underlies a region of approximately 259,000 km^2 throughout southern Alabama, southeastern Georgia, southern South Carolina, and the entire Florida peninsula; it is one of the most prolific and extensive aquifers in the world.

The Paleocene to Lower Miocene Floridan aquifer system (FAS) consists of the following stratigraphic units (from oldest to youngest): The Oldsmar, Cedar Keys, and Avon Park Formations, and the Ocala and Suwannee Limestones (Figure 3). The Tampa Member and the lower part of the Arcadia Formation of the Hawthorn Group

are included in the upper part of the FAS where it comprises permeable carbonate lenses (Scott, 1991).

Arcadia Formation

The Arcadia Formation unconformably overlies the Oligocene Suwannee Limestone and achieves its maximum thickness of about 183 m (600 ft) in the Okeechobee Basin (Scott, 1988). It was initially interpreted to be primarily Lower Miocene (Scott, 1988), but is now recognized to be Lower Oligocene to Middle Miocene (Brewster-Wingard et al., 1997; Missimer, 1997).

The Arcadia Formation is comprised of the undifferentiated Arcadia Formation, the Tampa Member and the Nocatee Member (Figure 2).

Throughout the research area the undifferentiated Arcadia Formation is principally composed of variable amount of siliciclastics within carbonate matrix (Figures 3, 4). The carbonates of the Arcadia Formation are typically composed of fossiliferous, yellowish gray to light greenish gray to light brown, micro- to finely crystalline limestones and dolostones with variable amounts of quartz sands, gray to greenish gray clays, chert and phosphatic material (Scott, 1990). The clays are palygorskite, sepiolite, illite/smectite mixed layer, and insignificant amounts of kaolinite (Compton et al., 1993). Thin beds of sand and clay are widespread and molds and casts of mollusks are commonly found in the dolostones.

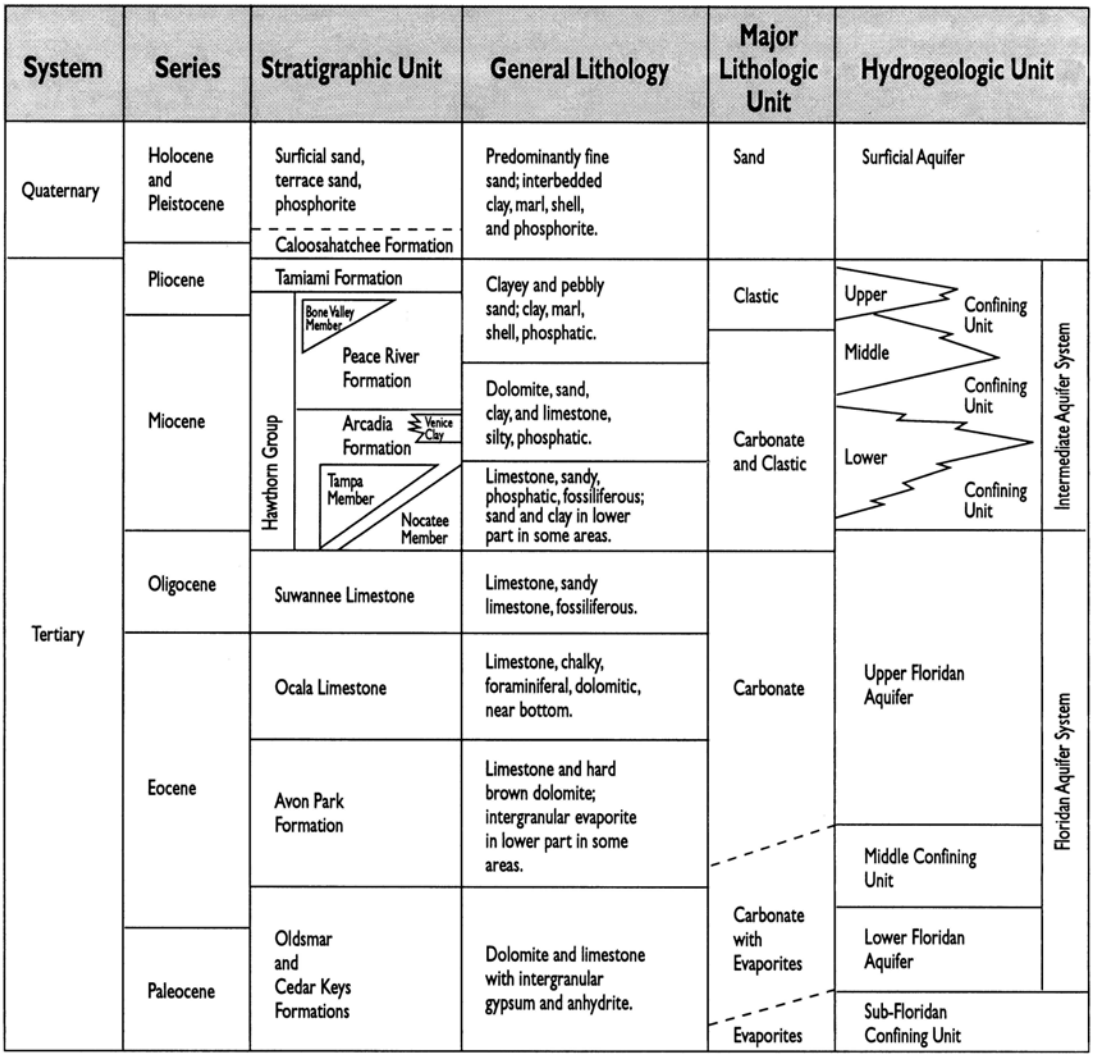

Figure 2. Lithostratigraphic and hydrogeologic units of the study area

(Modified from SWFWMD Report, 2000; Scott, 1989).

Tampa Member

The lithology of the Upper Oligocene to Lower Miocene Tampa Member of the Arcadia Formation (Figures 3, 4) varies from a white to yellow-gray marine wackestone to packestone containing variable amounts of dolostone, clay, quartz sand, and minor occurrences of phosphate material (Wingard et al., 1993; Scott, 1988). Thin carbonate, quartz sand and clay beds are commonly observed throughout the Tampa Member. The Tampa Member is typically a poor to well indurated limestone and in some areas it contains variable amounts of fossils such as mollusks, corals, and foraminifera (Scott, 1988). The Tampa Member usually has intergranular or moldic porosity. The contact between the undifferentiated Arcadia Formation and Tampa Member in central Florida is sporadically marked by a chert layer at the top of the Tampa Member (Gilboy, 1985).

Nocatee Member

The Nocatee Member forms the base of the Arcadia Formation (Figure 2) in the southern area of SWFWMD. The study of Scott (1988) showed that the Upper Oligocene to Lower Miocene Nocatee Member of the Arcadia Formation contains the highest amount of siliciclastic material compared to the entire Arcadia Formation.

Peace River Formation

The Peace River Formation unconformable overlies the Arcadia Formation and reaches a maximum thickness of 198 m (650 ft) in the Okeechobee Basin (Scott, 1990).

The lithological composition of the Middle Miocene to Lower Pliocene (Missimer et al., 1994) Peace River Formation consists of gray to greenish gray clays (palygorskite, sepiolite, illite/smectite mixed layer), sandy clays, and carbonates with variable amounts of phosphate sand and gravel (Green at al., 1995). The carbonates are comprised of dolosilts, dolostones, and interbedded limestones (Figures 3, 4). The siliciclastic component is dominant throughout the Peace River Formation (Scott, 1988). The Peace River Formation contains substantial amounts of phosphate material and is currently being exploited.

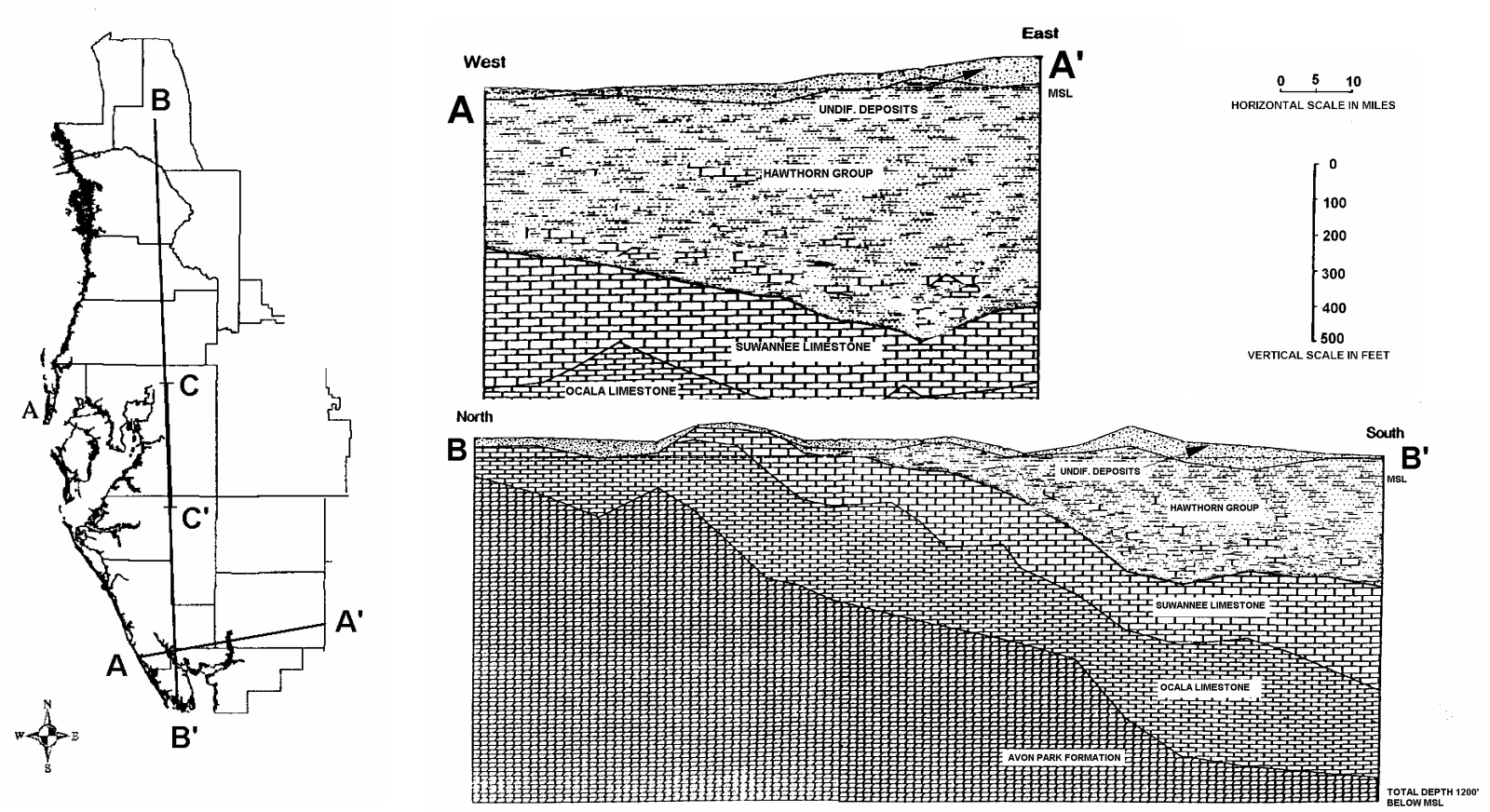

Figure 3. Geological cross sections of southwestern Florida (*Modified from Gilboy, 1985*).

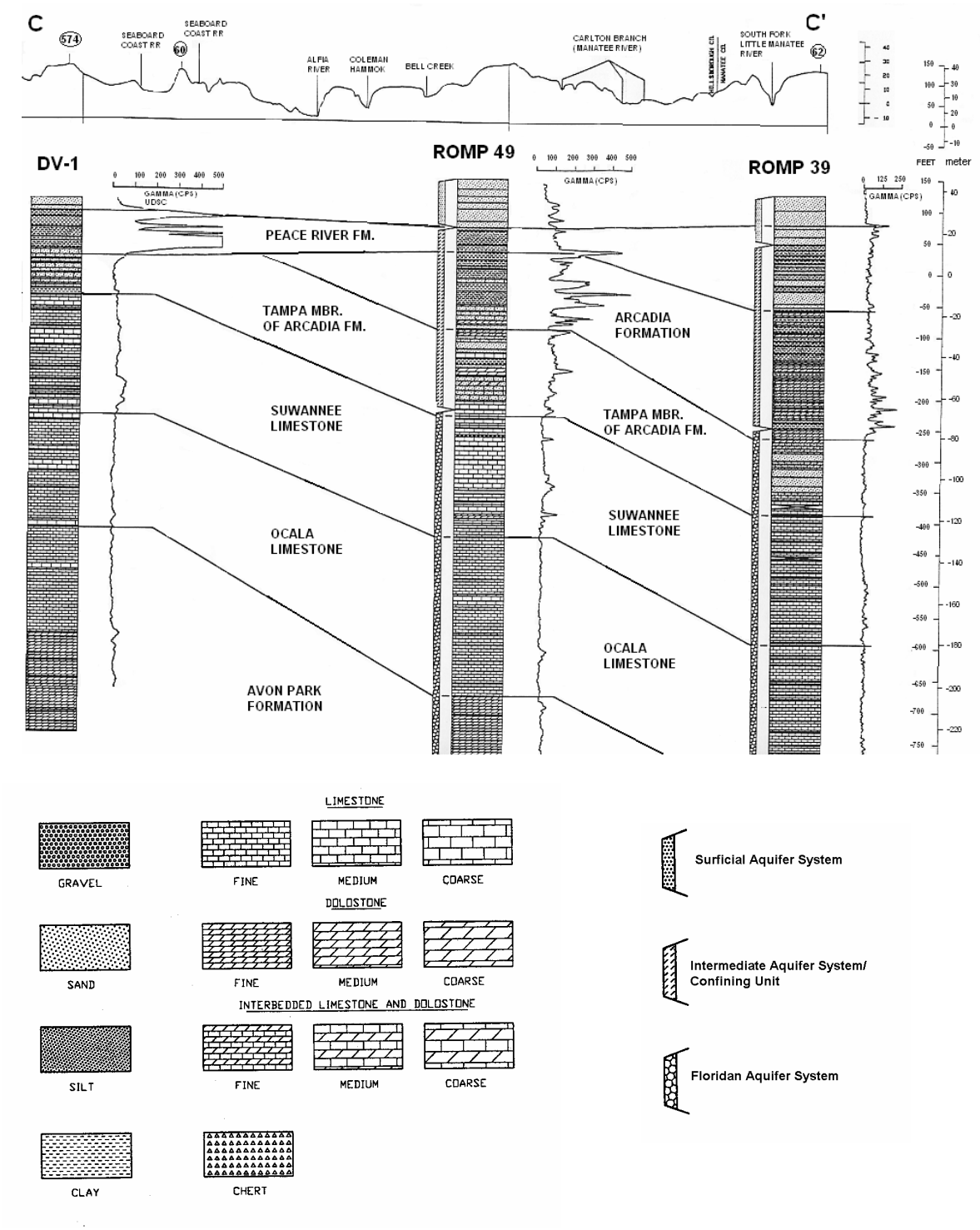

Figure 4. Geological cross sections of southwestern Florida

Hillsborough and Manatee Counties (*Modified from Green et al., 1995*).

Origin of Florida's Phosphorite Deposits

Changes in global climate and sea level during the Miocene were associated with the development of widespread phosphorite deposits of the Hawthorn Group in Florida (Riggs, 1979, 1984; Compton et al., 1993). Phosphorite sediments in Florida consist of the carbonate fluorapatite mineral francolite. Other phosphorous-bearing minerals, such as crandallite and wavellite, are a weathering product of francolite (Compton et al., 1993). These phosphorite sediments occur as sand- to pebble- sized peloidal grains that show no internal structure and are composed of black, brown or gray massive or cryptocrystalline francolite. Other types of phosphorite particles are skeletal grains (teeth and bones) and molds of mollusks (Compton et al., 1993).

The precipitation of phosphorite in the Hawthorn Group is related to the upwelling of deep phosphorite-rich ocean waters along the continental margin during periods of high or rising sea level (Kazakov, 1937). The upwelling of deep cold water to shallow warmer regions caused the increase of the surface productivity that contributed organic matter to sediments (Compton et al., 1993). Degradation of organic substance in the sediment by bacterial activity caused the releasing of phosphorus to the pore water and eventual precipitation of pore-filling francolite. Hydrogen sulfide (H_2S) that formed during sulfate reduction under anoxic conditions resulted in the deposition of pyrite and dolomite rhombs or caused diffusion of H_2S to bacterial mats with the subsequent oxidation back to sulfate. The inclusions of pyrite in the fibrous clay material (palygorskite and sepiolite) and numerous phosphorite

grains indicate the same diagenetic environment within the sulfate-reduction zone (Compton et al., 1993).

Reworking of the Hawthorn sediment occurred during periods of marine regressions or low sea level. Alteration of the deposits concentrated phosphorite grains and incorporated dolomite rhombs into dolomite beds and dolosilt layers. In the same time much of the organic substance and pyrite were altered by oxidation.

Possible Sources of Arsenic in the Hawthorn Group

Generally, there are four major possible sources of arsenic in the Hawthorn Group:

- Francolite (Carbonate Fluorapatite);
- Sulfide minerals such as pyrite and arsenopyrite;
- Clay and organic matter;
- Hydrous ferric oxides (HFO).

Hinkle and Polette (1999) reported two principal processes that mainly control arsenic mobility in aquifers: (1) adsorption and desorption and (2) solid-phase precipitation and dissolution reactions. Arsenic adsorption and desorption reactions are influenced by changes in pH, redox (reduction/oxidation) reactions and the presence of competing anions. Solid-phase precipitation and dissolution reactions are primarily controlled by pH, redox state and chemical composition (saturation).

Francolite (Carbonate Fluorapatite)

Francolite chemistry is extremely complex, but its chemical composition can be given as a general formula: $Ca_{10-a-b}\,Na_aMg_b\,(PO_4)_{6-x}\,(CO_3)_{x-y-z}\,(CO_3.F)_y\,(SO_4)_{zF2-p}\,OH_p$. The highly open crystal structure of francolite permits substantial substitution at any of the fluorapatite sites, e.g. Na^+, Mg^{2+}, Sr^{2+} for Ca^{2+}; OH^-, AsO^{3-} CrO^{2-}, VO^{3-} for PO^{3-}; and Cl^-, Br^- for F (Shields, 2002). A tendency to accumulate elements, such as As, Mo, Se, Y, Zn, and the REE during diagenesis is a poorly understood characteristic of francolite (Shields, 2002).

According to Smedley and Kinniburgh (2003) calcium phosphate or apatite can contain up to 1000 mg/kg of arsenic. On the other hand, Stow (1969) did not reveal any correlation between arsenic and phosphorous in the Bone Valley Member of the Hawthorn Group.

Sulfide Minerals (Pyrite)

Prior studies of sulfide minerals such as the abundance and occurrence of pyrite in the Suwannee Limestone (Price and Pichler, 2004, in review; Price, 2003; Price and Pichler, 2002) revealed significant enrichment of arsenic in pyrite with concentrations as high as 11,200 ppm. Thomas and Sanders (1998) reported arsenic concentrations in pyrite framboids of up to 1000 ppm as a substitute element for sulfur in the FeS_2 structure. Huerta-Diaz and Morse (1990) found arsenic

concentrations in marine sedimentary pyrites of as much as 0.93 wt. %. Therefore, sedimentary pyrite can be a significant sink and source of arsenic.

Clay and Organic Matter

It has been reported that soil constituents, such as clays and organic substances, can easily interact with heavy metals such as arsenic via ion exchange or surface adsorption (Manning, Goldberg, 1997; Evangelou, 1995). Clays readily adsorb arsenic because of the oxide-like character of the edges of its grains (Claesson et al., 2003). Clays and organic substance have very small particle size, which therefore result in a large surface area per unit volume and ability to adsorb arsenic. Moreover, the potential of humic substances to complex with heavy metals is due to the existence of oxygen-containing functional groups such as carboxyl (COOH), hydroxyl (Oh), and carbonyl (C=O) (Evangelou, 1995).

Hydrous Ferric Oxides (HFO)

Reworking of the Hawthorn Group sediment during periods of marine regressions caused oxidation of some pyrite and formation of iron oxyhydroxides or hydrous ferric oxides (HFO) (Compton et al., 1993). It has been shown that arsenic integrates into sediments by co-precipitation as hydrous ferric oxides (HFO), or is adsorbed onto extremely high surface area of precipitated HFO (Hongshao and Stanforth, 2001; Hinkle et al., 1999; Evangelou, 1995). High concentrations of arsenic are found in HFO (Bowell, 1994; Chao, Theobald, 1976). It has been reported

the close connection between hydrous ferric oxides and arsenic (Pichler et al., 2000; Chao, Theobald, 1976). Stow (1969) concludes that most of the arsenic in the Bone Valley Member of the Hawthorn Group is adsorbed on HFO.

Nickson et al. (2000) found high arsenic in the groundwater of Bangladesh that had been derived from reductive dissolution of arsenic-rich hydrous ferric oxides that exists as a coating on sedimentary grains.

CHAPTER THREE

METHODS

Sample Collection and Preparation

The present study addresses the detailed mineralogy and geochemistry of arsenic in the Miocene Hawthorn Group. In order to conduct the research, 55 samples from the Peace River Formation, 205 samples from the Arcadia Formation, 75 samples from the Tampa Member, and 27 samples from the Nocatee Member of the Hawthorn Group were collected and analyzed from the 16 ROMP wells (Figure 1).

During sampling, each core was taken at an even distance to demonstrate the entire Hawthorn Group interval. Samples at intervals of 7.6 m (25ft) and samples of special interest were obtained. Samples of interest were taken from sections likely to have high arsenic concentrations such as areas with pyrite crystals, hydrous ferric oxides, green clays, and organic material. Samples were sealed and labeled in plastic bags and brought back from the Florida Geological Survey in Tallahassee to the University of South Florida. The sediment samples were powdered in an agate mortar and stored in plastic vials. The cross-contamination between samples was minimized by cleaning mortar and pestle with pure silica sand and deionised water (DI) of 17.9 mΩ, and with nitric acid (1:1 HNO_3) if softy greenish clays were present.

Approximately 0.5 g ± 0.001 g of dried, powdered, homogenous sample was weighted into a digestion vessel and 10 mL of a 3:1 mixture of hydrochloric (HCl) and nitric acid (HNO_3) was added. The digestion vessel was immediately capped with a reflux cup to avoid the escape of arsine gas. The sample was heated to a temperature of 95^0C for 30 minutes. After digestion, the solution was cooled down, diluted to 50 mL (5:1) with DI water, centrifuged for 15 minutes to remove non-soluble particles, and filtered.

Mineralogy and Petrography

Stereo and Petrographic Microscopy

Hand samples were examined and lithologically described in the field and laboratory using a 10x hand lens and a SZ-PT Olympus stereo microscope with Fostec^R 150 watt tungsten halogen light source. When high arsenic concentrations were determined by chemical analyses (explained below), the stereo microscope was used again for a more detailed study.

Approximately 60 thin sections of selected samples were made to get a detailed mineralogical composition of the Hawthorn Group. Thin sections have been made as polished sections with blue dye impregnation and were described using a Meiji Techno ML 9400 polarizing microscope with reflected and transmitted light. Subsequently, about 18 thin sections were selected for the EMPA to study chemical composition of individual minerals (explained below).

Scanning Electron Microscopy

Based on geochemical data, several samples with high arsenic levels were selected for a more focused mineralogical analysis using scanning electron microscopy (SEM). The Hitachi S-3500N variable pressure scanning electron microscope is located at the College of Marine Science, University of South Florida. The SEM is equipped with a Robinson Backscattered detector for atomic number contrast. This type of analysis consists of mounting small sample chips onto an aluminum stub. The sample was sputter coated with Au/Pd coating (for imaging).

Chemistry

Inductively Coupled Argon Plasma Optical Emission Spectroscopy and Hydride Generation Atomic Fluorescence Spectrometry

To determine the concentration of arsenic (As), calcium (Ca), iron (Fe), magnesium (Mg), manganese (Mn), sulfur (S), phosphorous (P), silica (Si) and aluminum (Al) of the Hawthorn Group, samples were analyzed by a combination of Inductively Coupled Argon Plasma Optical Emission Spectroscopy (ICP-OES) and Atomic Fluorescence Spectrometry (HG-AFS) at the Center for Water Analysis, University of South Florida.

Total arsenic concentration for each sample was analyzed by HG-AFS on a PSA 10.055 Millennium Excalibur system. In preparation for AFS analysis, 10 mL of the sample solution was treated with 30% concentrated HCl, 2% saturated potassium iodide (KI) solution, and deionised water (DDI) with a final dilution volume of 50

mL (5:1). This special treatment of the samples cause the reduction of As (V) to As (III) prior to the formation of the arsenic hydride (AsH_3) via addition of sodium tetraborohydride ($NaBH_4$).

The arsenic hydride generator is based on the reaction of sodium borohydride, hydrochloric acid and the sample.

Formation of hydrogen free radical:

$NaBH_4 + 3\ H_2O + HCl \rightarrow H_3BO_3 + 8H^- + NaCl$

Formation of the volatile arsenic hydride (gas)

$8H^- + As^{3+} \rightarrow AsH_3 + H_2$ excess

In a consequence, the AsH_3 is then atomized in a hydrogen flame and concentrations are determined by fluorescence spectrometry.

The elements Ca, Fe, Mg, Mn, S, P, Si and Al were analyzed by ICP-OES on a Perkin-Elmer Optima 2000 DV spectrometer. Sample preparation consisted of measuring 2 mL of the stored sample solution and was diluted with 8 mL of deionized water into a 10 mL centrifuge tube. The sample dilution (5:1) is needed due to high acid concentration. The final solution is carried into the IC-OES via peristaltic pumps and the elements are atomized by high temperature argon plasma and detected by emission spectrometry.

Acid blanks for digestion, HG-AFS, and HG-ICP-OES did not revealed any detectable arsenic concentrations. Background signal drift monitor was less that 2%.

Electron-Probe Microanalyser – Wave Dispersive Spectrometry

The 16 polished thin sections with variable arsenic concentrations and lithological compositions from each Formation/Member of the Hawthorn Group were chosen for the electron-probe microanalysis – wave dispersive spectrometry (EMPA or Electron Microprobe) using a JEOL 8200 instrument at the Earth & Planetary Sciences Department, University of New Mexico. Operating conditions of the electron microprobe were 20 kV accelerating voltage, a spot size of 5 μm, and a 20nA current. The electron microprobe was used for spot analysis and to create several chemical maps for examination of arsenic distribution in matrix and individual minerals.

Statistical Methods

To estimate statistical properties of the analyzed elements the SPSS statistics software was used. The probability P-P plots for the decimal logarithm of arsenic, iron and sulfur concentrations were created to determine if the variable is normally distributed (Landau and Everitt, 2004). The normal P-P statistics plot compares the observed cumulative distribution function of the variable against the cumulative distribution function that would be expected if the data were normally distributed (Swan and Sandilands, 1995). Therefore, if a value comes from a normal distribution, points on the plot will group around a straight line.

In addition, the bell-shaped frequency histograms of the Hawthorn Group samples were generated to evaluate the distribution of a single numeric variable

(Landau, Everitt, 2004). A histogram displays the distribution of a quantitative variable by showing the relative concentration of data points along different intervals or sections of the scale on which the data are measured (Landau, Everitt, 2004).

Determination of the normal P-P plots and frequency histograms allowed to find a mean (μ) and standard deviation (σ) from the normal arsenic distribution and to get a normal cumulative distribution function (CDF.Normal). The CDF.Normal (*quant*, *mean, stddev*) function gives the area under a normal curve with the given mean and standard deviation for values less than *quant* (known concentration) (Landau, Everitt, 2004), or in other words, CDF.Normal shows the probability of a concentration Q to be less than *quant*, i.e.

CDF.Normal (*quant, mean, stddev*) = *P (Q< quant)*

$P\ (Q< quant) = \int_{-\infty}^{quant} f(x)dx$, where $f(x) = (2\pi\sigma^2)^{-1/2} e^{-(x-\mu)^2/2\sigma^2}$ is a density function for normal distribution with the given mean (μ) and standard deviation (σ) (Shiryaev, 1996).

The normal P-P plots, frequency histograms and normal cumulative distribution functions were created for all Hawthorn samples and for selected interval samples.

In addition, the survivor functions for each formation/member of the Hawthorn Group were found. The survival function is the probability that a concentration Q has a value greater than *quant*, i.e.

S (quant) = P (Q > quant) = 1 – P (Q < quant) (Evans et al., 2000; Shiryaev, 1996).

CHAPTER FOUR

RESULTS

Petrography and Mineralogy

Stereo and Petrographic Microscopy

Arcadia Formation

The inspection of the Arcadia Formation samples including the Tampa and the Nocatee Members demonstrates diverse lithologic and mineralogic compositions. Most samples consist of carbonate material (limestones and dolostones) with a variable amount of siliciclastic component. The general lithologic characteristics of the Arcadia Formation, Tampa and the Nocatee Members are demonstrated in Appendices A-C. The siliciclastics are primarily composed of gray and grayish green clays, quartz, and phosphatic material. The Tampa Member contains no or only a minor amount of phosphatic matter. In addition, the examination of sediments reveals presence of some minor mineral phases, such as pyrite, gypsum, chert, secondary calcite, feldspar, and hydrous ferric oxides. The HFO were frequently observed as stains or rings around pyrites. Framboidal and euhedral pyrite crystals are ubiquitous throughout the Arcadia Formation. Organic matter was observed in several samples and revealed heterogeneous distribution throughout the undifferentiated Arcadia

Formation. Detailed lithologic descriptions of the Arcadia sediments correspond to the reported studies of the Arcadia Formation (Wingard et al., 1993; Scott, 1990, 1988).

Thin sections with variable arsenic concentrations were investigated with the polarizing microscope with reflected and transmitted light, and demonstrated the presence of different mineralogies, such as phosphate, calcite, dolomite, feldspar, pyrite, quartz, clays, and hydrous ferric oxides. Pyrite crystals were observed in about 90% of the thin sections occurring in the sediment matrix and as inclusions in phosphate grains and calcite crystals. Figure 5 illustrates the presence of framboidal pyrites in the Arcadia Formation.

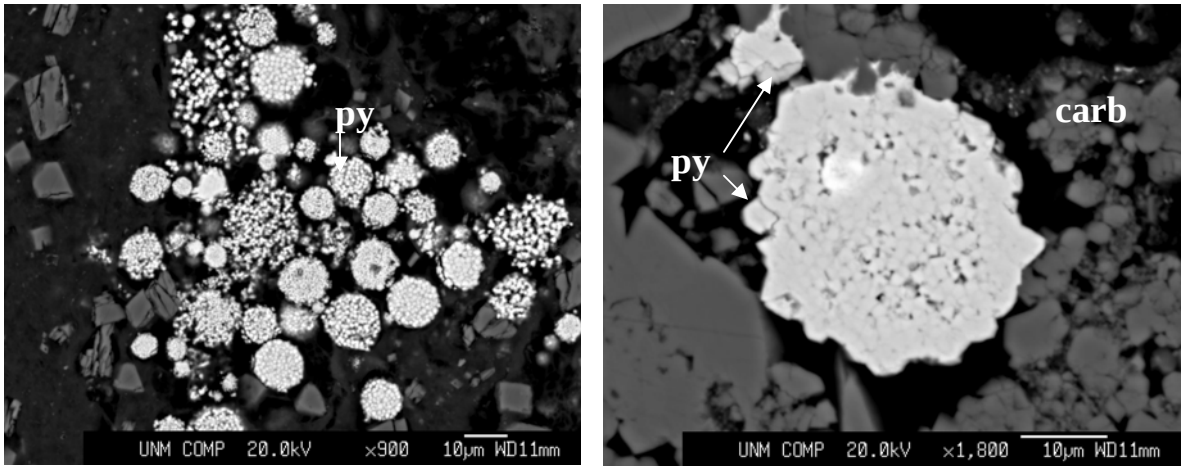

Figure 5. Backscattered images of framboidal pyrite (py) in carbonate matrix (carb) from sample 20-143 (Arcadia Formation).

Peace River Formation

The analyses of Peace River samples displays that the majority of sediments are generally composed of siliciclastics such as quartz sands, gray to dark greenish gray clays, and substantial amount of phosphates. The occurrence of several minor mineral phases revealed framboidal and euhedral pyrite, gypsum, native sulfur, secondary calcite, feldspar, and hydrous ferric oxides (HFO) or Fe-oxyhydroxides. These lithologic descriptions coincide with the reported studies of the Peace River Formation (Green at al., 1995; Compton et al., 1993; Scott, 1990, 1988). The general lithologic characteristics of the Peace River sediments are illustrated in Appendix D.

Using the polarizing microscope with reflected and transmitted light on thin sections of the Peace River sediments with variable arsenic concentrations revealed the presence of different mineralogies, such as pyrite, phosphate, calcite, gypsum, dolomite, feldspar, quartz, clays, and hydrous ferric oxides. Generally, about 90% of all thin sections contained pyrite crystals in the sediment matrix and several samples revealed the inclusions of pyrite in phosphate grains.

Scanning Electron Microscopy

Based on geochemical results several samples with high arsenic levels were selected for a more focused mineralogical analysis using scanning electron microscopy (SEM). The SEM of the selected samples from the Arcadia Formation and the Tampa Member confirm the existence of both framboidal and euhedral pyrite crystals (Figures 6, 7). Framboidal pyrites are approximately less than 10 μm in

diameter and consisted of euhedral pyrite micro-crystals (Figure 6). SEM shows that pyrite was randomly scattered, occurring with clays, phosphate nodules and organic material.

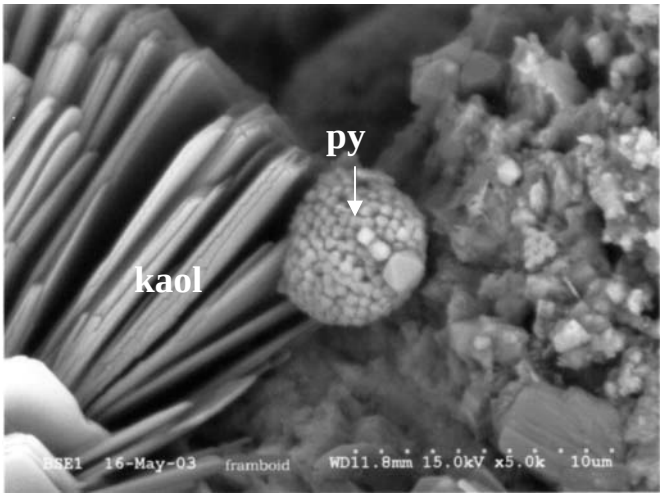

Figure 6. Scanning electron micrograph of framboidal pyrite (py) and kaolinite (kaol) in sample 22-170 from the Tampa Member (arsenic concentration of the bulk sample is 14.0 ppm).

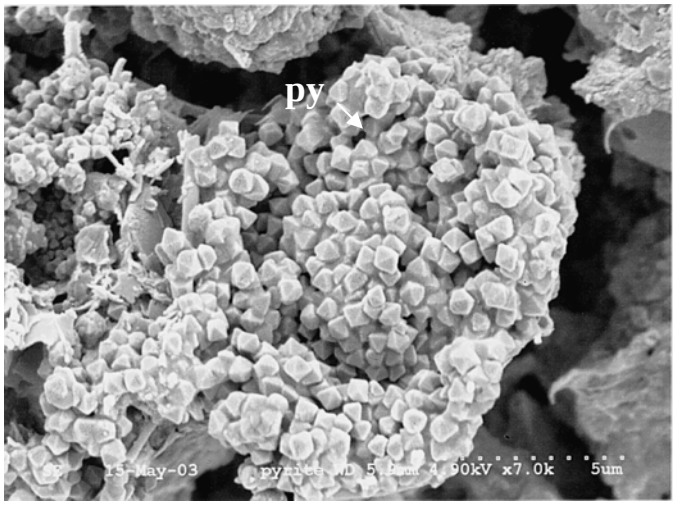

Figure 7. Scanning electron micrograph of euhedral pyrite (py) in sample 4-1-599 from the Arcadia Formation (arsenic concentration of the bulk sample is 7.5 ppm).

Bulk Chemical Composition

Hawthorn Group (All samples)

In the 362 Hawthorn Group samples, concentrations of arsenic vary from 0.1 ppm to as high as 69.0 ppm with a mean (μ) of 5.6 ppm and standard deviation (σ) of 7.1 ppm (Table 2). The mean includes both interval samples and samples of the special interest and, therefore, should be used with caution.

Bulk-rock chemical analyses by ICP-OES show that the most appreciable linear correlation for the Hawthorn Group sediments exists between S and Fe with R^2 of 0.87, which could be due to the outlier effect (Swan and Sandilands, 1995) caused by sample 12 - 125(2) (Figure 8A). Elimination of the outlier point with the anomalously high concentration of Fe and S show a correlation of $R^2 = 0.77$ (Figure 8B). Figure 8 displays the pyrite line in case if only pyrite as a source of Fe and S is dissolved and analyzed. Some of the Hawthorn samples plot above and under the pyrite line indicating that iron is probably present within hydrous ferric oxides and sulfur within gypsum.

Correlation matrix between Ca, Fe, Mg, Mn, Si, S, P, Al, and As for all 362 samples from the Hawthorn Group is demonstrated in Table 3.

Hawthorn Group (Interval samples)

The arsenic concentrations of the 285 interval samples from the Hawthorn Group range from 0.1 ppm to 40.8 ppm with a mean of 5.0 ppm (σ is 5.8 ppm) (Table 2).

Table 2. Maximum, Minimum, Mean and Standard Deviation of arsenic concentrations in ppm for the Hawthorn Group and its Formations/Members.

	Maximum	**Minimum**	**Mean**	**Standard Deviation**	**(n)**
Hawthorn Group (all samples)	69.0	0.1	5.6	7.1	362
Hawthorn Group (interval samples)	40.8	0.1	5.0	5.8	285
Peace River Formation	40.8	0.4	8.8	8.6	55
Undifferentiated Arcadia Formation	36.0	0.1	5.7	6.2	205
Tampa Member	15.2	1.2	3.0	3.7	75
Nocatee Member	69.0	0.5	6.5	13.1	27

(A)

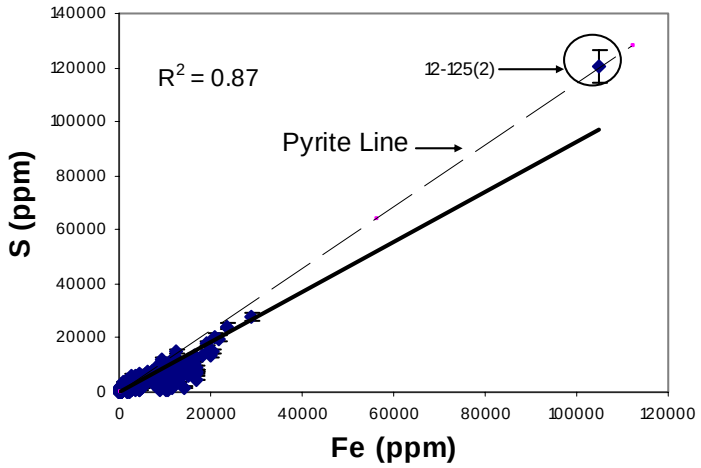

(B)

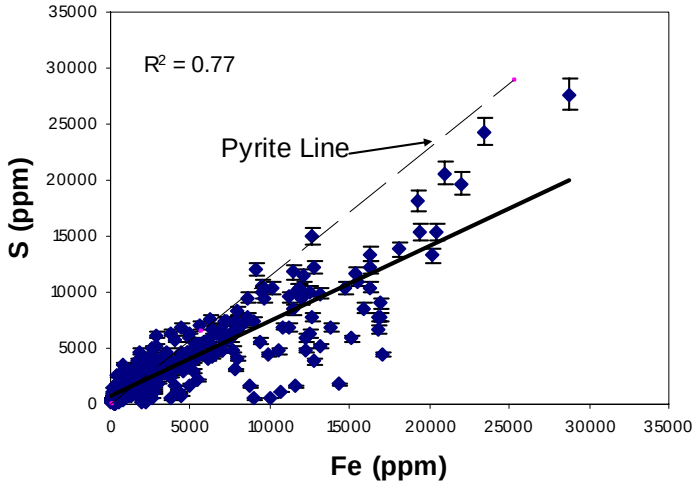

Figure 8. Diagrams showing correlation between Fe and S in the Hawthorn Group all data (A) and without the outlier (B); see text for additional information.

Table 3. Correlation matrix for the Hawthorn Group (all 362 samples); significant correlations are in bold.

	Ca	Fe	Mg	Mn	Si	S	P	Al	As
Ca	1.00	-0.43	-0.13	-0.24	-0.29	-0.27	-0.12	-0.64	-0.29
Fe		1.00	-0.03	0.38	0.25	**0.87**	0.27	0.57	0.35
Mg			1.00	0.23	0.09	-0.01	0.00	0.04	0.04
Mn				1.00	0.11	0.30	0.36	0.41	0.27
Si					1.00	0.22	0.28	0.24	0.28
S						1.00	0.29	0.35	0.40
P							1.00	0.28	0.14
Al								1.00	0.25
As									1.00

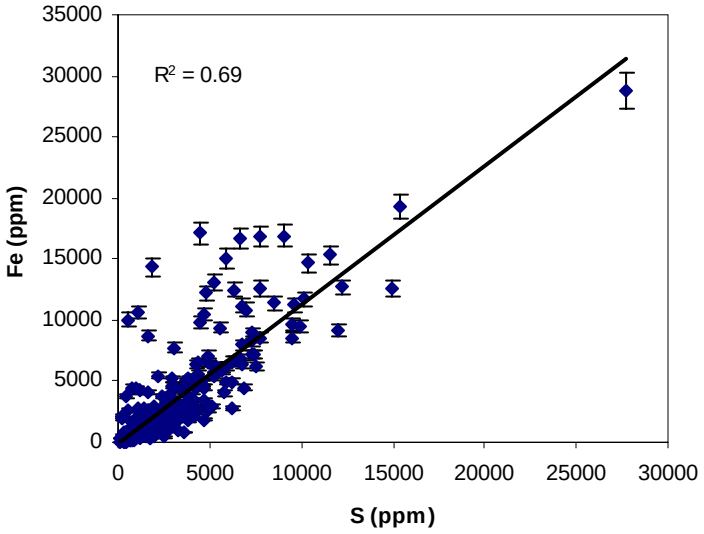

Figure 9. Correlation between Fe and S for the Hawthorn Group interval samples.

Bulk-rock analyses by ICP-OES revealed a significant degree of linear correlation between Fe and S, with R^2 value of 0.69 for the all interval samples (Figure 9). Correlation matrix for all 285 interval samples from the Hawthorn Group is demonstrated in Table 4.

Table 4. Correlation matrix for the Hawthorn Group (285 interval samples); significant correlations are in bold.

	Ca	**Fe**	**Mg**	**Mn**	**Si**	**S**	**P**	**Al**	**As**
Ca	1.00	-0.55	-0.17	-0.24	-0.25	-0.40	-0.16	-0.59	-0.09
Fe		1.00	0.04	0.47	0.31	**0.69**	0.30	0.63	0.32
Mg			1.00	0.27	0.09	0.09	-0.02	0.07	0.01
Mn				1.00	0.15	0.42	0.38	0.42	0.07
Si					1.00	0.37	0.32	0.26	0.06
S						1.00	0.37	0.35	0.26
P							1.00	0.33	0.19
Al								1.00	0.25
As									1.00

Undifferentiated Arcadia Formation

The arsenic concentrations of the undifferentiated Arcadia Formation vary from 0.1 ppm to 36.0 ppm (Table 2). The mean of 205 samples is of 5.7 ppm (σ is 6.2 ppm). Appendix B shows total arsenic concentrations for 205 samples from the undifferentiated Arcadia Formation.

About 88% of all samples have less that 10 ppm of arsenic and approximately 11% less that 1 ppm (Appendix E). Samples with mostly pure limestone and

dolostone show low concentration of arsenic. High arsenic concentrations associate with the contribution of pyrite, clays, hydrous ferric oxides, and phosphates.

Bulk-rock chemical analyses by ICP-OES illustrate that the most significant linear correlation for the undifferentiated Arcadia Formation sediments exists between S and Fe with R^2 of 0.81 (Figure 10) and between Al and Fe (clay material) with R^2 of 0.74. Correlation matrix for all 204 samples from the Arcadia Formation is shown in Table 5.

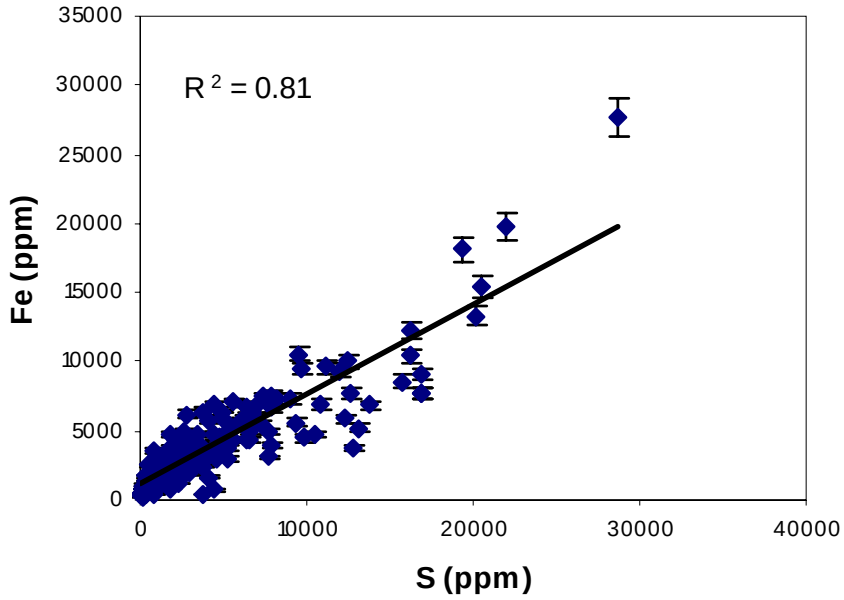

Figure 10. Correlation between Fe and S for the Undifferentiated Arcadia Formation.

Table 5. Correlation matrix for the undifferentiated Arcadia Formation (205 samples); significant correlations are in bold.

	Ca	Fe	Mg	Mn	Si	S	P	Al	As
Ca	1.00	-0.46	-0.17	-0.19	-0.28	-0.32	-0.06	-0.51	-0.14
Fe		1.00	-0.06	0.38	0.18	**0.81**	0.14	**0.74**	0.30
Mg			1.00	0.19	-0.01	-0.08	-0.11	-0.03	0.00
Mn				1.00	0.03	0.37	0.33	0.35	0.12
Si					1.00	0.18	0.23	0.23	0.02
S						1.00	0.27	0.51	0.28
P							1.00	0.21	0.10
Al								1.00	0.35
As									1.00

Tampa Member

The arsenic concentrations of the Tampa Member of the Arcadia Formation range from 0.2 ppm to 15.2 ppm (Table 2). The mean value for 75 samples is of 3 ppm (σ is 3.7 ppm). Values for all 75 samples from the Tampa Member are listed in Appendix B.

Approximately 92% of all samples contain less that 10 ppm of arsenic and about 39% less that 1 ppm (Appendix B). Samples of a pure carbonate sandstone, limestone and dolostone consistently demonstrate low arsenic concentrations. Arsenic concentrations increase with increasing abundance of pyrite, clays, and phosphates.

Bulk-rock analyses by ICP-OES revealed a significant degree of linear correlation between Al with Fe and S (clay material), with R^2 of 0.76 and 0.78

respectively. In addition, high degree of linear correlation found between Fe and S, with R^2 value of 0.63 (Figure 11). Correlation matrix for all 75 samples from the Tampa Member is shown in Table 6.

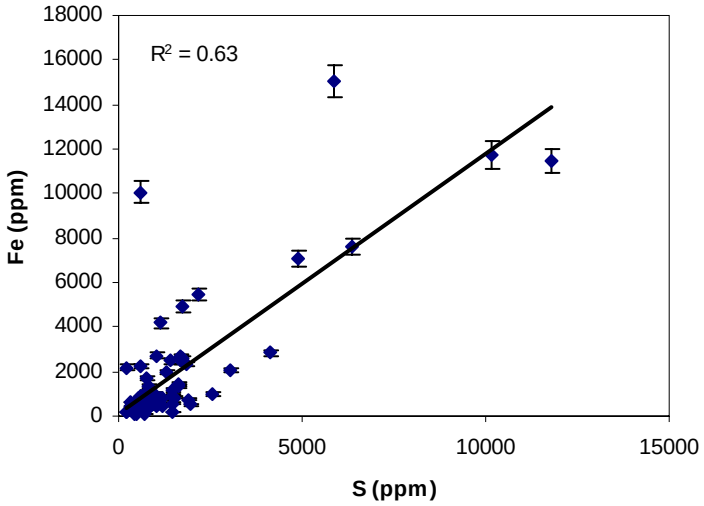

Figure 11. Correlation between Fe and S for the Tampa Member.

Table 6. Correlation matrix for the Tampa Member of the Arcadia Formation (75 samples); significant correlations are in bold.

	Ca	**Fe**	**Mg**	**Mn**	**Si**	**S**	**P**	**Al**	**As**
Ca	1.00	-0.52	-0.27	-0.18	-0.28	-0.34	-0.29	-0.58	-0.17
Fe		1.00	0.24	0.44	0.19	**0.63**	0.51	**0.76**	0.53
Mg			1.00	0.54	0.23	0.24	0.03	0.22	0.11
Mn				1.00	0.25	0.30	0.05	0.29	0.23
Si					1.00	0.16	0.08	0.16	0.23
S						1.00	0.58	**0.78**	**0.61**
P							1.00	0.48	0.16
Al								1.00	0.55
As									1.00

A combination of ICP-OES and HG-AFS results revealed a significant degree of linear correlation between As and S, with R^2 of 0.61(Figure 12).

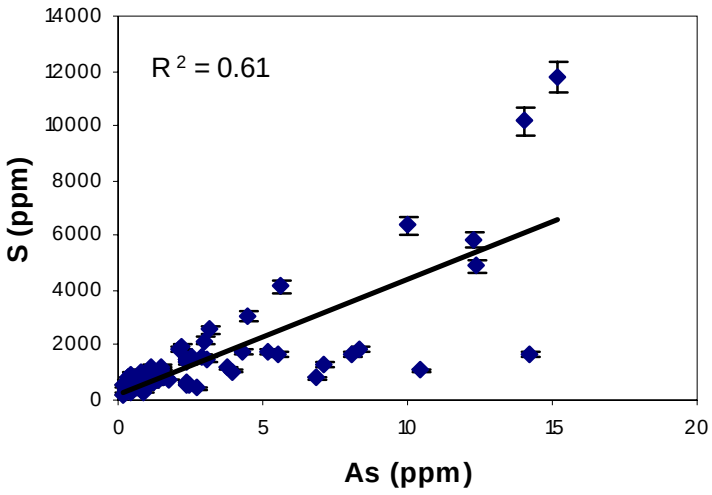

Figure 12. Correlation between As and S for the Tampa Member.

Nocatee Member

The arsenic concentrations of the Nocatee Member of the Arcadia Formation range from 0.5 ppm to as high as 69.0 ppm (Table 2). The mean value for 27 samples is 6.5 ppm (σ is 13.1 ppm). Arsenic values for all 27 samples from the Nocatee Member are demonstrated in Appendix C.

Approximately 88% of all samples contain less that 10 ppm of arsenic and roughly 23% less that 1 ppm (Appendix C). Arsenic concentrations increase with the abundance of pyrite, hydrous ferric oxides, clays, and phosphate. The sample 12-529

from the Nocatee Member represents the highest arsenic concentration (69.0 ppm) of the all Hawthorn Group samples.

Bulk-rock analyses by ICP-OES revealed a significant degree of linear correlation between Fe and S, with R^2 of 0.85 (Figure 13). In addition, a high degree of linear correlation found between Fe and Al (clay material), with a R^2 value of 0.81. Correlation matrix for all 27 samples from the Nocatee Member is shown in Table 7.

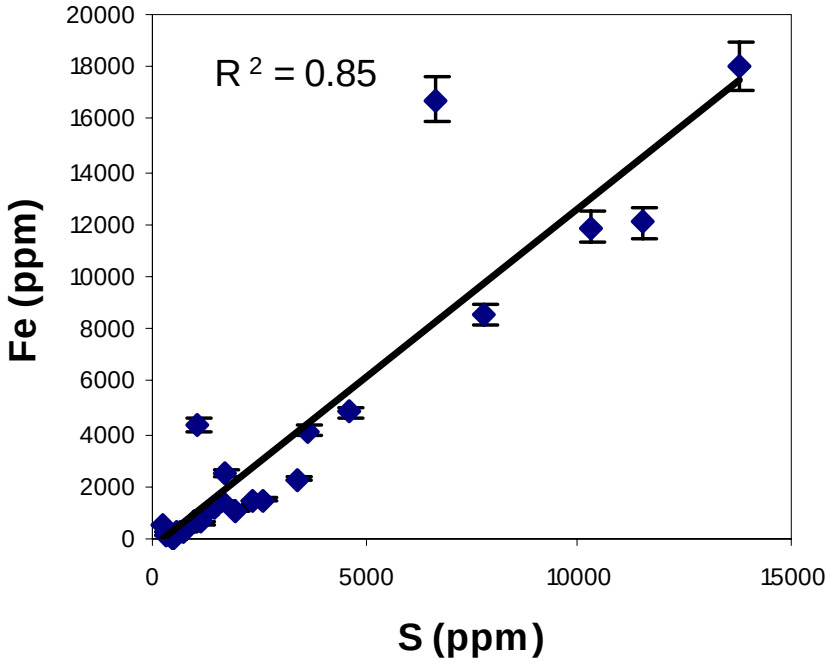

Figure 13. Correlation between Fe and S for the Nocatee Member.

Table 7. Correlation matrix for the Nocatee Member of the Arcadia Formation (27 samples); significant correlations are in bold.

	Ca	Fe	Mg	Mn	Si	S	P	Al	As
Ca	1.00	-0.44	-0.12	-0.39	-0.28	-0.38	-0.01	-0.36	-0.08
Fe		1.00	0.25	**0.77**	0.50	**0.85**	0.03	**0.81**	0.49
Mg			1.00	0.31	-0.05	0.13	0.29	0.42	0.002
Mn				1.00	0.58	0.61	0.10	0.45	0.11
Si					1.00	**0.74**	0.16	0.44	0.61
S						1.00	0.12	0.51	0.51
P							1.00	0.05	0.001
Al								1.00	0.28
As									1.00

Peace River Formation

The total arsenic concentrations of the Peace River Formation range from 0.4 ppm to 40.8 ppm (Table 2). The mean value for 54 samples is 8.8 ppm (σ is 8.6 ppm). Values for all 55 samples from the Peace River Formation are listed in Appendix D.

Arsenic concentrations of the Peace River Formations are diverse but can be explained by different lithological compositions of sediments. Approximately 70% of all samples have arsenic concentrations less that 10 ppm, and about 7% less than 1 ppm (Appendix D). Samples that represent pure carbonate matrix, sandstone with no visible trace minerals contain low arsenic concentrations. Arsenic concentrations increase with increasing abundance of pyrite, clays, hydrous ferric oxides, and phosphates.

The ICP-OES results show that the strongest linear correlation for the Peace Formation exists between Fe and S, with corresponding R^2 of 0.94 (Figure 14A), which could be due to the outlier effect (Swan and Sandilands, 1995). According to geochemical studies, the outlier (sample 12-125(2)) has anomalously high values of iron, sulfur and phosphorous compared to all Hawthorn Group sediments. Removing the outlier from the plot results in a significantly lower degree of linear correlation, $R^2 = 0.59$ (Figure 14B). This is because analyzed samples contain not only pyrite, but also composed of hydrous ferric oxides (HFO) and gypsum, as a source of iron and sulfur. The correlation matrix for all 55 samples from the Peace River Formation is shown in Table 8.

(A)

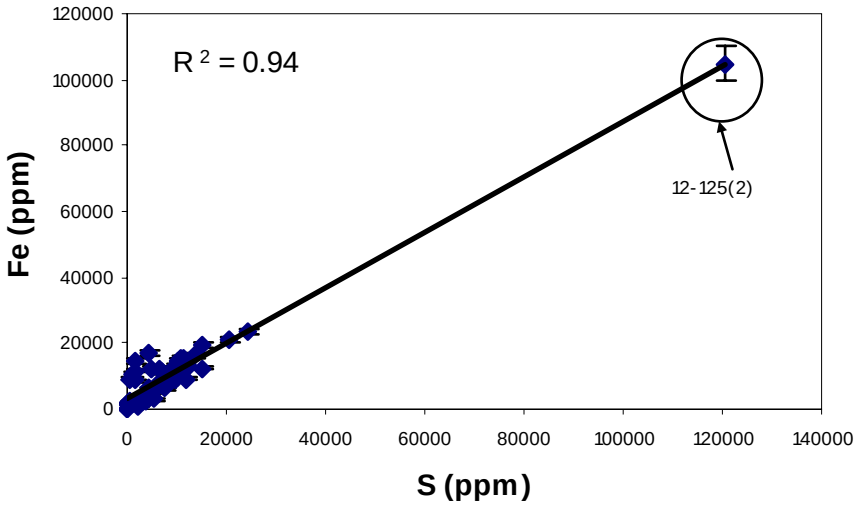

(B)

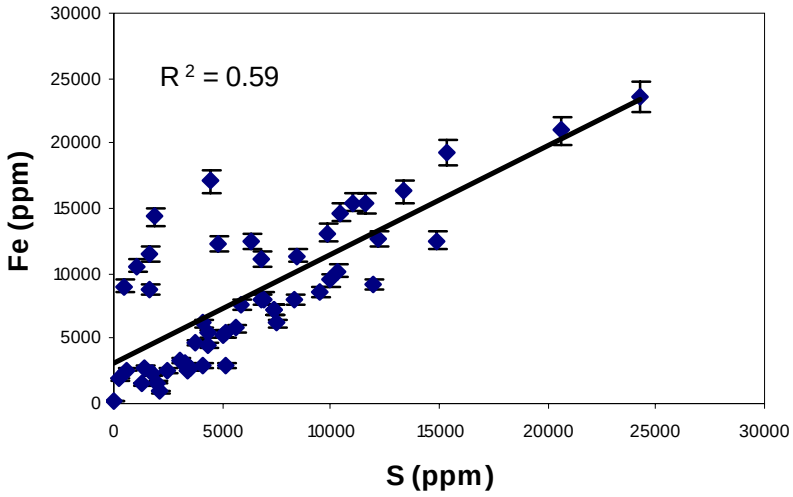

Figure 14. Diagrams showing correlation between Fe and S in the Peace River Formation for all data set (A) and with removed outlier (B); see text for additional information.

Table 8. Correlation matrix for the Peace River Formation (55 samples); significant correlations are in bold.

	Ca	Fe	Mg	Mn	Si	S	P	Al	As
Ca	1.00	-0.05	0.44	0.04	0.11	0.03	0.30	-0.39	0.06
Fe		1.00	-0.16	0.23	0.18	0.94	0.27	0.15	0.15
Mg			1.00	0.14	-0.19	-0.10	-0.26	-0.23	-0.003
Mn				1.00	-0.09	0.19	0.21	0.29	0.01
Si					1.00	0.19	0.29	-0.02	0.02
S						1.00	0.27	0.02	0.12
P							1.00	0.13	0.29
Al								1.00	0.004
As									1.00

Electron-Probe Microanalyser – Wave Dispersive Spectrometry

Hawthorn Group (All samples)

After determination of the total arsenic concentrations, 60 polished thin sections of the Hawthorn Group samples with the high bulk arsenic concentrations were selected for a more detailed chemical investigation and mineralogical association. The electron- probe microanalyses of 16 thin sections with different lithological composition revealed that substantial arsenic concentrations are present in framboidal and euhedral pyrite. The EMPA was used for spot analysis and to generate several chemical maps for examination of arsenic distribution in matrix and individual minerals.

About 126 single pyrite crystals were examined by EMPA. Arsenic concentrations in these pyrites ranged from 0 ppm to as high as 8260 ppm with mean value of 1272 ppm and standard deviation of 1379 ppm (Table 9). Values of arsenic concentrations for all 126 pyrites from the Hawthorn Group are listed in Appendix I. Prior studies of framboidal pyrite in Suwannee Limestone (Price and Pichler, 2004, in review; Price, 2002) revealed significant arsenic enrichment ranging from 100 to as high as 11,200 ppm.

The EMPA elemental mapping of clays, pyrite, dolomite, quartz and phosphorite demonstrates that high concentrations of arsenic are associated with the framboidal, euhedral pyrite and hydrous ferric oxides and shows heterogeneous distribution of arsenic within all analyzed samples.

Table 9. Electron microprobe results for arsenic in pyrites for the Formation/Member of the Hawthorn Group (in ppm).

	Maximum	Minimum	Mean	Standard Deviation	(n)
Peace River Formation	4160	0	772	1082	30
Undifferentiated Arcadia Formation	8260	0	1437	1569	48
Tampa Member	3220	0	1004	770	39
Nocatee Member	5710	560	2884	1896	9

Undifferentiated Arcadia Formation

Arsenic concentrations in pyrites from the undifferentiated Arcadia Formation range from 0 ppm to 8260 ppm (Table 9). The mean for 48 pyrites is 1437 ppm (σ is 1569 ppm). Values for all 48 pyrites from the undifferentiated Arcadia Formation are listed in Appendix I.

The elemental mapping of the internal chemical composition of the phosphate nodule (sample 5-1-235) reveals the occurrence of pyrite crystals (Figure 15) and demonstrates arsenic enrichment in pyrites to as high as 3700 ppm (0.37 weight %) compared to phosphate matrix with arsenic of 0 ppm (Table 10).

The EMPA elemental mapping of sample 4-1-501 demonstrates arsenic enrichment in both pyrites and hydrous ferric oxides (Figure 16, Table 11), and shows heterogeneous distribution of arsenic within the sample.

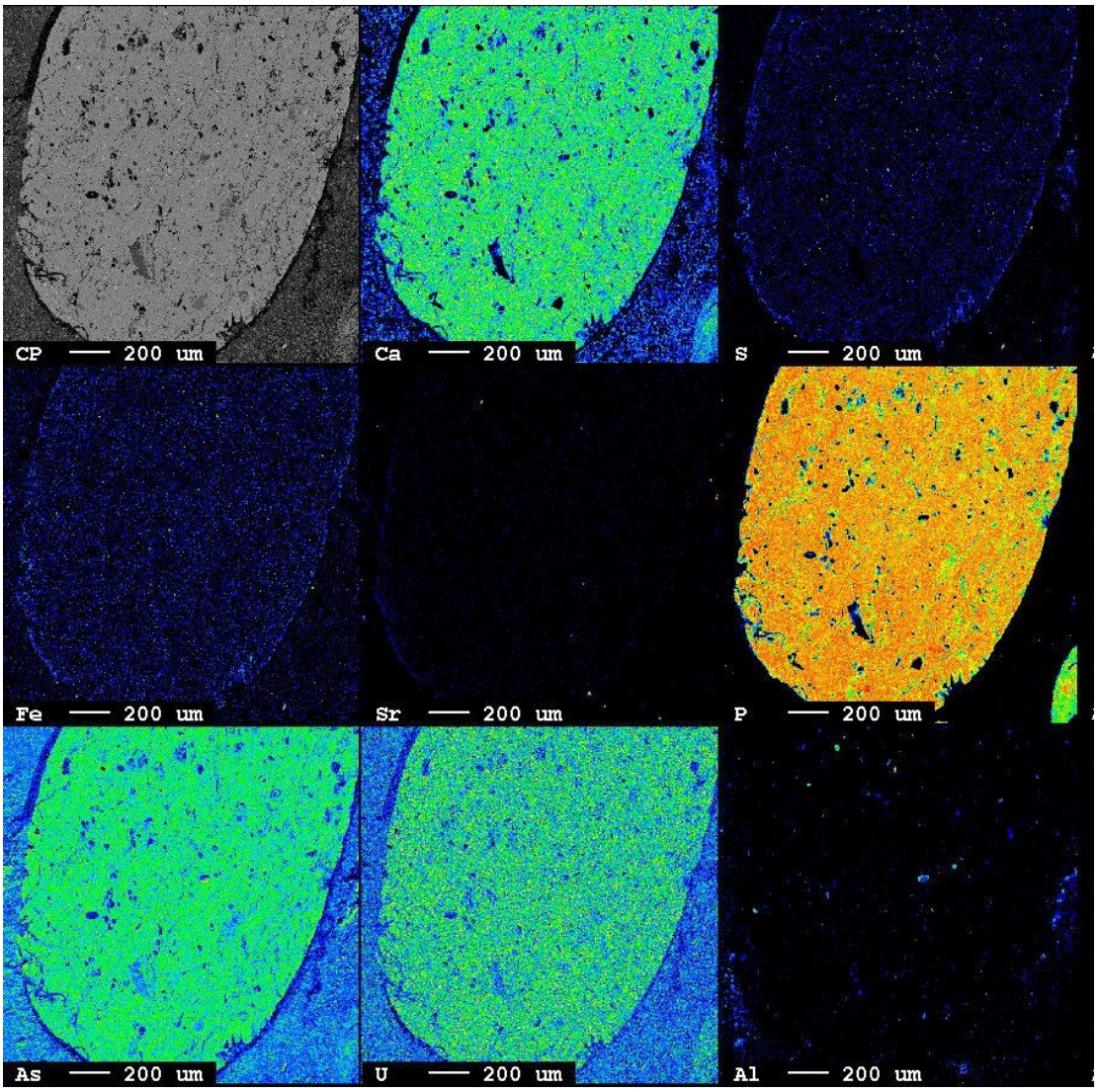

Figure15. Elemental mapping of phosphorite in sample 5-1-235 (Arcadia Formation). Background was not subtracted; relative concentrations increase with a change in color from blue to yellow to red.

Table 10. Electron microprobe results for arsenic in pyrites and phosphate matrix in sample 5-1-235 for the undifferentiated Arcadia Formation (wt. %)

Sample	S	As	Fe	P	Ca	Total
5-1-235map-1	51.21	0.03	44.57			95.80
5-1-235map-2	47.18	0.12	41.48			88.78
5-1-235map-3	45.73	0.37	41.72			87.83
5-1-235map-4	1.46	0.00	0.82	5.00	33.11	40.39
5-1-235map-5	0.65	0.00	0.45	4.73	26.96	32.79
5-1-235map-6	0.66	0.00	0.43	4.58	25.86	31.52

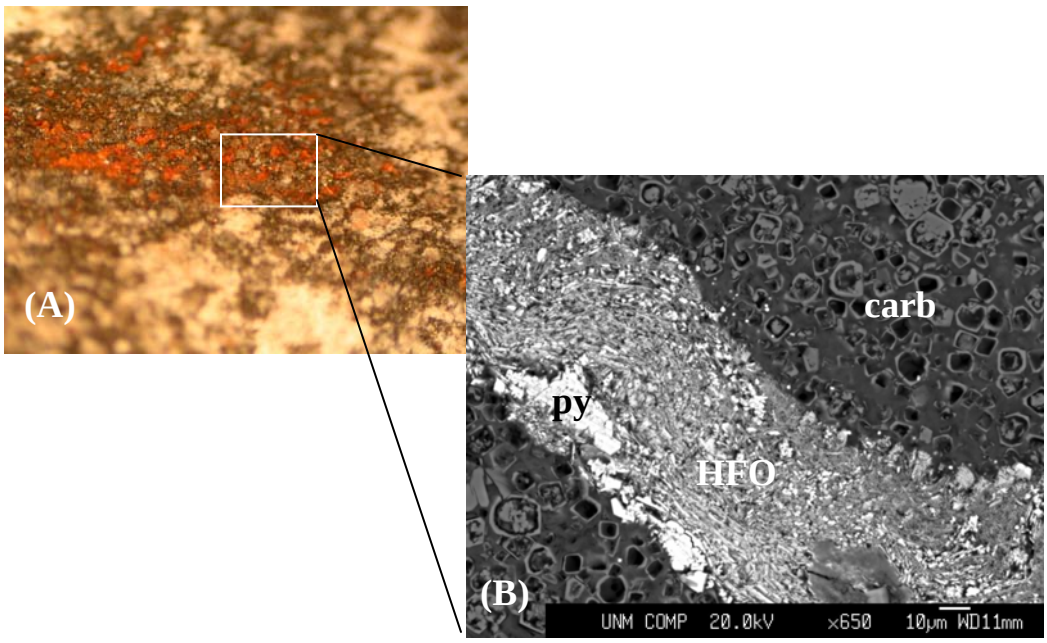

Figure 16. (A) Photograph of sample 4-1-501 (undifferentiated Arcadia Formation); (B) Backscattered image of pyrites (py), hydrous ferric oxides (HFO), and carbonate matrix (carb).

Table 11. Electron microprobe results for arsenic in pyrites and hydrous ferric oxides in sample 4-1-501 for the undifferentiated Arcadia Formation (in wt% percent)

Sample	S	As	Fe	Total
4-1-501-1	34.333	0.046	35.593	69.97
4-1-501-2	33.371	0	39.865	73.24
4-1-501-3	41.008	0	43.05	84.06
4-1-501-4	38.601	0.047	48.143	86.79
4-1-501-5	35.618	0	45.718	81.34
4-1-501-6	2.235	0.054	38.535	40.82
4-1-501-7	2.282	0.018	38.457	40.76
4-1-501-8	1.026	0.018	39.687	40.73

Tampa Member

Arsenic concentrations in pyrites from the Tampa Member range from 0 ppm to 3220 ppm (Table 9). The mean value for 39 pyrites is 1004ppm (σ is 770 ppm). Values for all 39 pyrites from the Tampa Member are listed in Appendix I.

The electron microprobe analysis of sample 22-170 for 31 pyrites evidently illustrates significantly range of arsenic from 10 ppm to as high 2,180 ppm in pyrite crystals (Appendix I). These results confirm occurrence of diverse arsenic concentrations in pyrite crystals even within one analyzed sample.

Nocatee Member

The electron microprobe analysis of sample 12-529 from the Nocatee Member for nine pyrites showed that arsenic concentrations vary from 560 ppm to as high as 5710 ppm with mean value of 2884 ppm and standard deviation of 1896 ppm (Table 9). Bulk arsenic analysis of all Hawthorn Group samples showed that sample 12-529 has the highest arsenic concentration of 69 ppm (Appendix C).

Peace River Formation

Arsenic concentrations in pyrites from the Peace River Formation range from 0 ppm to 4160 ppm (Table 9). The mean value for 30 pyrites is 772 ppm (σ is 1082 ppm). Values for all 30 pyrites from the Peace River Formation are demonstrated in Appendix I.

The elemental mapping of sample 12 – 125 clearly shows the dominated arsenic concentrations in pyrite compare to clays and phosphate (Figure 18). For the bulk-rock analysis, sample 12-125 was divided into two parts due to its heterogeneity (Figure 17). Total arsenic for sample 12-125(1) was 8.1 ppm and 26.7 ppm for 12-125(2) (Appendix D). Sample 12 – 125 (2) possibly represents a burrow fill with a significant amount of pyrite in the phosphate matrix.

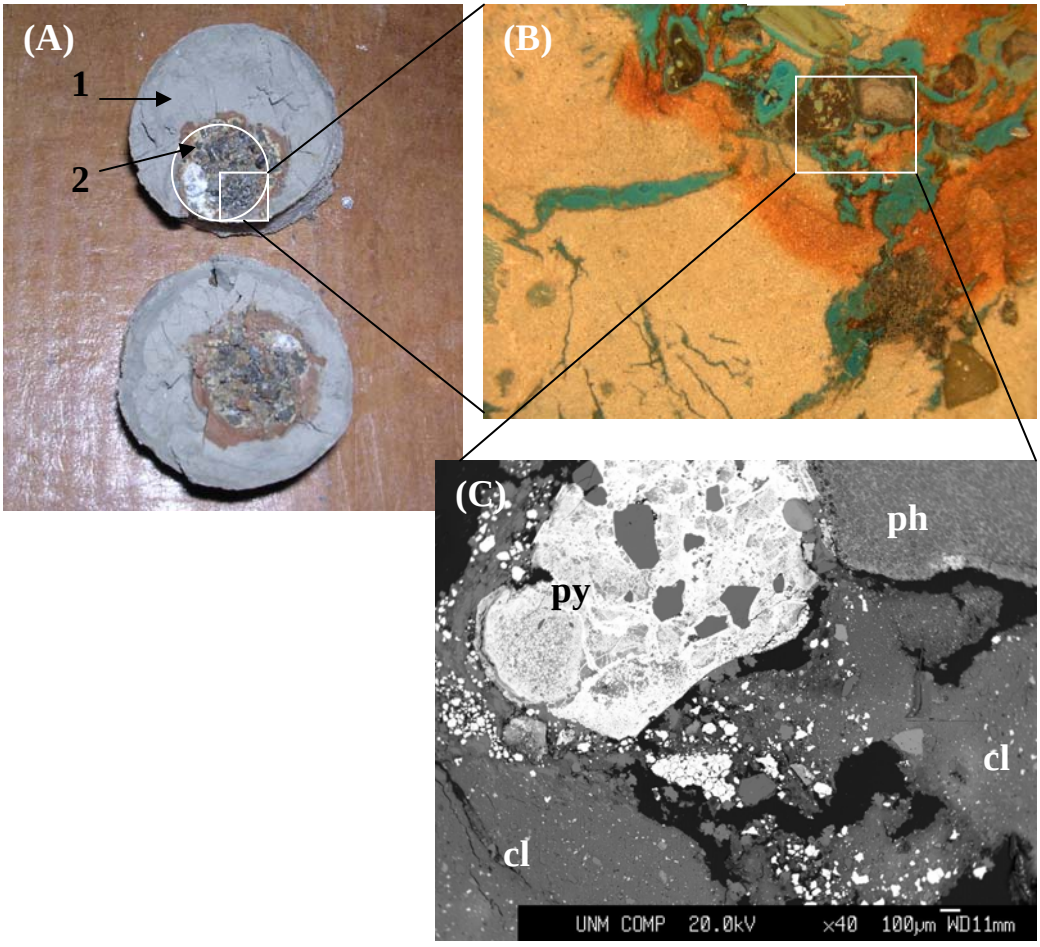

Figure 17. (A) Photograph of sample 12 – 125 (Peace River Formation) composed of clays (1 = 12 – 125(1)) and pyrite – phosphate matrix (2 = 12-125(2)); (B) Photomicrograph of contact between sample (1) and (2); (C) Backscattered image of pyrite (py), clay (cl) and phosphate (ph).

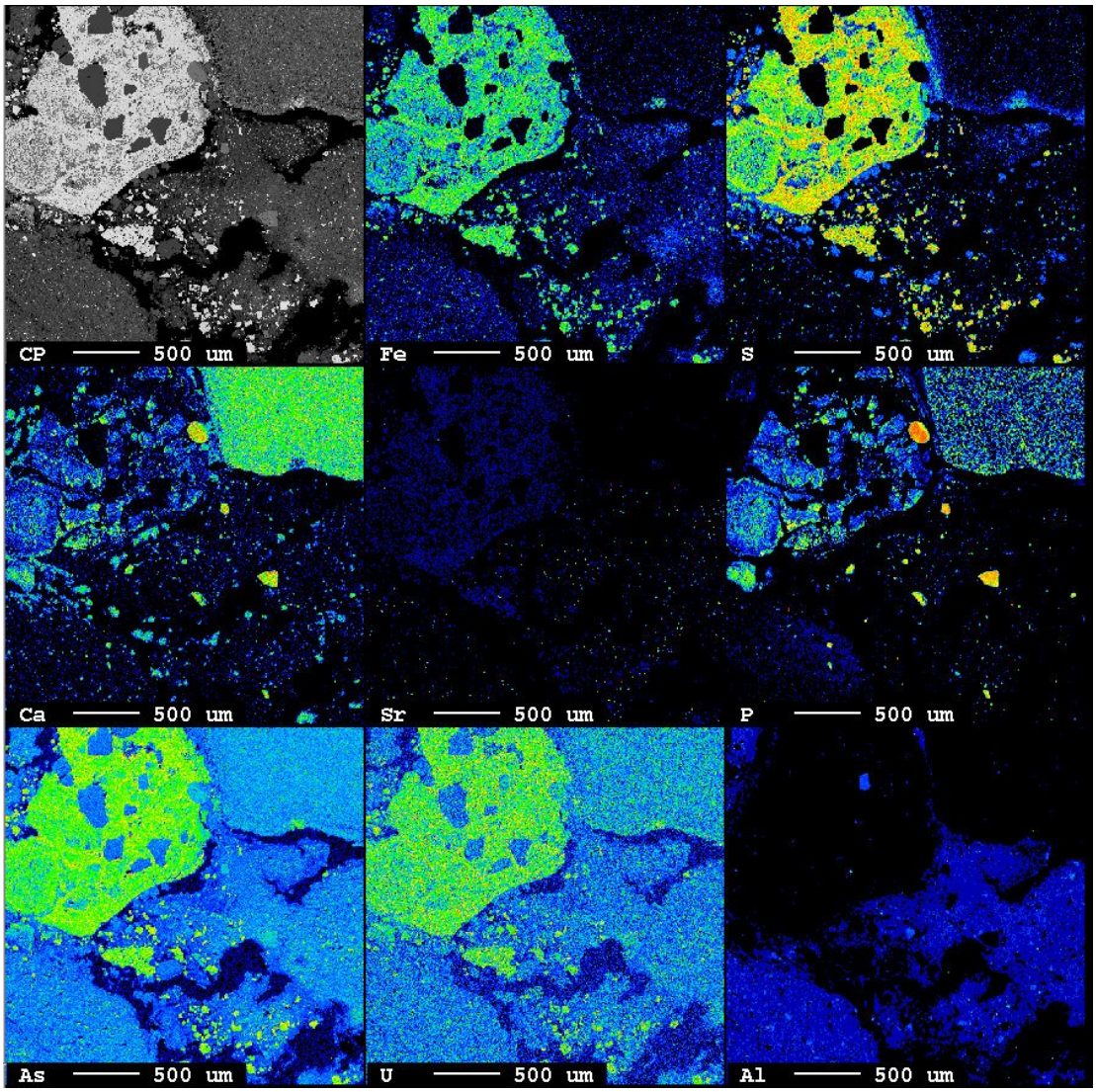

Figure 18. Elemental mapping of pyrite in sample 12 – 125 (Peace River Formation). Background subtracted; relative concentrations increase with a change in color from blue to yellow to red.

Probability Analysis

The statistical analysis indicated that arsenic (As), sulfur (S) and iron (Fe) concentrations for all Hawthorn samples follow a lognormal distribution (Figures 19-21), i.e., all points follow a straight line.

Figures 19-21 demonstrate the bell-shaped frequency histograms indicating the lognormal distribution of analyzed elements (As, S and Fe). Histograms were generated to evaluate the distribution of an element and to calculate values of a mean (μ) and standard deviation (σ). Determination of μ and σ of the normal arsenic distribution allow the application of the normal cumulative distribution function (CDF.Normal) (Figures 22, 24).

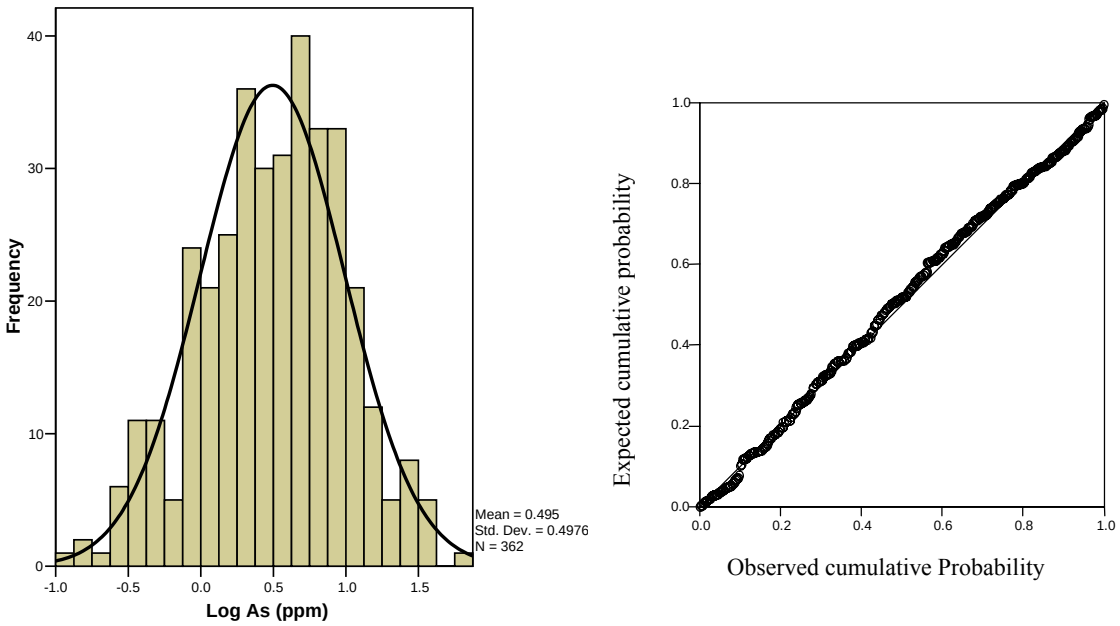

Figure 19. Frequency histogram and normal P-P plot of log-transformed arsenic concentrations from the Hawthorn Group

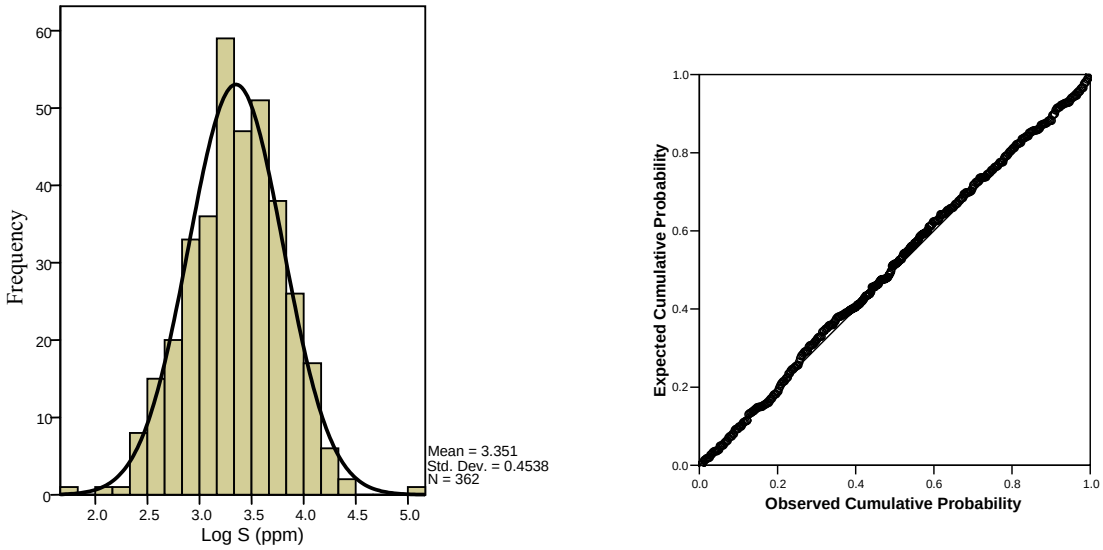

Figure 20. Frequency histogram and normal P-P plot of log-transformed sulfur concentrations from the Hawthorn Group

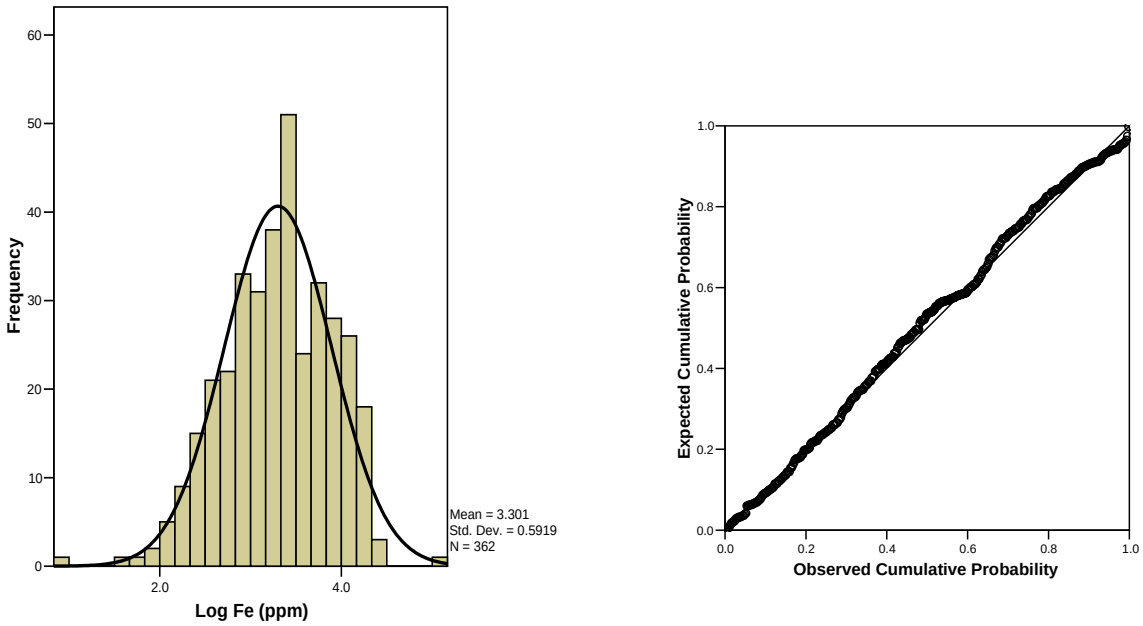

Figure 21. Frequency histogram and normal P-P plot of log-transformed iron concentrations from the Hawthorn Group

The CDF.Normal (*quant, mean, stddev*) function gives the area under a normal curve with the given mean and standard deviation for values less than *quant* (known concentration) (Landau, Everitt, 2004).

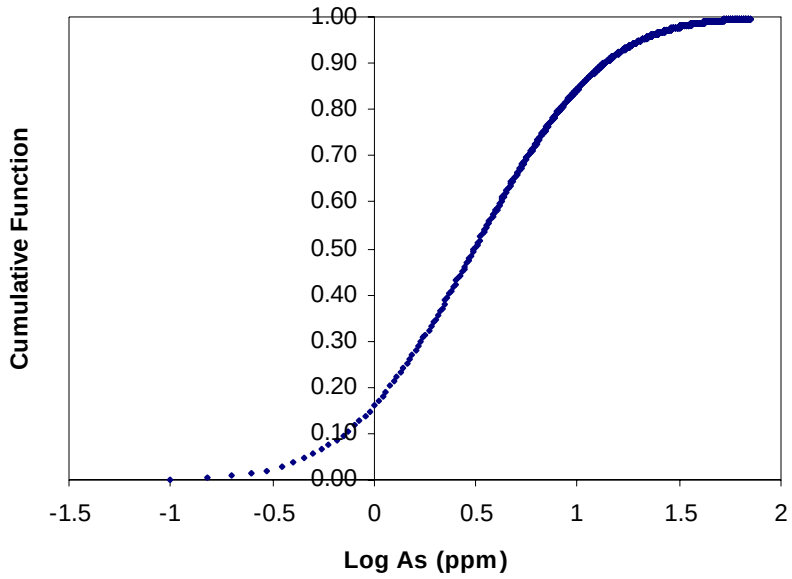

Figure 22. Cumulative distribution function of log-transformed arsenic concentrations for the all Hawthorn Group

The statistical analysis indicated that arsenic concentrations for the interval Hawthorn samples also follows a lognormal distribution (Figure 23).

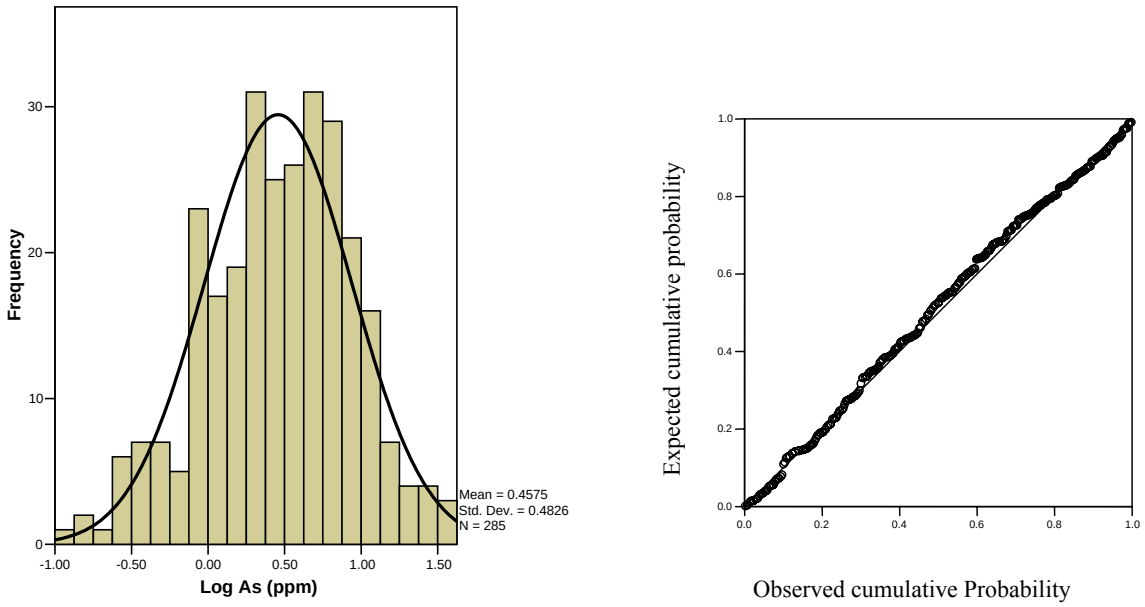

Figure 23. Frequency histogram and normal P-P plot of log-transformed arsenic concentrations from the Hawthorn Group interval samples

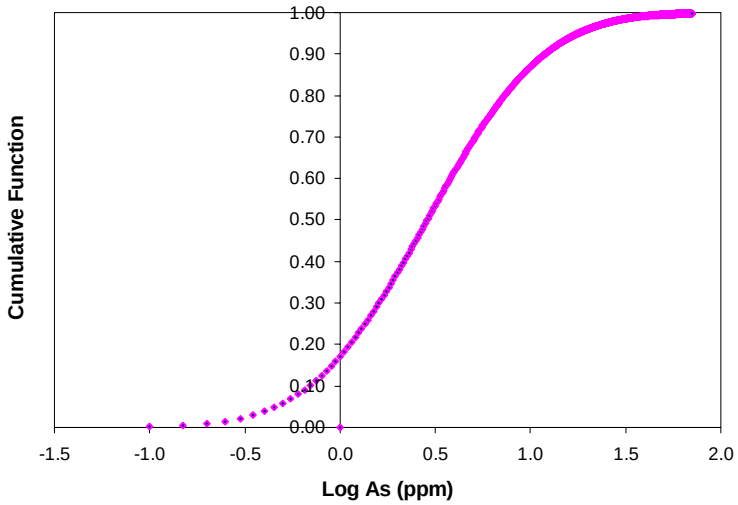

Figure 24. Cumulative distribution function of log-transformed arsenic concentrations for the interval Hawthorn samples.

In addition, survivor probability functions of log-transformed and actual arsenic concentrations were created for Arcadia Formation (Figure 25), Tampa (Figure 26) and the Nocatee (Figure 27) Members of the Arcadia Formation, and the Peace River Formation (Figure 28). The survival function is the probability that a concentration Q has a value greater than *quant*, i.e.

$S\ (quant) = P\ (Q > quant) = 1 - P(Q < quant)$ (Evans et al., 2000; Connor et. al., 2003).

Detailed examinations of the survivor functions indicate a general decrease of arsenic concentration from the Peace River Formation to the Tampa Member of the Arcadia Formation with the increasing values in the Nocatee Member of the Arcadia Formation (Table 12, Figure 29). For example, it shows that, there is a probability of 0.06 of finding a sample from the Peace River Formation with arsenic concentration greater than 30 ppm and only 0.01 for the Tampa Member of Arcadia Formation. On the other hand, probabilities of arsenic with corresponding values for the Arcadia Formation and the Nocatee Member of Arcadia Formation are approximately the same (Table 12). Generally, the distribution of arsenic concentrations depends on the presence of pyrite, clays and phosphate material, and, according to Scott (1988), the siliciclastics are dominant throughout the Peace River Formation and more prevalent within the Nocatee Member as compared to the entire Arcadia Formation.

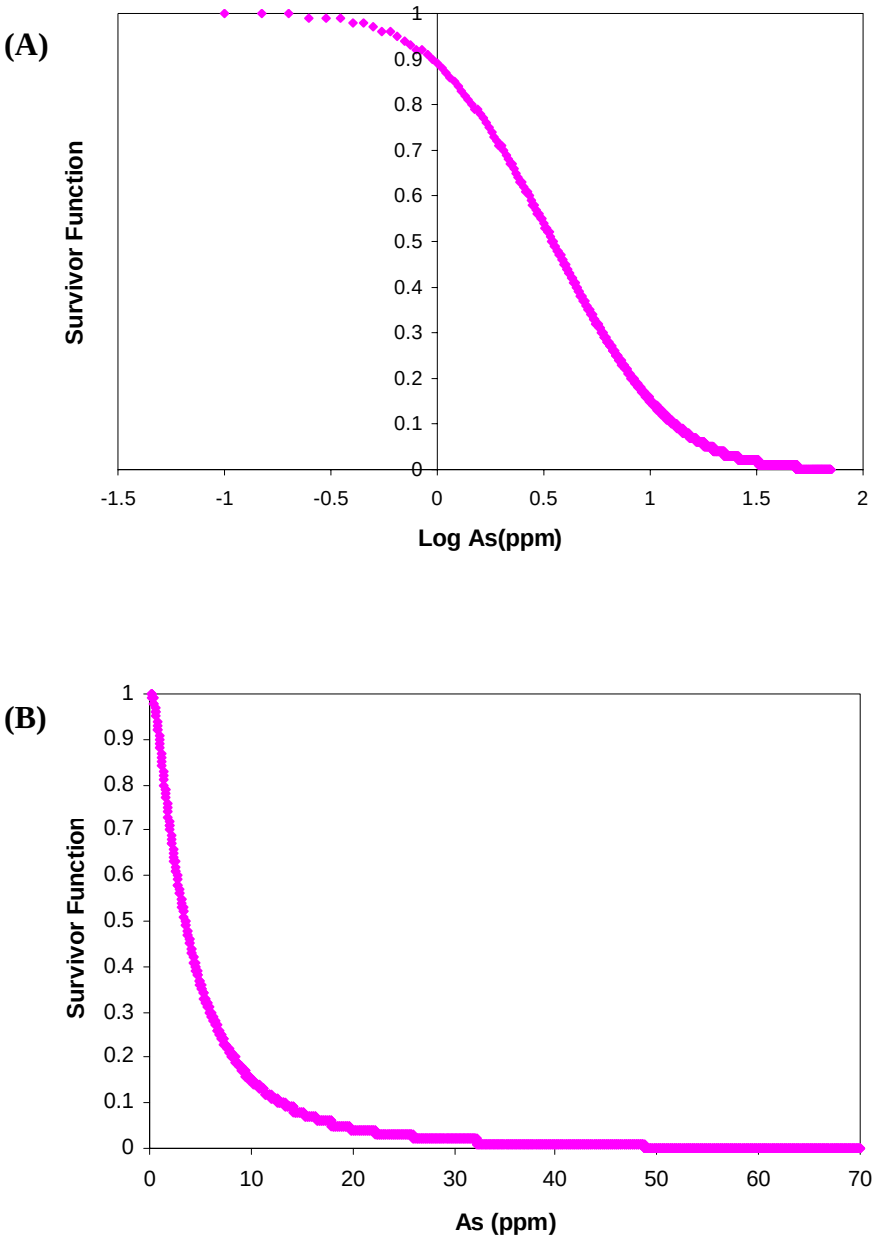

Figure 25. Survivor probability functions of log-transformed (A) and actual (B) arsenic concentrations for the Arcadia Formation.

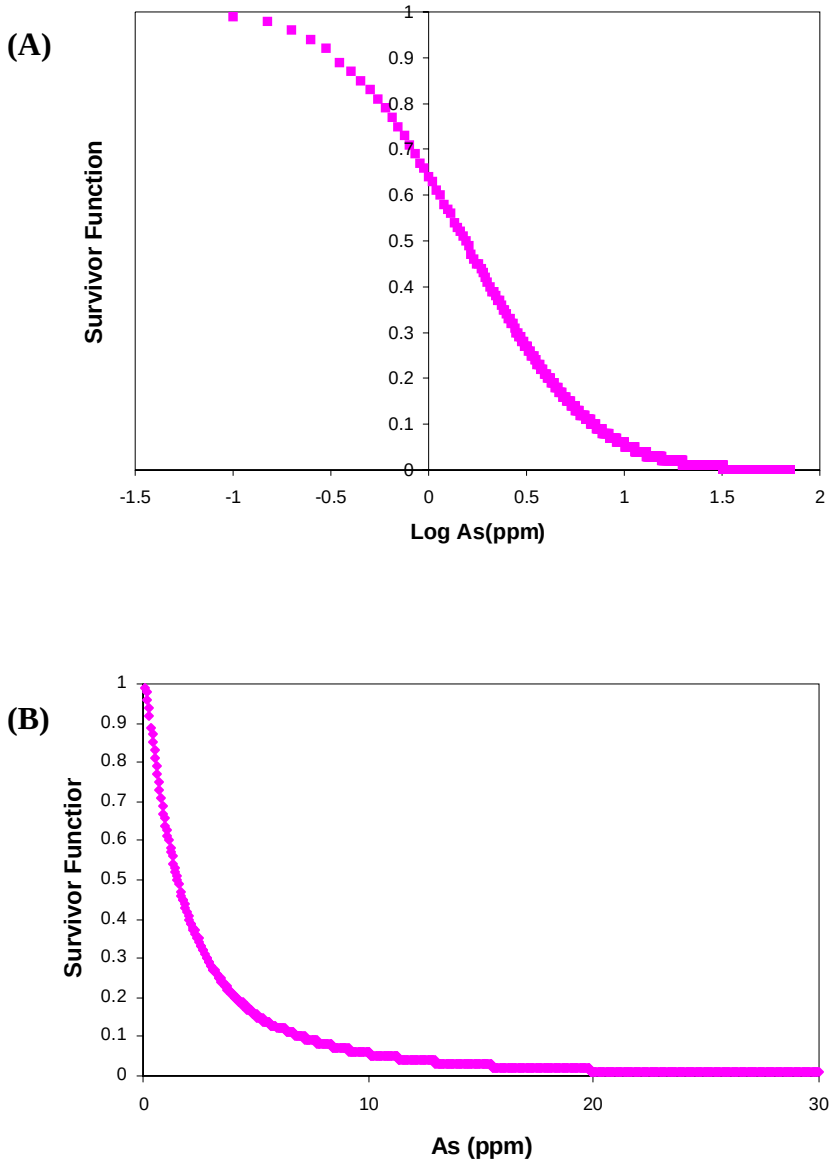

Figure 26. Survivor probability functions of log-transformed (A) and actual (B) arsenic concentrations for the Tampa Member of the Arcadia Formation.

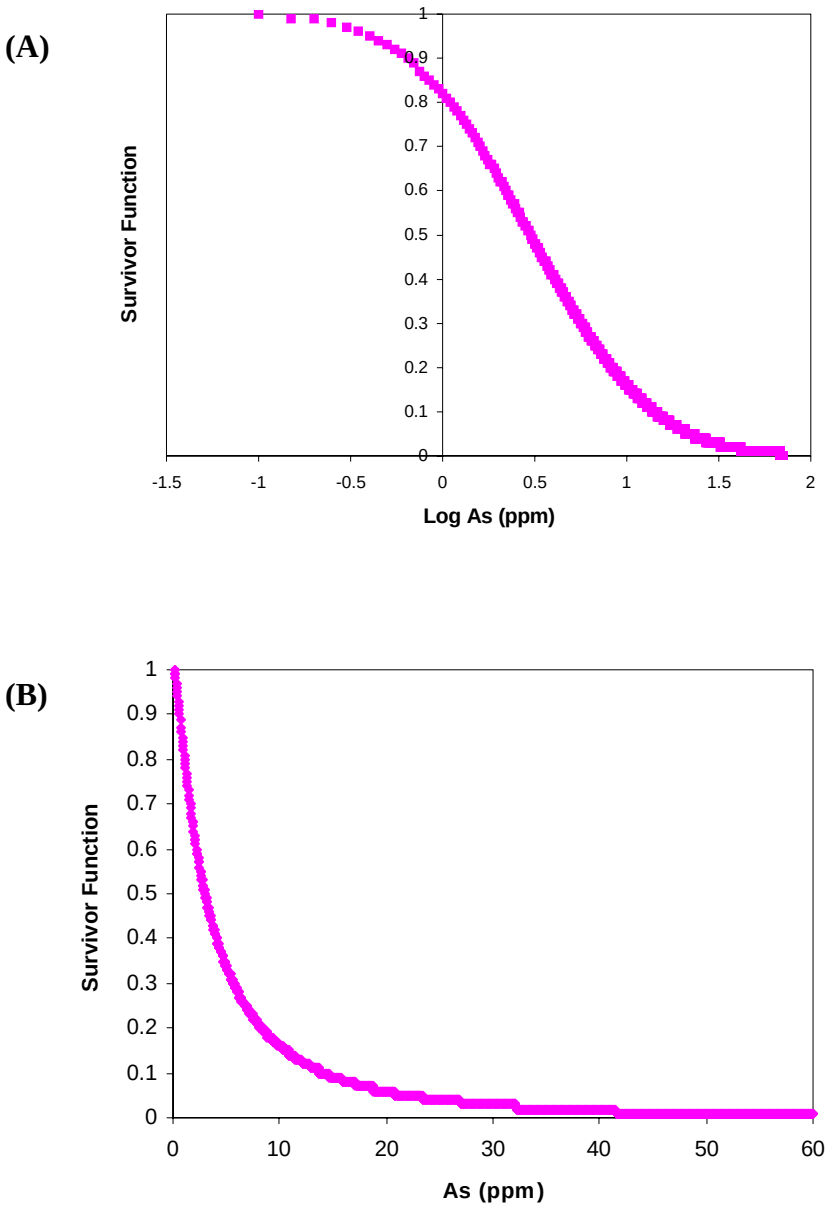

Figure 27. Survivor probability functions of log-transformed (A) and actual (B) arsenic concentrations for the Nocatee Member of the Arcadia Formation.

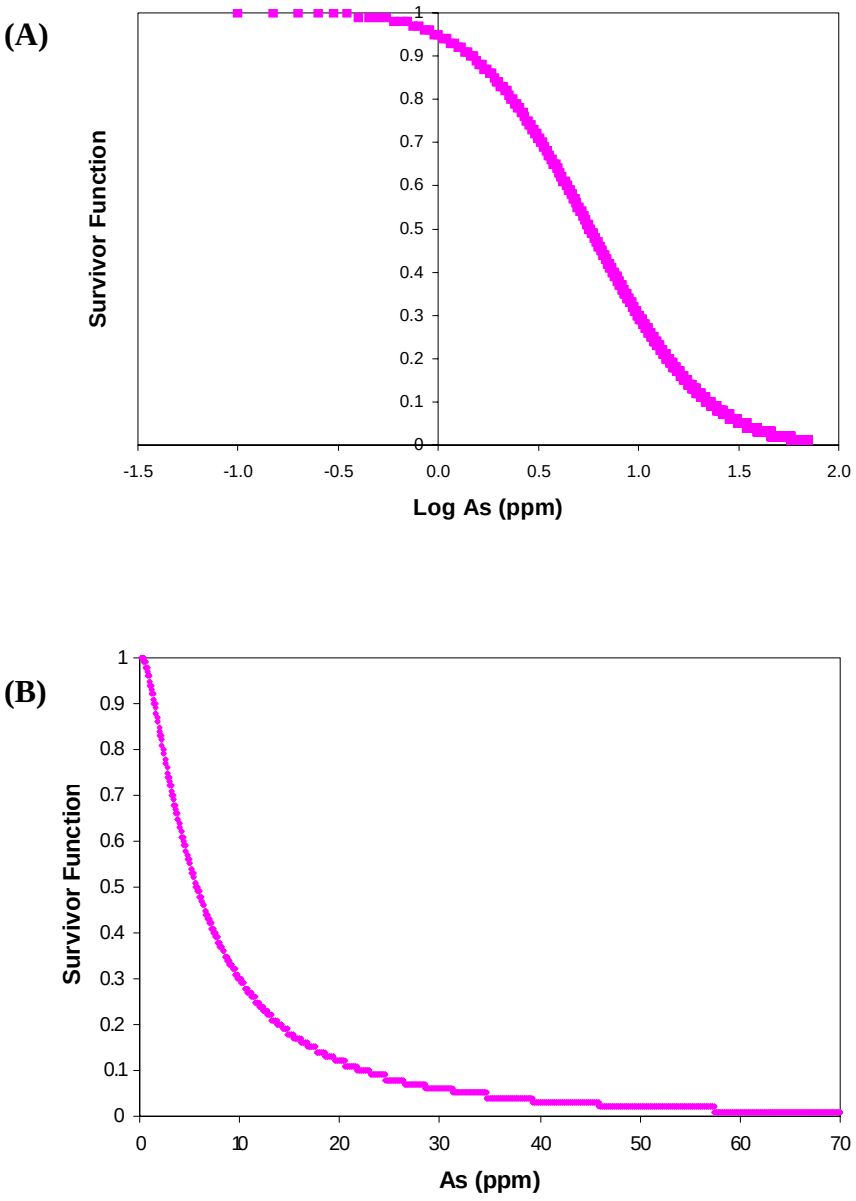

Figure 28. Survivor probability functions of log-transformed (A) and actual (B) arsenic concentrations for the Peace River Formation

Table 12. Probability of arsenic concentrations being larger than corresponding values throughout the Hawthorn Group

Hawthorn Group Unit	Probability			
Q >	*1ppm*	*5ppm*	*15ppm*	*30ppm*
Peace River Formation	0.95	0.55	0.18	0.06
Arcadia Formation	0.89	0.36	0.08	0.02
Tampa Member	0.64	0.16	0.03	0.01
Nocatee Member	0.82	0.34	0.09	0.03

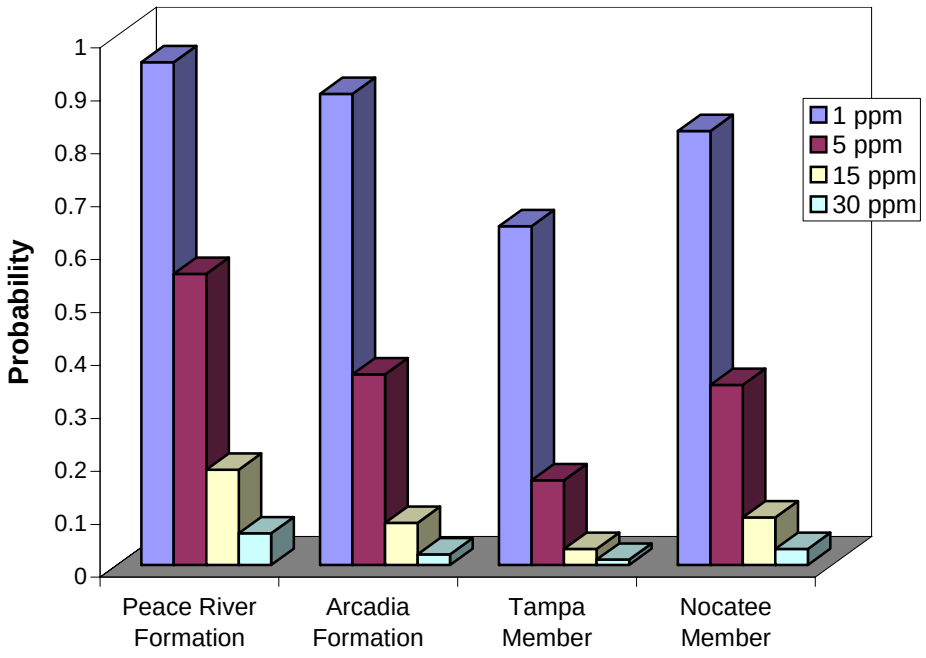

Figure 29. Diagram showing the probability of arsenic distribution throughout the Hawthorn Group

CHAPTER FIVE

DISCUSSION

Abundance of Arsenic in the Hawthorn Group

The abundance of arsenic in the upper continental crust significantly varies from 1.5 ppm (Taylor et al., 1985) to 4.8 ppm (average data from Sims et al., 1990; Gao et al. 1998). These values of arsenic concentrations depend on the lithology of individual rocks. The average for limestone geostandard GSR-6 is reported as 2.6 ppm (Baur, Onishi, 1969). The average concentrations for shale and river mud are 12.4 and 8.4 ppm respectively (Govindaraju, 1994). The average value for phosphorite is 23 ppm (Li, 2000).

The present research demonstrates that arsenic occurs throughout the whole Hawthorn Group and varies drastically from the formation to formation (Table 2).

Figure 30 shows the distribution of arsenic mean values for the each formation and member of the Hawthorn Group. It noticeably indicates the decrease of arsenic concentration with depth from the Peace River Formation to the Tampa Member of the Arcadia Formation. The same distribution patterns occur for iron (Fe), sulfur (S), aluminum (Al), and phosphorous (P) (Figure 32). According to Scott (1988), the siliciclastic component, such as clay, phosphate, and quartz sand is dominant in the Peace River Formation and its input to the Hawthorn Group decreases with depth.

Therefore, the overall decrease of the arsenic concentrations with depth correlate with a source of siliciclastic content. The Nocatee Member of the Arcadia Formation reveals much higher arsenic mean concentration which could be due to the outlier effect (Swan and Sandilands, 1995) caused by sample 12 - 529 with the highest arsenic value of the all Hawthorn Group samples (69 ppm) (Figure 30A). Elimination of the outlier results in lower arsenic mean value (4.1 ppm) for the Nocatee Member (Figure 30B). In addition, the higher contribution of siliciclastic material in the Nocatee Member (Scott, 1988) demonstrates the elevated values of Fe, S, Al and P compared to those in the Tampa Member (Figure 31).

Spatial distribution of the mean arsenic concentrations for each core was determined for the Hawthorn Group all data (Figure 32), Arcadia Formation (Figure 33), Tampa (Figure 34) and the Nocatee (Figure 35) Members of the Arcadia Formation, and the Peace River Formation (Figure 36).

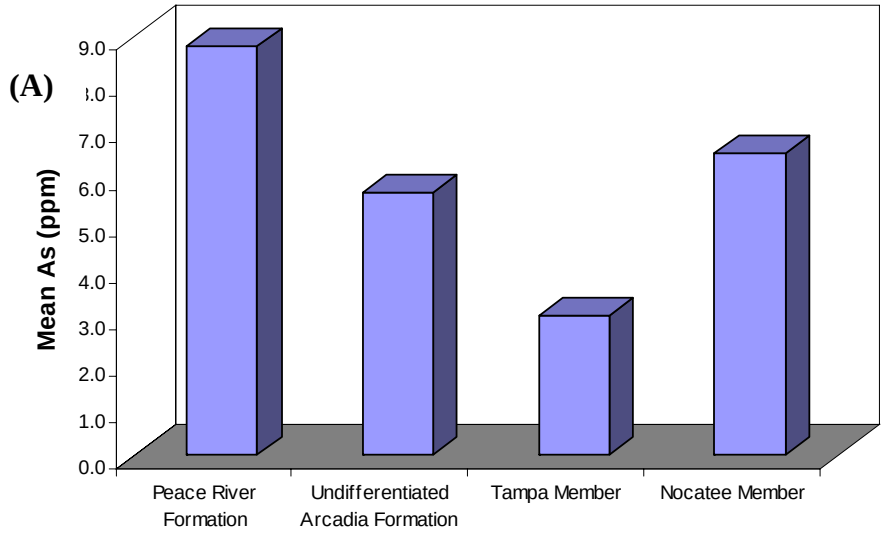

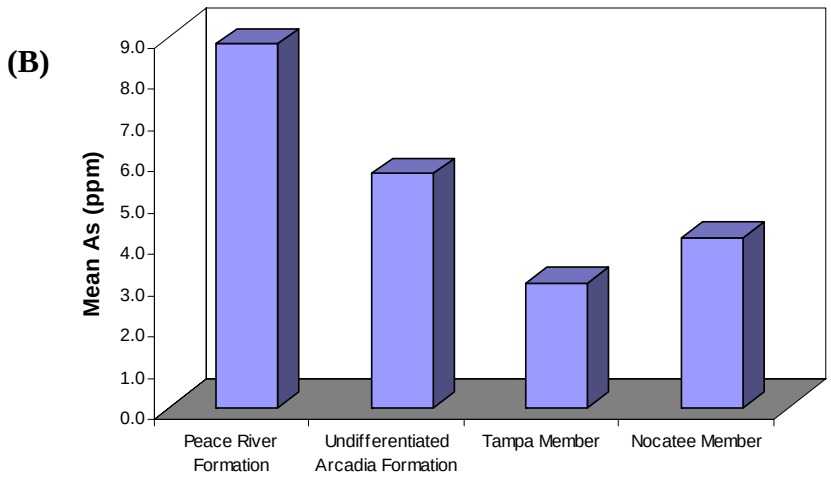

Figure 30. Distribution of the mean arsenic concentrations throughout the Hawthorn Group all data (A) and without the outlier (B); see text for additional information.

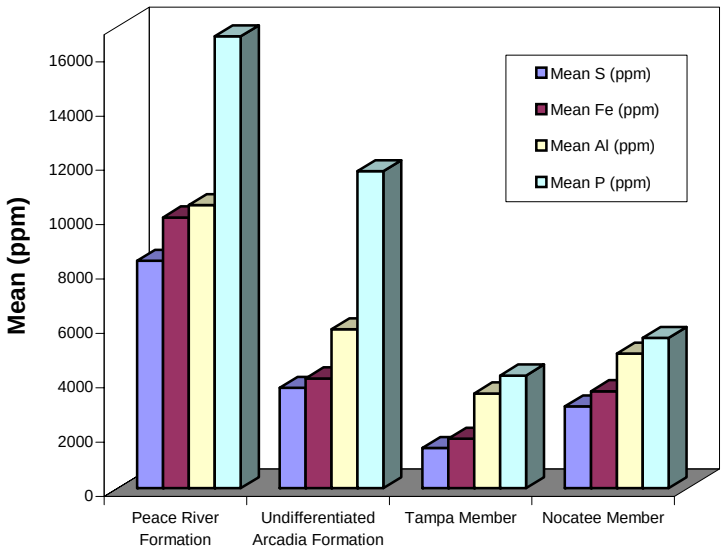

Figure 31. Distribution of the mean S, Fe, Al and P concentrations throughout the Hawthorn Group

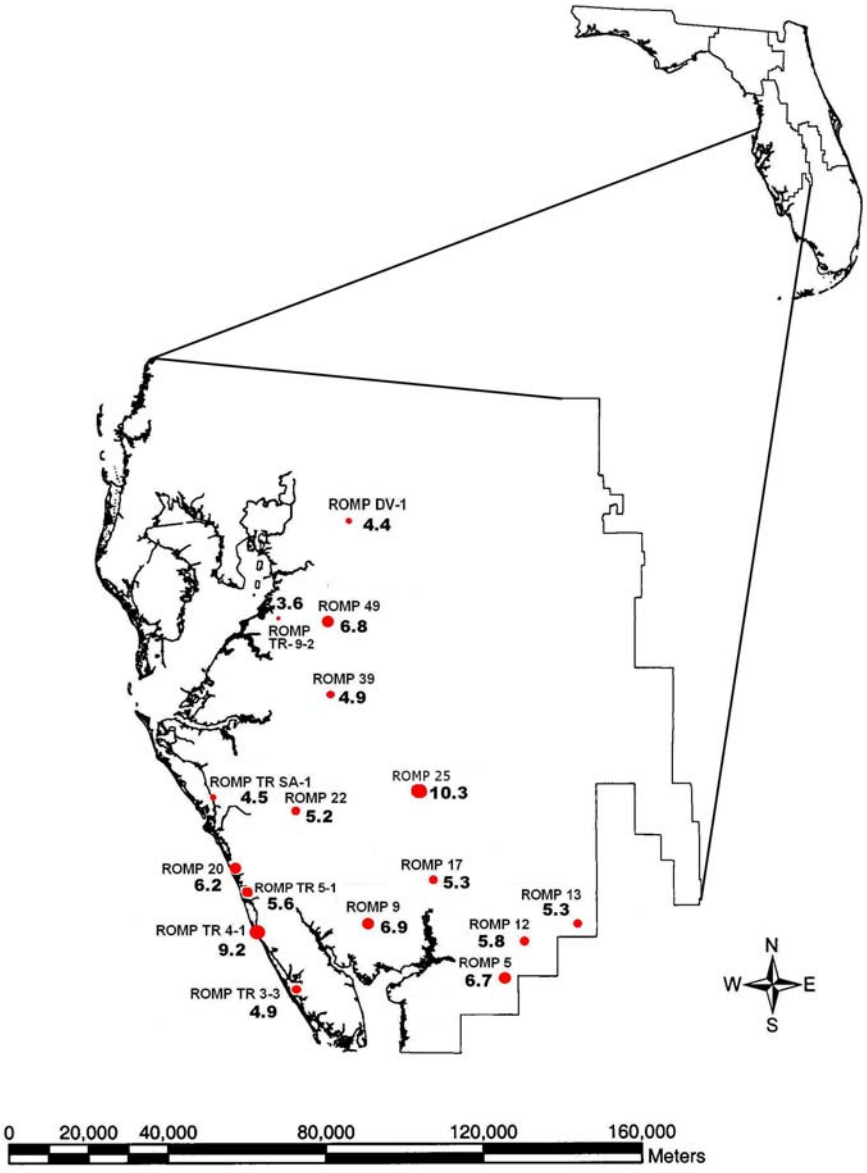

Figure 32. Spatial distribution of the mean concentrations (in ppm) in the Hawthorn Group all data; size of point indicates relative mean of arsenic concentration.

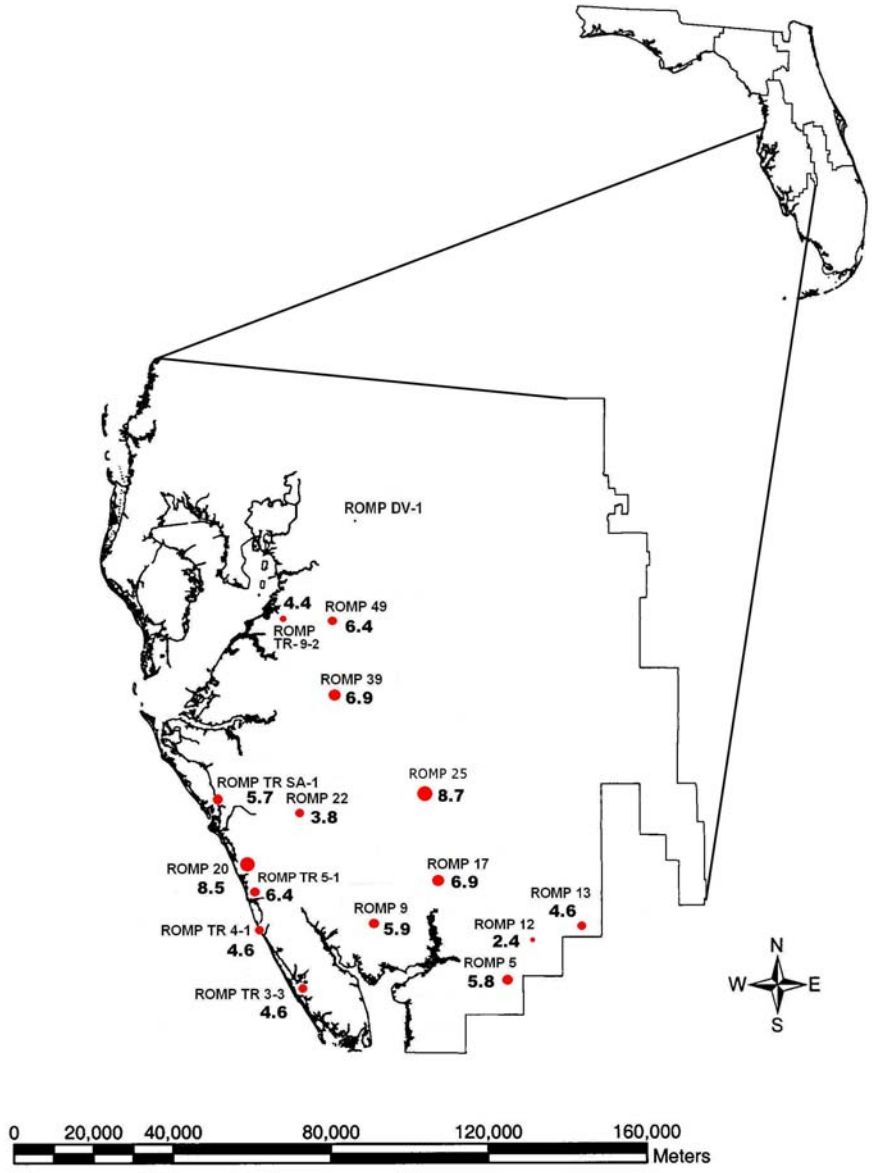

Figure 33. Spatial distribution of the mean concentrations (in ppm) in the Arcadia Formation; size of point indicates relative mean of arsenic concentration.

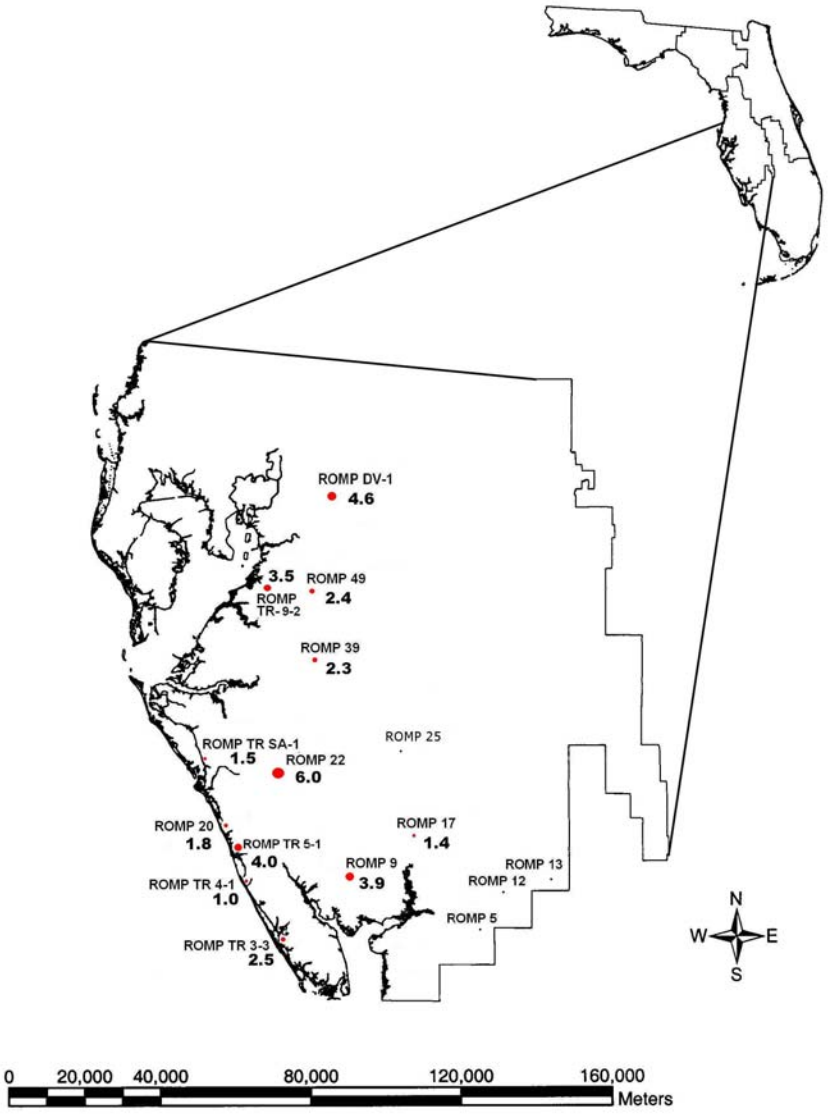

Figure 34. Spatial distribution of the mean concentrations (in ppm) in the Tampa Member of the Arcadia Formation; size of point indicates relative mean of arsenic concentration.

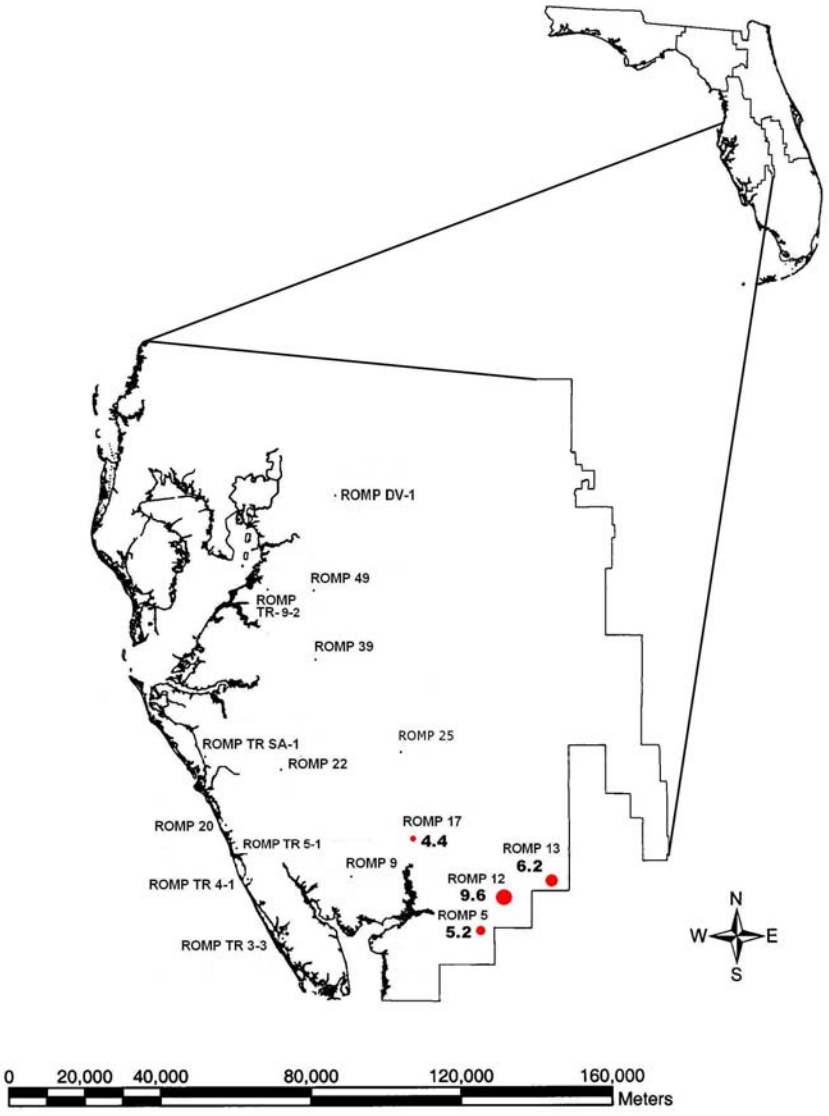

Figure 35. Spatial distribution of the mean concentrations (in ppm) in the Nocatee Member of the Arcadia Formation; size of point indicates relative mean of arsenic concentration.

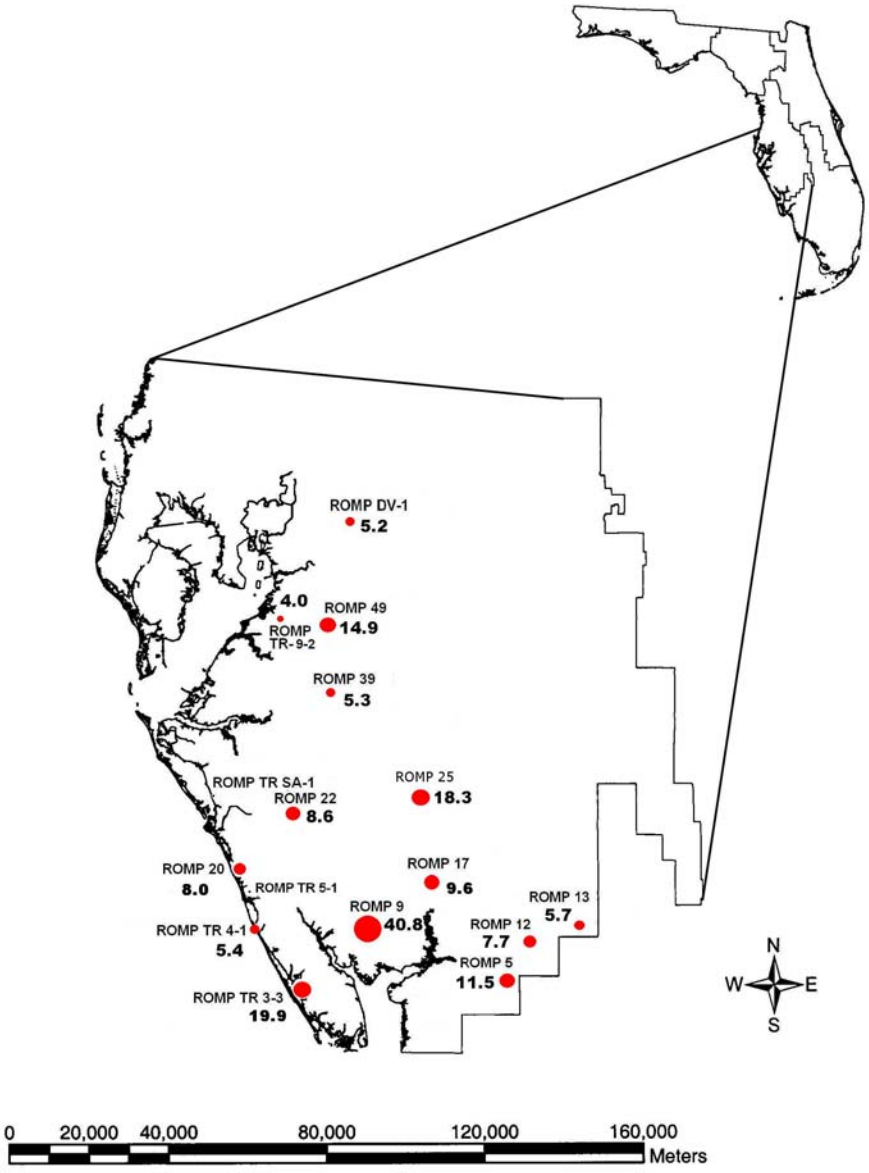

Figure 36. Spatial distribution of the mean concentrations (in ppm) in the Peace River Formation; size of point indicates relative mean of arsenic concentration.

Sources of Arsenic in the Hawthorn Group

Detailed mineralogical and geochemical study the Hawthorn Group sediments demonstrates four major possible sources of arsenic:

- Substitution at any of the fluorapatite sites in Francolite;
- Substitution in the crystal structure of sulfide minerals such as pyrite and arsenopyrite;
- Adsorption or ion exchange onto clay and organic matter;
- Adsorption or coprecipitation with hydrous ferric oxides (HFO).

The following section is a brief explanation of arsenic sources in the Hawthorn Group.

Francolite (Carbonate Fluorapatite)

The highly open crystal structure of francolite permits substitution at any of the fluorapatite sites, e.g. Na^{+}, $Mg^{2+,}$ Sr^{2+} for Ca^{2+}; OH^{-}, AsO^{3-} CrO^{2-}, VO^{3-} for PO^{3-}; and Cl^{-}, Br^{-} for F (Shields, 2002). According to Smedley and Kinniburgh (2003) calcium phosphate or apatite can contain up to 1000 mg/kg of arsenic. On the other hand, Stow (1969) did not reveal any correlation between arsenic and phosphorous in the Bone Valley Member of the Hawthorn Group. The combination of the ICP-OES and HG-AFS showed no correlation between arsenic and phosphorous. However, the

EMPA elemental mapping of the internal chemical composition of the phosphate nodule from the undifferentiated Arcadia Formation revealed the occurrence of pyrite crystals with arsenic enrichment as high as 3700 ppm (0.37 wt. %) compared to phosphate matrix with arsenic of 0 ppm (Table 10, Figure 15).

Pyrite

Detailed lithologic examinations of the Hawthorn Group sediments with stereo microscope and SEM revealed the existence of unevenly distributed pyrite occurring mostly with greenish clays, phosphate and organic material. These lithological components are deposited under the reducing environment. Examination of thin sections with the polarizing microscope demonstrated that euhedral and framboidal pyrites occur in about 90% of all samples as a minor mineral phase in the sediment matrix and as inclusions in phosphate grains and calcite crystals. Prior studies of sulfide minerals such as the abundance and occurrence of pyrite in the Suwannee Limestone (Price, Pichler, 2004, in review; Price, 2003; Price, Pichler, 2002) revealed significant enrichment of arsenic in pyrite with concentrations as high as 11,200 ppm. Thomas and Sanders (1998) reported arsenic concentrations in pyrite framboids of up to 1000 ppm as a substitute element for sulfur in the FeS_2 structure. Huerta-Diaz and Morse (1990) found arsenic concentrations in marine sedimentary pyrites of as much as 0.93 wt. %. Therefore, sedimentary pyrite can be a significant sink and source of arsenic.

The ICP-OES results revealed strong linear correlation between sulfur and iron ($R^2 = 0.87$) confirming presence of pyrite (Figure 8). Lack of significant correlation between arsenic and sulfur or iron is probably due to the contribution of other sources of arsenic.

The electron microprobe analyses of 16 thin sections with a different lithological composition revealed that substantial arsenic concentrations are present in framboidal and euhedral pyrite. Arsenic concentrations in 126 analyzed pyrites crystals range from 0 ppm to as high as 8260 ppm showing the heterogeneous distribution of arsenic within all samples (Table 9).

Clay and Organic Matter

Clays readily adsorb arsenic because of the oxide-like character of the edges of its grains (Claesson et al., 2003). Lithologic examinations of the Hawthorn Group sediments revealed the abundance of green or even brownish green clays mostly in the Peace River Formation. Generally, green clays contained unevenly distributed pyrite and phosphate. The HG-AFS analysis of clay material generally showed high arsenic concentrations (Appendix A-D).

Clays and organic substance have very small particle size, which therefore result in a large surface area per unit volume and ability to adsorb arsenic. Moreover the potential of organic material to generate complexes with heavy metals is due to the existence of oxygen-containing functional groups such as carboxyl (COOH), hydroxyl (Oh), and carbonyl (C=O) (Evangelou, 1995). Detailed lithologic

examinations of the Hawthorn Group samples revealed the abundance of organic matter mostly in the Arcadia Formation. The AFS analysis of samples with organic substance revealed arsenic concentration of about 5 ppm. At the same time, concentration of arsenic in samples containing green clays with pyrite was as high as 69 ppm (Appendix C).

Hydrous Ferric Oxides (HFO)

It has been shown that arsenic incorporates into sediments by co-precipitation as hydrous ferric oxides (HFO), or is adsorbed onto extremely high surface area of precipitated HFO (Hongshao, Stanforth, 2001; Hinkle et al., 1999; Evangelou, 1995; Bowell, 1994; Chao, Theobald, 1976). It has been reported the close connection between hydrous ferric oxides and arsenic (Pichler et al., 2000; Chao, Theobald, 1976). Stow (1969) reported that most of the arsenic in the Bone Valley Member of the Hawthorn Group is adsorbed onto HFO. Detailed lithologic examinations revealed the occurrence of hydrous ferric oxides throughout the Hawthorn Group as stains or rings around pyrites. According to Compton et al. (1993) reworking of the Hawthorn Group sediment during periods of marine regressions caused oxidation of some pyrite and formation of hydrous ferric oxides. The electron microprobe elemental mapping showed that hydrous ferric oxides from the undifferentiated Arcadia Formation contain as high as 540 ppm (0.054 weight %) of arsenic (Table 11, Figure 16).

Quantified Role of Pyrite

Based on the data presented above it appears evident that most arsenic is present in pyrite crystals. In order to quantify the responsibility of pyrite (FeS_2) to contain arsenic we can calculate its abundance in the Hawthorn Group sediments. According to the strong linear correlation between S and Fe ($R^2 = 0.87$) suppose that Fe and S in our bulk rock studies are completely derived from dissolved pyrite crystals. The calculated percent of pyrite amount was multiplied by arsenic concentration in pyrite of the each analyzed thin section and finally compared to the actual bulk concentration of arsenic obtained by AFS (Table 13).

Table 13. Measured bulk arsenic concentrations and calculated arsenic in pyrite

Sample	Hawthorn Formation/ Member	S, ppm	Fe, ppm	FeS_2, ppm	FeS_2 (%)	As, ppm (pyrite)	Number of pyrite crystals	As, ppm (pyrite) calc.	As, ppm (bulk), meas.
9-30	Peace River	4479	3905	8384	1	1337	15	11	41
13-195	Peace River	7545	6579	14124	1	688	4	10	18
12-48	Peace River	5833	5086	10919	1	15	4	0	3
20-215	Arcadia	7293	6358	13651	1	1096	10	15	36
20-143	Arcadia	7429	6477	13906	1	2570	11	36	32
49-154.5	Arcadia	10563	9210	19773	2	2620	3	52	28
5-1-235	Arcadia	7350	6408	13758	1	1468	8	20	17
25-299	Arcadia	9356	8158	17514	2	1734	5	30	28
4-1-501	Arcadia	2839	2475	5314	1	186	5	1	1
5-320	Arcadia	9595	8365	17960	2	34	5	1	24
22-170	Tampa	10190	8883	19073	2	929	31	18	14
3-3-275	Tampa	4892	4265	9157	1	2036	5	19	12
12-529	Nocatee	13805	12036	25841	3	2884	9	75	69

Figure 37A demonstrates the distribution of the calculated and measured arsenic concentrations in pyrites. For those samples that lie significantly above the equal concentration line of pyrite, calculated arsenic concentrations are lower than these measured in the bulk sample (Figure 37A). These results can be explained by existence of other sources of arsenic (clays, phosphate and organic material, hydrous ferrous oxides) or underestimation of the possible amount of pyrite, or an insufficient number of analyzed pyrite crystals. Sample 49 – 154.5 shows much higher calculated arsenic concentration compared to a measured result probably due to overestimation of pyrite constituent or a insufficient number of analyzed pyrites. Elimination of the outlier data points results in strong linear correlation, with corresponding R^2 value of 0.89 for arsenic calculated versus measured by AFS (Figure 37B).

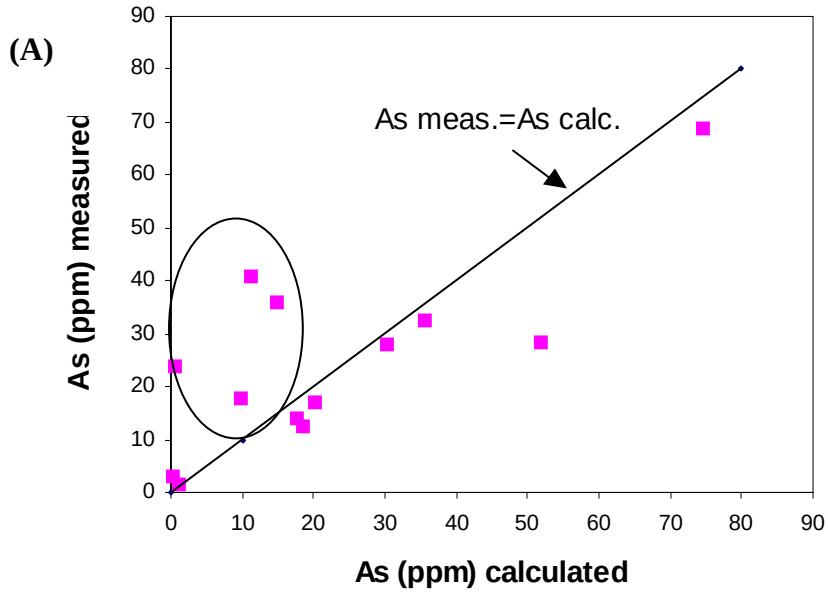

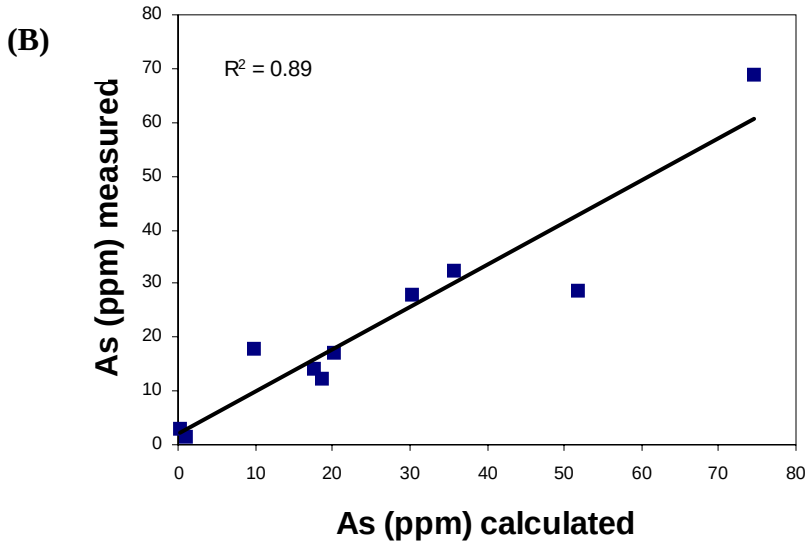

Figure 37. Diagram showing arsenic calculated vs. arsenic measured from the Hawthorn Group including all data (A) and excluding points from the circle (B); see text for additional information.

Mobilization of Arsenic during Phosphate Mining

Apatite group minerals are stable under a broad range of geologic conditions for millions of years (Nriagu, 1974; Wright 1990). The trace elemental composition of the apatite fossil teeth and bones, and analyses of the sedimentary phosphorite deposits by Wright (1990) and others (Kovach and Zartman, 1981; Shaw and Wasserburg, 1985; Keto and Jacobsen, 1987) revealed that biogenic and sedimentary apatite incorporates considerable amounts of radionuclides and metals from seawater. Different elements substitute for calcium, phosphate, and hydroxide in the apatite crystal structure (Deer et al., 1992; Skinner, 1989, 2002). Apatite locks these metals

and radionuclides in a crystal structure for billions of years with no consequent leaching, exchange, desorption, even due to diagenetic changes in water chemistry, pH, and temperatures. This is because the apatite mineral structure is very stable in a broad range of environmental conditions, such as pH 2 to 12, temperature as high as 1000 degrees C, in the presence of aqueous and non-aqueous solutions (Shields, 2002).

Central Florida has extensive phosphorite mining facilities for the Miocene Hawthorn Group sediments. The mineable phosphate sources expand through central Florida from Hillsborough and Polk Counties south throughout Hardee, Desoto, Manatee, Sarasota, and Charlotte Counties (Blakey, 1973).

The Peace River Formation of the Hawthorn Group contains substantial amounts of phosphate and is currently being exploited for phosphate ore. According to our comprehensive geochemical studies, the Peace River Formation contains the highest concentration of arsenic (μ = 9 ppm) compared to the Arcadia Formation, Tampa and Nocatee Members (Table 2). Detailed mineralogical analyses confirm the presence of ubiquitous pyrite crystals harboring considerable amounts of arsenic. In addition, EMPA elemental mapping revealed that pyrite crystals are located both inside the francolite matrix with arsenic as high as 3730 ppm (Table 10, Figure 15) and as a minor mineral phase in the sediment with varying concentrations.

Therefore, even if phosphate minerals are stable in a wide range of environmental conditions, arsenic contamination of the mineable Peace River Formation can cause several latent problems for the phosphate industry. First of all,

there have been several incidences of swine fatalities due to arsenic poisoning as a result of phosphate feed supplements (El Bahri, Romdane, 1991). In addition, oxidation of pyrite in aerobic conditions will release significant amounts of sulfate, acidity and naturally occurring arsenic (Smedley and Kinniburgh, 2003). Furthermore, these results could lead to contamination of water supplies, pollution of rivers and bays in Florida, hamper the operation of wetlands, affect wildlife and aquatic life, and cause serious health problems, such as leukemia, colon cancer and lung cancer.

Mobilization of Arsenic during Aquifer Storage and Recovery (ASR)

Recently, ASR facilities in central Florida reported that arsenic concentrations in recovered water are in excess of 100 μg/L (Arthur et al., 2001; Arthur et al., 2002). The ASR storage zone in the study area is the Suwannee Limestone, which directly underlies the Hawthorn sediments. The mobilization of arsenic from the aquifer is caused by the change in redox conditions via the pumping of oxygen-rich surface water into groundwater that is under reducing conditions (Arthur et al., 2002). The arsenic in the Suwannee Limestone probably could migrate from the Hawthorn Group deposits through the downward leaching processes (Price, Pichler, 2002).

When pyrite is exposed to atmospheric O_2 and water at the earth's surface, it reacts to form H^+, SO_4^{2-}, and Fe^{2+} (Evangelou, 1995):

$$FeS_2 + 7/2O_2 + H_2O \rightarrow Fe^{2+} + 2SO_4^{2-} + 2H^+$$

The Fe^{2+} formed can be further oxidized into Fe^{3+}, which hydrolyzes into iron hydroxide to discharge extra amounts of acid into the environment:

$Fe^{2+} + 1/4O_2 + H^+ \rightarrow Fe^{3+} + ½\ H_2O$ and

$Fe^{3+} + 3H_2O \rightarrow Fe(OH)_3 + 3H^+$ (Evangelou, 1995)

Eh-pH diagram (Figure 38) is used to show if a particular geologic site is under pyrite oxidizing conditions or pyrite stabilizing conditions (Evangelou, 1995). The diagram clearly demonstrates that $Fe(OH)_3$ is not stable under reducing subsurface environment and pyrite is not stable under oxidizing conditions resulting in release of possible arsenic.

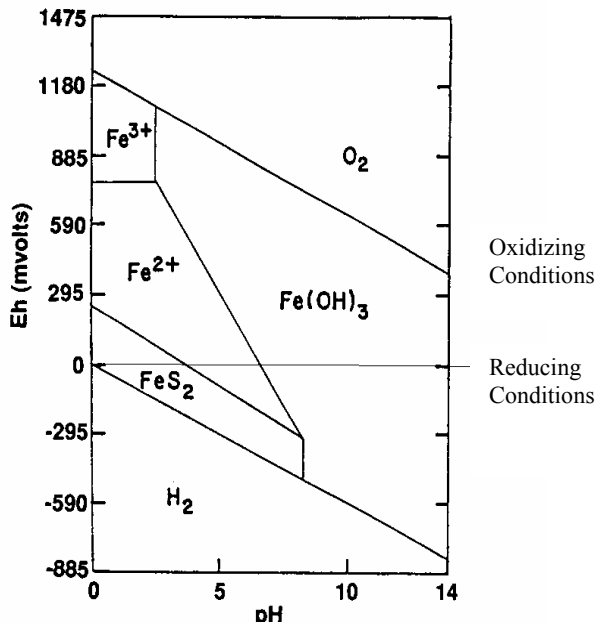

Figure 38. Stability diagram of pyrite and $Fe(OH)_3$ in water at 25ºC and 1 atmosphere total pressure (*Modified from Evangelou, 1995)*

CHAPTER SIX

CONCLUSIONS

Our detailed mineralogical and geochemical study demonstrates that:

(1) Arsenic in the Hawthorn Group varies from the formation to formation and is mostly concentrated in trace minerals, such as pyrite;

(2) Average arsenic concentrations significantly change from 9.0 ppm in the Peace River Formation to 3.0 ppm in the Tampa Member of the Arcadia Formation. As concentrations for all Hawthorn samples vary from 0.07 to 69.0 ppm;

(3) Pyrite occurs in framboidal and euhedral forms and is unevenly distributed throughout the Hawthorn Group;

(4) Concentrations of the arsenic in pyrite crystals can vary drastically from a minimum of 0 ppm to a maximum of 8260 ppm;

(5) Hydrous ferric oxides can contain arsenic as high as 540 ppm;

(6) Phosphate, organic material, and clays contain lower arsenic concentrations than in pyrite;

(7) Arsenic, sulfur and iron have lognormal distribution throughout the Hawthorn Group;

(8) Phosphorous, arsenic and sulfur are chemically closely related; they often occur together in nature, thus posing a potential problem for the phosphate industry;

(9) Aquifer storage and recovery processes could cause migration of released arsenic from the Hawthorn Group to the Suwannee Limestone through downward leaching processes, depending on chemical gradient in ground water;

(10) Further investigations should be applied to understand the ultimate source of arsenic in Florida deposits.

Information about the concentration, distribution and mineralogical association of naturally occurring arsenic in the Hawthorn Group is important, because this is a first step to forecast its behavior during anthropogenic induced physico-chemical changes in the aquifer and to understand its cycling in the Florida platform.

REFERENCES

Andrews, J.E., Brimblecombe, P., Jickells, T.D., Liss, P.S., 1996, An introduction to environmental chemistry, Blackwell Science Ltd., London, pp. 136-138.

Arthur, J.D., Dabous A.A., Cowart J.B., 2002, Mobilization of arsenic and other trace elements during aquifer storage and recovery, Southwest Florida, Open-File Report - U. S. Geological Survey, Report: OF 02-0089, pp.47-50.

Arthur, J.D., Cowart J.B., Dabous A.A., 2001, Florida aquifer storage and recovery geochemical study; year three progress report, Open File Report - Florida Geological Survey, Report: 83, 46 pp.

Arthur, J.D., Cowart J.B., Dabous A.A.,2000, Arsenic and uranium mobilization during aquifer storage and recovery in the Floridan Aquifer system, Geological Society of America, vol.32, no.7, pp.356.

Bang, B.S., 1994 - Framboidal pyrite and associated organic matrices. A risky composite for preservation of fossils. In: Kejser, U.B. (ed.), Surface Treatment: Cleaning, Stabilization and Coatings. IIC Nordic Group, Danish Section, XIII Congress, Copenhagen, pp 66-82.

Baur, W.H., Onishi, B.H., 1969, Arsenic. In: K.H. Wedepohl (Ed.), Handbook of Geochemistry. Springer Verlag, Berlin, A1-33.

Belzile, N., Tessier, A., 1990, Interactions between arsenic and iron oxyhydroxides in lacustrine sediments, Geochimica et Cosmochimica Acta, vol.54, no.1, pp.103-109.

Bhattacharya, R., Jana J., DeDalal, S.S. et. al, Groundwater arsenic contamination in the Bengal delta plain; use of geological material, laterite as the remedial option, Memoires des Sciences de la Terre, vol.40, pp.19-22, 2001.

Blakey, A.F., 1973, The Florida phosphate industry: a history of the development and use of a vital mineral, Harvard University press, Cambridge, 199 pp.

Bowell, R.J., 1994, Sorption of arsenic by iron oxides and oxyhydroxides in soils, Applied Geochemistry, vol.9, no.3, pp.279-286.

Brewster-Wingard, G.L., Scott, T.M., Edwards, L.E., Weedman, S.D., Simmons, K.R., 1997, Reinterpretation of the peninsular Florida Oligocene; an integrated stratigraphic approach, Sedimentary Geology, vol.108, no.1-4, pp.207-228.

Chao, T.T., and Theobald, P.K., 1976, The significance of secondary iron and manganese oxides in geochemical exploration, Economic Geology and the Bulletin of the Society of Economic Geologists, vol.71, no.8, pp.1560-1569.

Chow, L.C., Eanes E.D., 2001, Solubility of calcium phosphates, Monographs in oral science, vol.18, pp. 94-111.

Claesson, M., Fagerberg, J., 2003, Arsenic in groundwater of Santiago del Estero, Argentina; sources, mobilization controls and remediation with natural materials, Minor field studies, 62pp.

Compton, J.S., Mulabisana, J. and McMillan, I. 2002, Origin and age of phosphorite from the Last Glacial Maximum to Holocene transgressive succession off the Orange River, South Africa, Marine Geology 186, 243-261.

Compton, J.S., Donald, H.L., Mallinson, D.J., and Hodell, D.A., 1994. Origin of dolomite in the phosphatic Miocene Hawthorn Group of Florida, J. Sediment. Res., 64: 638–649.

Compton, J. S., D. A. Hodell, J. R. Garrido and D. J. Mallinson. 1993. Origin and age of phosphorite from the south-central Florida Platform: Relation of phosphogenesis to sea-level fluctuations and d13C excursions. Geochimica et Cosmochimica Acta 57:131-146.

Connor, C.B., Sparks R.S.J., Mason R.M., Bonadonna C., 2003, Exploring links between physical and probabilistic models of volcanic eruptions: the Soufriere Hills Volcano, Monserrat, Geophysical Research Letters vol.30, no.13, 1701.

Deer, F.R.S., Howie, R.A., Zussman, J., 1992, An introduction to the rock-forming minerals, Longman Scientific Technical, Harlow, United Kingdom (GBR).

El Bahri, L., Romdane, S.B., 1991, Arsenic poisoning in livestock, Veterinary and Human Toxicology, vol. 33, no. 3, pp. 259-264.

Evangelou, V.P. (Bill), 1995, Pyrite oxidation and its control, CRC Press, Inc., Corporate Blvd., N.W., Boca Raton, Florida.

Evans, M.; Hastings, N.; and Peacock, B. Statistical Distributions, 3rd ed. New York: Wiley, pp. 6-8, 2000.

Gao S., Luo, T.-C., Zhang B.-R., Zhang,H.-F., Han, Y.-W., Hu, Y.-K., and Zhao, Z.-D, 1998, Chemical composition of the continental crust as revealed by studies in east China. Geochimica et Cosmochimica Acta 62, 1959–1975.

Govindaraju, K., 1994, Compliation of working values and sample description for 383 geostandards. Geostandards Newletter, 18, 1-158.

Gilboy, A.E., 1985, Hydrogeology of the Southwest Florida Water Management District, regional Analysis Section Technical Report 85-01.

Green, R.C., Arthur J.D., DeWitt D., 1995, Lithostratigraphic and hydrostratigraphic cross sections through Pinellas and Hillsborough counties, Southwest Florida, Open File Report - Florida Geological Survey, Report: 61, 26 pp.

Hinkle, S.R., Polette, D.J., 1999, Arsenic of the Willamette Basin, Oregon, Geochemistry of Arsenic, report 8 (Accessed March, 2003)

Hodges, A., Mulkey, D., Philippakos, E., Economic Impact of Florida's Agricultural Chemical and Mining Industries, 2001, Department of Food and Resource Economics, Institute of Food and Agricultural Sciences, University of Florida, 4pp.

Hongshao, Z., Stanforth, R., 2001, Competitive adsorption of phosphate and arsenate on goethite, Environ. Sci. and Technol., 35, 4753-4757.

Huerta-Diaz, M.A., Morse J. W., 1990, Geochemistry of trace metals associated with sedimentary pyrite from anoxic marine sediments, Eos, Transactions, American Geophysical Union, vol.71, no.2, pp.98.

Jain, C. K. and Ali. I., 2000, Arsenic: occurrence, toxicity and speciation techniques, Water Research, 34(17), 4304-4312.

Jones, S.K. and Owen, R.S., 2001, Regional Water Supply Plan. Southwest Florida Water Management District Report, Brooksville Florida.

Kolker, A., Cannon, W. F., Westjohn, D. B., Woodruff, L. G., 1998, Arsenic-rich pyrite in the Mississippian Marshall Sandstone: Source of anomalous arsenic in southeastern Michigan ground water: Geological Society of America, Abstracts with Programs, v. 30, no. 7, p. A-59.

Kolker, A., Goldhaber, M. B., Hatch, J. R., Meeker, G. P., and Koeppen, R. P., 1999, Arsenic-rich pyrite in coals of the Warrior Field, northwestern Alabama: Mineralogical evidence for a hydrothermal origin: Geological Society of America, Abstracts with Programs, v. 31, no. 7, p. A-402.

Kazakov, A.V., 1937. The phosphate facies: origin of the phosphorite and the geologic factors of formation of the deposits. Proc. Sci. Inst. Fertilizers and Insectofungicides, 145:1-106.

Keto, L.S., Jacobsen S.B., 1987, Nd and Sr isotopic variations of early Paleozoic oceans, Earth and Planetary Science Letters, vol.84, no.1, pp.27-41.

Kovach, J., Zartman R.W., 1981, U-Th-Pb dating of conodonts, Geological Society of America Abstracts with programs 13:285.

Landau, S., Everitt, B.S., 2004, A handbook of statistical analyses using SPSS, Chapman & Hall/CRC Press, 354pp.

Lebel, J., Belzile, N., Silverberg, N., Sundby, B., 1983, Geochemistry of arsenic in coastal marine sediments, Eos, Transactions, American Geophysical Union, vol.64, no.45, pp.735.

Lepertier, C., 1969, A simplified statistical treatment of geochemical data by graphical representation, Economic Geology, vol.64, pp.538-550.

Li, Y.H., 2000, A compendium of geochemistry: from solar nebula to the human brain, 55. Princeton University Press, Princeton, 476.

Manning, J.A., Goldberg, S., 1997, Adsorption and stability of arsenic (III) at the clay mineral-water interface, Environ. Sci. Technol, vol. 31, pp. 2005-2011.

Miller, J.A., 1986, Hydrogeologic framework of the Floridan aquifer system in Florida and in parts of Georgia, South Carolina, and Alabama, U. S. Geological Survey Professional Paper, Report: P 1403-B, pp. B1-B91.

Missimer, T.M., 1997, Late Oligocene to Pliocene sea level history of the southern Florida Platform based on sequence stratigraphy, Geological Society of America, vol.29, no.3, pp.59.

Missimer, T.M., McNeill, D.F., Ginsburg, R.N., Mueller, P.A., Covington, J.M., Scot, T.M., 1994, Cenozoic record of global sea level events in the Hawthorn Group and Tamiami Formation on the Florida Platform, Geological Society of America, vol.26, no.7, pp.151.

Nickson R.T., McArthur J. M., Ravenscroft, P., Burgess W. G., Ahmed K.M., 2000, Mechanism of arsenic release to groundwater, Bangladesh and West Bengal, Applied Geochemistry, vol.15, no.4, pp.403-413.

Nriagu, 1974, Lead orthophosphates, IV. Formation and stability in the environment, Geochimica et Cosmochimica Acta 38:887-898.

Pichler, T., Arthur, J.D., Price R.E., Jones, G.W., 2004, The arsenic problem during aquifer storage and recovery (ASR), Goldschmidt Conference, Copenhagen, Denmark.

Pichler, T., Hendry, J. and Hall, G.E.M., 2001, The Mineralogy of Arsenic in Uranium Mine Tailings at the Rabbit Lake In-pit Facility, Northern Saskatchewan, Canada. Environmental Geology, v.40, 4-5, p. 495-506.

Price, R.E., Pichler T., 2004, Abundance and mineralogical association of arsenic in the Suwannee Limestone (Florida): implications for arsenic release during water-rock interaction, (in review).

Price, R., 2003, Abundance and mineralogical associations of naturally occurring arsenic in the upper Floridan Aquifer, Suwannee Limestone, University of South Florida, Tampa, Florida, 80 p.

Price, R. and Pichler, T., 2002, Naturally occurring arsenic in the Upper Floridan Aquifer, southwest Florida: Implications for aquifer storage and recovery. in Kenny, J. F. (Ed.) GroundWater/Surface Water Interactions, American Water Resources Association, Middleburg, Virginia, TPS-02-2, p. 387-392.

Pyne, R.D.G., 1994, Groundwater recharge and wells: A guide to Aquifer Storage and Recovery. CRC Press, Inc., 2000 Corporate Blvd., N.W., Boca Raton, Florida.

Riggs, S.R., 1984, Paleoceanographic model of Neogene phosphorite deposition; U.S. Atlantic continental margin, Science, vol.223, no.4632, pp.123-131.

Riggs, S.R., 1979, Phosphorite sedimentation in Florida; a model phosphogenic system, Economic Geology and the Bulletin of the Society of Economic Geologists, vol.74, no.2, pp.285-314.

Schreiber, M.E., Gotkowitz M.B., Simo J.A., Freiberg, P.G., 2003, Mechanism of arsenic release to groundwater from naturally occurring sources, eastern Wisconsin, Kluwer Academic Publishers, Boston, MA, United States.

Scott, T M., 1991, Depositional patterns of the Hawthorn Group in Florida, Geological Society of America, vol.23, no.1, pp.126.

Scott, T.M., 1990, The lithostratigraphy of the Hawthorn Group of peninsular Florida, Open File Report - Florida Geological Survey, Report: 36, 12 pp.

Scott, T.M., 1989, Florida's phosphorites; deposition to reclamation, Geological Society of America, vol.21, no.3, pp.57.

Scott, T.M., 1989, The lithostratigraphy and hydrostratigraphy of the Floridan Aquifer system in Florida, Am. Geophys. Union, Washington, DC, United States.

Scott, T.M., 1988, The lithostratigraphy of the Hawthorn Group (Miocene) of Florida: Florida Geological Survey Bulletin 59, 148 p.

Shaw, S.K., 1989, Occurrence, Geochemistry and origin of early diagenetic carbonates of the Hawthorn Group (Miocene), Marion County, Florida: University of South Florida, Tampa, Florida, 169 p.

Shaw, H.F., Wasserburg G.J., 1985, Sm-Nd in marine carbonates and phosphates: implications for Nd isotopes in seawater and crustal ages, Geochimica et Cosmochimica Acta, vol.49, no.2, pp.503-518.

Shields G., 2002, Phosphorites: a mine of information, Economic Geology Research Unit Newsletter, pp.6-7.

Shiryaev, A. N., 1996, Probability, 2nd edition New York: Springer, 621 pp.

Sims, K. W. W., Newsom, H. E., and Gladney, E. S.,1990, Chemical fractionation during formation of the Earth's core and continental crust: clues from As, Sb, W, and M., and In Origin of the Earth (eds. H. E. Newsom, J. H. Jones, and J. H. Newson). Oxford University Press, Oxford, pp. 291–317.

Skinner, H. C. W., 2002, In praise of phosphates, or why vertebrates chose apatite to mineralize their skeletal elements, International Book Series, vol.6, pp.41-49.

Skinner, H. C. W., 1989, Low temperature carbonate phosphate materials or the carbonate-apatite problem; a review, Plenum Press, New York, NY, USA.

Smedley, P. L., Kinniburgh, D.C., 2002, A review of the source, behavior and distribution of arsenic in natural waters, Applied Geochemistry, vol.17, no.5, pp.517-568.

SWFWMD, 2000, Aquifer characteristics within the Southwest Florida Water Management District, Report 99-1, 123 pp.

Stow, S.H., 1969, The occurrence of arsenic and the color-causing components in Florida land-pebble phosphate rock, Economic Geology, vol.64, pp.667-671.

Swan, A.R.H., Sandilands, M., 1995, Introduction to geological data analysis, Blackwell Science, United Kingdom, Oxford, 446pp.

Taylor, S.R. and McLennan, S.M., 1985, The Continental Crust; Composition and Evolution. Geoscience Texts. Blackwell Scientific Publications, Oxford, 312.

Thomas, R.C., Sanders, J.A., 1998, Arsenic coprecipitation in low temperature pyrites: implications for bioremediation via sulfate reducing bacteria. Geological Society of America Abstracts with Program, vol. 30, no. 7, pp. A-58.

Upchurch, S.B., 1989, Hydrology and chemistry of ground waters in the Central Florida phosphate district, Am. Geophys. Union, Washington, DC, United States.

USGS, 1999, Ground water atlas of the United States, Alabama, Florida, Georgia, South Carolina, HA 730-G, Reston, Va.: The Survey,

Welch, A. H., Westjohn D.B., Helsel, D.R., Wanty R. B., 2000,Arsenic in ground water of the United States; occurrence and geochemistry, Ground Water, vol.38, no.4, pp.589-604.

Wilkin, R.T., Barnes, H.L., 1997. Formation processes of framboidal pyrite. Geochimica and Cosmochimica Acta, 61 (2), 323-339.

Wingard, G.L., Weedman, S.D., McCartan, L., 1993, Age and diagenesis of Miocene and Oligocene strata of the intermediate and upper Floridan Aquifer systems in Southwest Florida, Geological Society of America, vol.25, no.6, pp.208.

Wright, J., 1990, Conodont apatite: structure and geochemistry, p.445-449, 28th International Geological Congress, Paleontological Society and American Geophysical Union, Washington, D.C.

APPENDICES

APPENDIX A

Detailed Lithological Descriptions of the Arcadia Formation Core Samples

Sorted by arsenic concentrations in ascending order

Sample	Lithological Composition	As (ppm)
TR-SA-1-55	dolostone;gray;quartz,phosphate	0.1
12-365	limestone;white gray;quartz,phosphate	0.2
4-1-100	dolostone;gray;phosphate,quartz,pyrite	0.3
12-660	limestone;gray;iron oxides,phosphate,pyrite	0.4
5-1-310	limestone;gray;quartz,phosphate	0.4
4-1-316	dolostone;creamy gray;quartz,phosphate	0.5
20-440	limestone;yellowish gray	0.5
20-90	dolostone;gray to light gray;pyrite	0.6
4-1-350	carbonate-quartz matrix;gray;phosphate	0.6
5-1-285	carb-quartz matrix;gray;phosphate	0.6
12-685	limestone;gray;iron oxides,phosphate,pyrite,quartz	0.8
4-1-275	limestone;white-gray;phosphate,quartz,iron oxides	0.8
4-1-375	quartz-carb.matrix;gray;phosphate,clay	0.8
5-1-110	dolostone;gray;phosphate,clay,pyrite	0.9
9-480	limestone;light to yellow-gray;iron oxides	0.9
49-225	dolostone;gray	0.9
TR-3-3-475	dolostone;light gray,quartz	0.9
TR-3-3-500	limestone;light gray	0.9
13-370	clay;white;calcite,quartz,phosphate	0.9
20-115	dolostone;light gray;iron oxides	1.0
20-465	limestone;yellowish gray	1.0
12-643	limestone;gray;iron oxides,phosphate,pyrite	1.1
12-380	dolostone;dark gray;pyrite,phosphate,iron oxides	1.1
17-120	dolostone;gray;oxidized pyrite(?)	1.1
TR-3-3-600	limestone;gray;pyrite(?),phosphate	1.1
5-170	dolostone;gray;phosphate,quartz,iron oxides	1.1
9-455	limestone;light gray	1.2
TRSA-1-255	dolostone;gray;quartz,phosphate,clay	1.2
TR-3-3-650	carbonate-quartz matrix;gray;clay, phosphate	1.2
TRSA-1-355	limestone;creamy gray;quartz,phosp.,pyrite,iron oxides	1.2
9-430	carbonate-clay matrix;light gray	1.3
12-615	limestone;gray;iron oxides,phosphate,pyrite	1.3
12-717	limestone;gray;iron oxides,phosphate,pyrite,quartz	1.3
4-1-425	carb-quartz matrix;gray;phosphate,clay	1.3
4-1-550	carbonate-clay matrix;gray;phosphate,quartz	1.3
TR-3-3-575	carbonate-clay matrix;gray;organics	1.4
4-1-501	dolostone;gray;pyrite,iron oxides,quartz,clay	1.5
5-470	limestone;gray;quartz,phosphate,pyrite	1.5
25-290	dolostone;light gray	1.5
4-1-450	limestone;gray;phosphate,quartz,clay	1.5
22-323.5-328.5	pure carbonate sand; gray	1.6
12-390	limestone;gray;phosphate,quartz	1.6
TR-3-3-544	carbonate-clay matrix;white-green;pyrite(?)	1.7
TR-3-3-611	calcilutite;gray; green clay (algae mats)	1.7
13-545	limestone;gray;quartz,phosphate,iron oxides	1.7
5-705	sandstone;gray;calcite,pyrite,phosphate	1.7

TR-3-3-175	dolostone;gray;oxidized pyrite(?)	1.8
9-380	sand;light gray	1.8
5-445	dolostone;gray;phosphate	1.8
9-405	calcilutite;gray,quartz,phosphate	1.8
5-1-360	carb.-quartz matrix;dark gray;pyrite,iron oxides,phosph.	1.9
12-315	limestone;gray;quartz,phosphate	1.9
5-145	carb.-quartz matrix;gray;phosphate,iron oxides	1.9
5-1-335	limestone;gray;quartz,pyrite,iron oxides,phosphate	1.9
12-340	limestone;gray;quartz,phosphate	1.9
12-265	limestone;gray;phosphate,clay,quartz	2.0
4-1-475	clay;gray;pyrite,phosphate,quartz,iron oxides	2.0
13-445	limestone;gray;clay,quartz,phosphate	2.0
22-348.5-353.5	carbonate sand; gray;clay	2.1
TR-3-3-678	carbonate-quartz matrix;gray	2.1
5-620	limestone;gray;quartz,phosphate,clay	2.1
25-203	dolostone;olive gray	2.1
13-395	limestone;gray;clay,quartz,phosphate	2.1
49-200	quartz-phosphate sand;light gray;oxidized pyrite(?)	2.1
9-130	dolostone;yellowish gray	2.1
13-470	quartz-carbonate matrix;gray;clay,phosphate	2.1
22-95	calcilutite; light gray	2.2
20-190	dolostone;light gray	2.2
4-1-325	limestone;gray;phosphate,quartz	2.2
13-320	limestone; gray;quartz,phosphate	2.3
39-275	dolostone; gray to yellowish gray	2.3
9-355	carbonate-clay matrix;gray,quartz	2.4
4-1-575	quartz-carb.matrix;gray;quartz,pyrite,phosphate	2.4
22-120	dolostone; gray to light gray,clay,phosphate	2.4
4-1-125	carb-quartz matrix;gray;phosphate,clay	2.4
4-1-150	dolostone;gray;phospate,quartz	2.4
5-1-210	quartz-carb.matrix;white;phosphate;clay	2.4
20-415	limestone;yellowish gray	2.5
TRSA-1-130	carbonate-quartz matrix;gray,pyrite,phosphate	2.5
4-1-75	dolostone;gray;phosphate,quartz,clay	2.7
13-220	limestone;gray;clay,phosphate,quartz,pyrite;iron oxides	2.7
20-165	dolostone;gray	2.8
TRSA-1-310	carb.-clay matrix;gray;quartz,pyrite,phosphate	2.8
TR-3-3-200	carbonate-quartz matrix;gray,phosphate	2.8
13-420	carbonate-quartz matrix;gray;clay,phosphate,pyrite	2.9
13-520	limestone;gray;clay,quartz,phosphate	3.1
4-1-200	quartz-carb.matrix;gray;phosph.,pyrite,iron oxides,clay	3.1
5-1-260	carb.-quartz matrix;green-gray;pyrite,clay,phosphate	3.1
9-95.5	carb.-clay matr.;gray;pyrite,iron ox.,phosph,org.(lignite)	3.2
12-215	limestone;gray;phosphate,pyrite,clay,quartz	3.2
4-1-175	carb-quartz matrix;gray;clay,phosphate	3.2
4-1-210	quartz-carb.matrix;green-gray;clay,phosphate,pyrite	3.2
13-345	dolostone; gray;quartz,phosphate,clay	3.2
TRSA-1-105	carbonate-quartz matrix;gray,pyrite,phosphate	3.3

12-293	limestone;white gray;quartz,phosphate,pyrite	3.3
TRSA-1-205	carbonate-clay matrix;gray,quartz,pyrite,phosphate	3.3
TRSA-1-330	quartz-carb.matrix;dark brown;pyrite,phosphate,clay	3.3
22-70	carb.-quartz matrix; light gray,phosphate,clay	3.3
25-265	limestone;yellowish gray	3.3
13-495	limestone;gray;clay,quartz,phosphate	3.4
TR-SA-1-280	sandy clay;dark gray;phosphate	3.5
4-1-485	clay;dark gray;pyrite,phosphate	3.5
5-495	carb.-quartz matrix;dark gray;pyrite,clay,phosphate	3.6
5-195	limestone;gray;phosphate,quartz,iron oxides	3.6
TR-3-3-625	carbonate-quartz matrix;gray,clay, phosphate	3.7
5-595	carb.-quartz matrix;gray;phosphate,pyrite,iron oxides	3.7
12-240	carb.-clay matrix;dark gray;phosphate,pyrite,quartz	3.7
TR-3-3-125	carb.-quartz matrix;green-gray,clay,phoshate	3.7
49-117.5	carbonate-clay matrix;light gray;phosphate	3.9
4-1-225	quartz-carb.matrix;gray;phosphate,pyrite,iron oxides	4.0
TR-3-3-644	carbonate-clay matrix;green;iron oxides	4.2
4-1-400	sandstone;dark gray;phosphate,iron oxides,clay	4.2
5-646	limestone;gray;quartz,phosphate,clay,pyrite	4.3
9-505	clay;greenish gray	4.3
5-670	limestone;gray;quartz,phosphate,clay,iron oxides	4.3
25-313	limestone;light gray;pyrite	4.3
TR-9-2-65	carbonate-quartz matrix;gray;clay	4.4
5-284	carb.-clay matrix;green gray,phoshate,pyrite,organics	4.4
TRSA-1-80	carbonate-clay matrix;gray,quartz,pyrite,phosphate	4.4
5-295	carb.-clay matrix,green gray;pyrite,quartz,phosphate	4.6
39-325	dolostone;white to light gray,phosphate	4.6
5-245	quartz-carb.matrix;dark gray;clay,phosphate	4.8
4-1-514	clay;dark gray;pyrite,iron oxides	4.8
9-155	quartz-carb.matrix; gray; phosphate,clay	4.8
TRSA-1-155	carbonate-clay matrix;dark gray,pyrite,phosphate	4.8
TRSA-1-180	carbonate-clay matrix;white-gray,pyrite,phosphate	4.9
25-165	limestone;gray;phosphate	4.9
17-195	dolostone;light greenish gray,clay	4.9
TRSA-1-230	carb.-clay matrix;green-gray,quartz,pyrite,phosphate	4.9
TR-3-3-250	carbonate-quartz matrix;gray,phosphate	4.9
5-395	quartz-carb.matrix;gray;phosphate,clay	5.0
5-270	carb-quartz matrix;gray;pyrite,phosphate	5.1
TRSA-1-305	carb.-clay matrix;green-gray,quartz,pyrite,phosphate	5.3
TR-3-3-450	dolostone;yellowish gray;pyrite(?)	5.3
TR-3-3-525	limestone;light gray;pyrite(?) on organics	5.3
5-345	carb.-quartz matrix;gray;pyrite,clay,phosphate	5.6
39-375(2)	dolostone;light gray,phosphate,clay	5.7
25-115	carb.-quartz matrix;gray;pyrite,phosphate,clay	5.9
17-148	sand;grayish green;organics	5.9
TRSA-1-29	quartz-carb.matrix;gray;pyrite,iron oxides,phosph.,clay	5.9
TR-3-3-99	quartz-carb.matrix;green-gray,clay,phosphate	6.0
39-300	quartz-carb.matrix;light gray,clay,phosphate	6.0

5-695	carb.-quartz matrix;gray;phosphate,clay,pyrite	6.1
5-370	carb.-quartz matrix;gray;pyrite,phosphate,clay	6.1
5-570	quartz-carb.matrix;gray;phosphate,clay,pyrite	6.2
39-225	dolostone; gray	6.3
4-1-525	clay;gray;pyrite;iron oxides;phosphate,quartz,calcite	6.4
39-350	carb.-clay matrix;gray,quartz,phosphate	6.7
20-240	clay;greenish gray	6.7
13-295	limestone;dark gray;quartz,phosphate,clay,pyrite	6.7
13-570	carbonte-quartz matrix;green;pyrite,iron oxides	6.9
22-145	calcilutite; light gray	6.9
25-284.5	carbonate-clay matrix;light gray	7.0
39-250	clay;gray to greenish gray	7.1
5-220	carb.-clay matrix,gray;pyrite,quartz,phosphate	7.2
17-95	limestone;light gray;quartz,clay	7.3
TR-3-3-225	dolostone;yellowish gray,phosphate	7.4
9-105	limestone;grayish olive,phosphate,clay	7.4
9-207	dolomitic sandstone; gray	7.4
4-1-599	limestone;dark gray;phosphate,iron oxides	7.5
TRSA-1-300	carb.-clay matrix;green-gray,quartz,pyrite,phosphate	7.7
49-175	quartz-carbonate matrix;light gray;pyrite,phosphate	8.0
22-73.8	quartz-carb.matrix;light gray,clay	8.0
20-140	dolostone;yellow-gray;phosphate	8.2
25-178.5	carbonate-clay matrix;gray, phosphate	8.3
17-167	carb.-clay matrix;green-gray;pyrite	8.5
TR-3-3-138	clay;green;oxidized pyrite(?)	8.8
TR-3-3-550	carbonate-clay matrix;gray;oxidized pyrite(?)	8.8
25-140	calcilutite;gray	9.2
5-1-218	clay;gray-green;pyrite,quartz	9.3
5-1-135	carb.-quartz matrix;gray;pyrite,clay,phosphate	9.4
17-145	dolostone;gray;iron oxides	9.5
13-245	carbonate-clay matrix;gray,pyrite,phosphate,quartz	9.6
TR-3-3-150	carb.-quartz matrix;gray-brown,pyrite,clay,phosphate	9.7
25-215	dolomite-clay matrix;light gray,pyrite	9.9
49-150	carbonate-clay matrix;greenish gray;organics	9.9
TR-3-3-523.5	clay-carb.matr.;gray-brown,pyrite,quartz,phosphate	10.2
4-1-250	clay;gray;pyrite,calcite,iron oxides	10.3
9-55	carb.-clay matrix;green-gray,pyrite,phosph.,quartz	10.5
39-375(1)	clay;gray;phosphate	11.1
17-170	carb.-clay matrix;green-gray,quartz,phosphate,pyrite	11.1
TR-3-3-145	clay;green;iron oxides,quartz,pyrite,phosphate	11.2
9-80	carb.-clay matrix;green-gray,pyrite,phosph.,quartz	11.4
49-115	carbonate-clay matrix;green-gray;pyrite,phosphate	11.7
5-1-160	carb.-clay matrix;gray;quartz,pyrite,iron oxides,phosph.	11.9
39-200	carb.-clay;yellow-gray,pyrite,quartz,phosphate	12.1
49-125	carbonate-clay matrix;light gray;pyrite,phosphate	12.8
12-190	carb.-clay matrix;gray;pyrite,quartz,phosphate	14.6
25-190	calcilutite;green-gray;clay,quartz,pyrite,phosphate	15.4
9-530	limestone;light gray;clay,pyrite,quartz,phosphate	16.5

TRSA-1-44.8	clay;gray;pyrite,calcite,phosphate	17.1
5-1-235	carb.-clay matrix;gray;iron oxides,quartz,pyrite,phosph.	17.2
9-180	quartz-carb.matrix;yellow-gray,pyrite,phosphate	17.9
5-1-187	clay;gray-green;pyrite,iron oxides	18.1
4-1-115	clay;dark gray;pyrite,iron oxides,gypsum,calcite,quartz	18.1
13-270	clay;dark gray,pyrite on gypsum	18.7
5-320	carb.-clay matrix;gray;pyrite,quartz,phosphate	23.7
5-420	clay;dark gray;pyrite,quartz,iron oxides,phosphate	25.9
TRSA-1-213	clay;dark gray;pyrite,gypsum,phosphate	26.2
25-299	clay;dark green-gray;quartz,calcite,pyrite,phosphate	27.9
49-154.5	carbonate-clay matrix;green-gray;pyrite,iron oxides	28.5
20-143	dolostone;yellow-gray;pyrite,phosphate	32.3
4-1-111	clay;dark gray;pyrite,gypsum	33.1
20-215	dolomite-clay matrix;light gray,pyrite	36.0

APPENDIX B

Detailed Lithological Descriptions of the Tampa Member of the Arcadia Formation

Core Samples

Sorted by arsenic concentrations in ascending order

Sample	Lithological Composition	As (ppm)
22-273.5-278.5	pure carbonate sand.;gray	0.2
20-290	limestone;light gray;pyrite(?)	0.2
39-425	sandstone;green-gray;clay	0.3
39-400	limestone; light gray	0.3
22-250	carbonate sand;yellowish gray	0.3
20-315	limestone;yellowish gray;pyrite(?)	0.3
39-450	carb.-quartz matrix; light to greenish gray	0.3
TR-3-3-400	limestone;yellow-gray;pyrite(?)	0.3
TR-3-3-404	limestone;light gray;pyrite(?)	0.4
DV-1-139.5	carbonate-quartz matrix;gray;pyrite(?)	0.4
TR-3-3-309.5	limestone;yellow-gray;pyrite(?)	0.4
9-255	limestone;light to yellow-gray;pyrite(?)	0.4
5-1-385	sandstone;gray;phosphate,clay	0.4
20-279	limestone;yellowish gray;pyrite(?)	0.4
20-265	carbonate-quartz matrix;yellowish gray	0.5
49-350	limestone;yellow-gray;pyrite(?)	0.5
TR-3-3-300	limestone;yellow-gray;pyrite(?)	0.5
39-510	limestone; white to yellowish gray	0.5
TR-9-2-140	limestone;yellowish gray	0.6
TRSA-1-380	limestone;white-gray;quartz,phosphate,iron oxides	0.6
49-375	limestone;yelllow-gray;Tampa/Suwannee contact	0.7
17-245	limestone;light gray;oxidized pyrite(?)	0.8
39-467	limestone; yellowish gray	0.8
9-230	limestone;light to yellow-gray;pyrite(?)	0.9
DV-1-125	limestone;light gray	0.9
22-300	carbonate sandstone; gray	0.9
TR-9-2-190	dolostone;brownish gray	0.9
TRSA-1-405	limestone;white-gray;quartz,phosphate,iron oxides	0.9
TRSA-1-430	limestone;white-gray;quartz,phosphate,iron oxides	0.9
4-1-300	limestone;gray;phosphate,quartz	1.0
TR-9-2-165	dolostone;dark gray	1.1
TR-3-3-325	limestone;light gray;pyrite(?)	1.1
5-1-410	carbonate-quartz matrix;gray;phosphate	1.2
DV-1-106	limestone;yellowish gray	1.3
TRSA-1-455	limestone;white-gray;quartz,phosphate,iron oxides	1.3
TR-9-2-265	limestone;light gray;iron oxides	1.4
39-500	limestone; yellowish gray	1.4
17-270	carbonate-quartz matrix;gray	1.5
TRSA-1-419	quartz-carb.matrix;green-gray;pyrite,phosphate	1.5
9-280	limestone;light to yellow-gray;pyrite(?)	1.5
49-325	limestone;yellow-gray;pyrite(?)	1.6
49-300	cuttings;carb-quartz matrix;gray;iron oxides	1.8
17-220	limestone;light gray;oxidized pyrite(?)	2.1
20-365	limestone;yellowish gray;pyrite(?)	2.2
TR-9-2-115-119	quartz-carbonate matrix; light gray	2.3
TR-3-3-375	limestone;yellow-gray;pyrite(?)	2.3

5-1-488	limestone;gray;quartz,pyrite;iron oxides	2.4
9-305	limestone;light gray;pyrite(?)	2.4
TRSA-1-480	limestone;white-gray;quartz,phosphate,iron oxides	2.4
TRSA-1-484	limestone;white-gray;quartz,phosphate,iron oxides	2.5
TR-3-3-350	limestone;yellow-gray;pyrite(?)	2.6
49-250	carbonate-quartz matrix;grayish white	2.7
9-330	limestone;light gray	2.9
22-225	calcilutite;gray to white;clay	3.0
TR-3-3-425	dolostone;yellowish gray	3.0
20-390	clay;yellowish gray	3.2
TR-9-2-90	quartz-clay matrix;gray;iron oxides,phosphate	3.8
DV-1-150	quartz-carbonate matrix;gray;clay	3.9
39-390	carbonate-clay matrix;gray;pyrite(?)	4.3
5-1-436	quartz-carb.matrix;gray;phosphate,clay	4.5
TR-9-2-101.5	sandy clay; gray;oxideized pyrite(?),phosphate	5.2
20-340	quartz-carb.matrix;yellowish gray;pyrite(?)	5.5
5-1-460	dolostone;gray;clay,quartz,pyrite,phosphate	5.6
DV-1-100	limestone;light gray;pyrite(?)	6.8
49-275-280	cuttings;carb.-quartz matrix;gray-green;clay	7.1
TR-9-2-215	carb.-clay matrix;green-yellow-gray,quartz,pyrite	8.1
TR-9-2-240	sandy clay;green-gray;phosphate,pyrite	8.3
5-1-421	clay;dark brown;pyrite,iron oxides,quartz	10.0
39-475	dolostone;dark gray;pyrite	10.4
22-195	clay; grayish green	12.3
TR-3-3-275	carb.-clay matrix;grayish brown;pyrite,quartz	12.3
22-170	carb.-clay matrix;green-gray;pyrite,phosphate	14.0
DV-1-113	limestone;light gray;pyrite,quartz	14.2
9-352.5	clay;gray;pyrite,iron oxides,feldspar,quartz	15.2

APPENDIX C

Detailed Lithological Descriptions of the Nocatee Member of the Arcadia Formation

Core Samples

Sorted by arsenic concentrations in ascending order

Sample	Lithological Composition	As (ppm)
13-704	limestone;white gray,quartz,phosphate	0.5
13-690	limestone;gray;quartz,phosphate	0.5
12-462-467	sandstone;white gray,phosphate	0.5
12-545	limestone;gray;pyrite,iron oxides,phosphate,quartz	0.8
12-590	limestone;gray;iron oxides,phosphate,quartz	0.9
12-490	limestone;gray;pyrite,quartz,phosphate,iron oxides	0.9
17-395	limestone;light gray;pyrite	1.0
17-295	limestone;light gray	1.5
12-517	limestone;gray;pyrite,iron oxides,phosphate	1.5
12-567	limestone;gray;pyrite,iron oxides,phosphate,quartz	1.6
12-454	sandstone;green-gray,phosphate,clay	1.8
12-414-419	quartz-carb.matrix;gray;phosphate,clay	1.9
17-412	limestone;light gray;pyrite	2.0
17-420	limestone;light gray;pyrite	2.6
17-370	dolostone;gray;clay	2.7
13-644	sandstone;green-gray;clay,phosphate,calcite	3.5
5-520	limestone;gray;quartz,phosphate,clay	3.8
13-627	sandy clay;brown;pyrite,phosphate	5.2
17-320	carb.-quartz matrix;yellow-gray,phosphate	6.5
5-545	limestone;gray;quartz,phosphate,clay	6.6
13-620	sandstone;gray;clay,pyrite,iron oxides,phosphate	7.1
12-440	carb.-quartz matrix;gray;pyrite,clay	8.2
17-345	quartz-carb.matrix;light gray;pyrite,phosphate	8.8
17-434	carb.-clay matrix;gray,quartz,pyrite,phosphate	9.9
13-595	clay;gray;pyrite,iron oxides,feldspar,quartz	13.1
13-630	quartz-clay matrix;brown;pyrite,gypsum	13.8
12-529	clay;dark green-gray;pyrite,iron oxides,quartz,calcite	69.0

APPENDIX D

Detailed Lithological Descriptions of the Peace River Formation Core Samples

Sorted by arsenic concentrations in ascending order

Sample	Lithological Composition	As (ppm)
13-19	sandy clay;brown gray;phosphate	0.4
39-47.5-52.5	sand;brown	0.4
13-23	clay;green-gray,iron oxides,gypsum,quartz,phosphate	0.4
13-69	quartz-carb.matrix;gray,pyrite,clay,ir.ox.,phosphate	0.9
DV-1-6	sand;dark brown	1.1
DV-1-25-26	clay;brownish gray	1.1
13-134	sandstone;gray;clay,phosphate,pyrite,iron oxides	1.1
12-90	carb.-quartz matrix;gray;pyrite,phosphate,clay	1.8
20-65	carb.-quartz matrix;grayish green,clay	1.9
12-64.5	limestone;gray;pyrite,phosphate	2.1
12-48	carb.-clay;green-gray,iron oxides,pyrite,phosphate	2.9
DV-1-48.5-51	clay;brownish gray	3.0
13-108	dolomitic sandstone;gray,pyrite,phosphate	3.2
5-110	clay;dark green-gray;pyrite,quartz,phosphate	3.2
13-120	quartz-carb.matrix;gray;clay,phosphate,pyrite	3.3
5-95	clay;green-gray;pyrite,quartz,phosphate	3.8
12-115	carb.-clay matrix;green-gray;pyrite,phosphate,quartz	3.9
TR-9-2-40	clay;grayish green	4.0
39-125	carbonate matrix;gray,clay,quartz	4.3
25-45-47	sand;gray;clay, phosphate	4.5
22-29	sandy clay; grayish dark green	5.3
39-155	clay-carb.matrix;gray, phosp.,quartz	5.3
4-1-50	sandstone;dark brown;phosphate,iron oxides,clay	5.4
5-85	sandy clay;green-gray,pyrite,phosphate	5.4
12-41	clay;green-gray;phosphate,iron oxides,pyrite	5.6
39-173-178	sandstone;light bluish gray,clay, phosphate	5.9
39-100	clay;greenish gray	6.1
39-150	clay;dark gray	6.1
12-165	clay;dark gray;phosphate,quartz,calcite,pyrite	6.2
39-130	clay;greenish gray;iron oxides	6.5
12-125(1)	clay;gray-green;pyrite,iron oxides	7.7
12-125(1)dup.	clay;gray-green;pyrite,iron oxides	8.1
39-72.5-77.5	sand;gray; iron oxides,phosphate	8.1
13-45	carb.-clay matrix;green-gray;quartz,pyrite,phosphate	8.2
13-95	carb.-quartz matrix;gray,pyrite,clay,iron oxides	8.4
13-170	clay;dark gray;pyrite,quartz,calcite,phosphate	8.7
22-45	clay; grayish green	9.3
17-70	clay;greenish gray;iron oxides	9.4
17-50-56	cuttings;limestone;yellowish gray,phosphate	9.7
20-48.5	sandy clay;green.gray;iron oxides,pyrite,calc,phosp.	9.8
13-145	quartz-carb.matrix;gray,pyrite,clay,iron oxides	10.2
22-20	carb.-clay matrix;grayish green;pyrite,phosp.,quartz	11.2
DV-1-74.5-77	carb.-clay matrix;gray;iron oxides,pyrite,phosphate	11.4
12-140	carb.-clay matrix;dark gray;quartz,pyrite,phosphate	11.8
20-38.5	carb.-quartz matrix;yellowish gray,clay,phoshate	12.2

25-90	calcilutite;gray,clay,quartz,phosphate,pyrite	13.1
TR-3-3-81.5-86.5	cuttings;quartz-carb.matrix;greenish gray,clay,phosp.	13.9
49-77.3-82.3	phosphate-quartz sand;brown-gray,clay,pyrite,iron ox.	14.9
13-195	carbonate-clay matrix;gray;pyrite	17.7
5-69-74	phosphate-clay matrix;quartz,pyrite,iron oxides	20.0
5-120	carb.-clay matrix;dark gray;pyrite,quartz,ir.ox.,phosp.	25.1
TR-3-3-56.5-61	cuttings;phosphate-quartz sand;gray	25.8
12-125(2)	phosphate matrix;calcite,pyrite,iron oxides,gypsum	26.7
25-65-70	cuttings;carbonate -clay matrix;gray,quartz	37.2
9-30	clay;dark greenish gray,pyrite,phosphate	40.8

APPENDIX E

Inductively Coupled Plasma – Optical Emission Spectrometry (ICP-OES)

Results for the Arcadia Formation

Samples sorted by well

Sample	Ca (ppm)	Fe (ppm)	Mg (ppm)	Mn (ppm)	Si (ppm)	S (ppm)	P (ppm)	Al (ppm)	As (ppm)
39-200	257426	9653	73020	456.1	873	9481	52030	12129	12.1
39-225	327946	6204	150678	460.9	1174	5378	34620	7091	6.3
39-250	94756	16924	57569	317.0	1994	9064	21552	25805	7.1
39-275	227056	1782	120381	97.1	981	1481	10488	1990	2.3
39-300	202281	1921	108043	87.0	678	2306	17783	2797	6.0
39-325	240718	1980	123144	101.5	781	2494	22932	3775	4.6
39-350	126856	4239	39542	27.2	499	3474	28271	8354	6.7
39-375(1)	102041	12245	56391	43.5	877	5927	26992	21375	11.1
39-375(2)	246906	2401	125000	50.1	1378	3325	16992	2104	5.7
22-70	261185	2503	121524	35.1	500	3361	10074	1542	3.3
22-73.8	213535	3114	122865	32.9	479	3805	10202	4494	8.0
22-95	202881	2287	129052	61.8	373	1217	4063	3944	2.2
22-120	270696	1386	154402	49.9	302	1282	7360	1419	2.4
22-145	206771	3634	120314	42.9	291	2665	8593	5750	6.9
22-323.5-328.5	185340	3731	2312	27.4	132	465	3412	989	1.6
22-348.5-353.5	256785	4452	6367	32.4	367	720	4527	2234	2.1
9-55	183496	6189	39794	255.7	385	5877	40463	9229	10.5
9-80	228013	3675	116178	101.5	158	4046	9809	5863	11.4
9-95.5	229099	1553	103692	31.5	369	3051	13215	2894	3.2
9-105	265472	1819	83605	46.1	1615	4716	38760	3073	7.4
9-130	253529	1412	141694	51.6	149	1576	3072	2530	2.1
9-155	146037	1971	58632	30.9	401	2275	20232	4066	4.8
9-180	173673	4032	63053	32.6	823	5752	34243	6527	17.9
9-207	255139	3936	132406	39.9	217	2873	5296	4976	7.4
9-355	199642	2330	58164	62.0	298	3217	12428	3129	2.4
9-380	261621	2557	6734	31.6	439	3475	16882	2723	1.8
9-405	195795	3305	13403	32.9	370	3752	17056	5381	1.8

Sample	Ca (ppm)	Fe (ppm)	Mg (ppm)	Mn (ppm)	Si (ppm)	S (ppm)	P (ppm)	Al (ppm)	As (ppm)
9-430	275091	5574	108827	69.5	334	4399	5874	12515	1.3
9-455	479444	1620	6530	28.4	262	2044	9333	1300	1.2
9-480	379619	1305	6317	26.8	153	1351	3757	1210	0.9
9-505	21294	9845	96792	33.7	1719	4458	9209	18418	4.3
9-530	335534	2137	15066	12.6	817	1943	9970	2215	16.5
25-115	211058	1471	110577	53.8	1064	1716	11614	1462	5.9
25-140	204071	2923	103340	98.6	433	3068	10448	4880	9.2
25-165	277924	2628	99869	31.5	2161	3499	38240	3798	4.9
25-178.5	241584	3713	44010	16.8	3523	6386	72456	5941	8.3
25-190	205288	4952	46683	28.4	2238	6250	58068	6154	15.4
25-203	268176	1085	137068	47.1	708	1074	3369	757	2.1
25-215	258654	5769	112981	51.4	748	5288	26413	9808	9.9
25-265	238975	2640	24493	28.6	3335	2399	2823	2938	3.3
25-284.5	188461	5433	40144	20.7	1134	5433	48972	12500	7.0
25-290	326923	716	143269	18.8	658	1591	8787	1091	1.5
25-299	147030	12030	28069	43.6	819	9356	40082	19059	27.9
TR-9-2-65	173267	1802	97030	94.6	784	851	6321	2738	4.4
20-90	239011	577	126923	26.9	405	1181	1387	295	0.6
20-115	278230	1013	144354	76.8	519	1649	5469	757	1.0
20-140	223516	2689	108265	28.5	870	2439	17207	4302	8.2
20-143	309080	7334	142026	66.9	1436	7429	20278	1787	32.3
20-165	233467	1403	128257	26.6	570	1600	2506	1373	2.8
20-190	210922	1693	120240	33.6	1417	1270	1575	1849	2.2
20-215	157315	8267	98196	40.6	1140	7293	6323	9669	36.0
20-240	147796	6563	70641	53.1	905	4407	16159	10571	6.7
20-415	345650	769	7330	4.2	3442	2255	4474	1204	2.5
20-440	443981	353	6973	3.6	235	1193	172	<0.0009	0.5
20-465	360440	388	4346	2.7	2196	879	927	535	1.0

Sample	Ca (ppm)	Fe (ppm)	Mg (ppm)	Mn (ppm)	Si (ppm)	S (ppm)	P (ppm)	Al (ppm)	As (ppm)
17-95	276768	10505	49444	114.1	2223	4743	43311	4480	7.3
17-145	303535	1152	143434	61.1	609	1640	5537	1601	9.5
17-148	211765	2539	114706	40.2	510	2779	6569	3093	5.9
17-167	123529	2529	40049	26.0	935	3144	24259	5294	8.5
17-170	203407	6413	65631	26.1	1093	6716	37061	9068	11.1
17-195	241667	5637	48775	25.0	2221	7030	61471	9657	4.9
TR-3-3-99	245588	1799	117647	22.1	648	2045	3063	1701	6.0
TR-3-3-125	172772	4604	68812	80.2	960	2965	15725	2530	3.7
TR-3-3-138	400835	1931	63152	65.2	252	2572	6716	1508	8.8
TR-3-3-145	8549	16310	24353	60.2	358	10436	2635	20754	11.2
TR-3-3-150	83433	21990	54529	127.5	767	19717	3695	16925	9.7
TR-3-3-175	246699	3397	107443	29.4	884	3917	18750	3037	1.8
TR-3-3-200	238295	1164	129052	22.2	206	1573	2567	858	2.8
TR-3-3-225	193811	1059	85233	48.3	905	1825	16349	1732	7.4
TR-3-3-250	265440	1380	120237	19.1	924	2271	16900	1294	4.9
TR-3-3-450	171669	2251	65426	33.6	1011	2809	19271	2005	5.3
TR-3-3-475	234157	1096	126208	19.9	201	2793	2596	1042	0.9
TR-3-3-500	248657	806	127282	54.2	156	3609	749	2658	0.9
TR-3-3-523.5	296993	1896	25242	28.5	246	3269	7555	2089	10.2
TR-3-3-525	134282	7859	56993	60.0	405	6753	9699	27166	5.3
TR-3-3-544	336333	2672	22666	34.9	1183	2618	1560	4016	1.7
TR-3-3-550	141176	16225	65686	79.9	1211	12228	17179	18529	8.8
TR-3-3-575	135294	6765	53922	35.8	1225	6373	17779	9314	1.4
TR-3-3-600	243147	5012	151371	85.8	4112	3758	6573	7092	1.1
TR-3-3-611	453431	2828	29363	23.5	1279	6176	10897	3505	1.7
TR-3-3-625	116388	7933	111169	55.3	2445	4034	4204	15084	3.7
TR-3-3-644	298039	3309	49510	17.6	2342	2738	4281	4711	4.2
TR-3-3-650	58455	12787	100731	53.8	1275	3799	5858	14248	1.2

Sample	Ca (ppm)	Fe (ppm)	Mg (ppm)	Mn (ppm)	Si (ppm)	S (ppm)	P (ppm)	Al (ppm)	As (ppm)
TR-3-3-678	248352	3044	29121	19.2	1052	2648	14366	5390	2.1
49-115	267582	1544	4846	13.2	572	1564	5429	2247	11.7
49-117.5	220955	2676	123778	200.9	304	2109	7289	5212	3.9
49-125	148481	6355	59055	87.2	526	4281	28155	11136	12.8
49-150	193476	4561	109111	87.2	521	3090	11442	9224	9.9
49-154.5	221805	9560	26423	152.5	916	10563	63668	15789	28.5
49-175	193584	4928	19082	67.5	3126	5944	72306	7799	8.0
49-200	144544	1265	75928	92.8	300	1456	10680	3830	2.1
49-225	232420	781	125745	78.7	868	655	3842	638	0.9
13-220	320833	935	30602	47.7	2708	3222	30093	1255	2.7
13-245	166063	3489	58371	80.5	1869	4706	28824	8597	9.6
13-270	10000	10856	76577	43.2	1856	6937	4068	20631	18.7
13-295	378995	1557	18402	40.6	1041	2292	4840	1954	6.7
13-320	381448	422	2149	5.9	1900	2502	26244	418	2.3
13-345	273756	1796	29276	10.9	2154	1620	6199	6697	3.2
13-370	19801	28756	15025	71.1	657	27662	2194	12239	0.9
13-395	377561	634	30732	8.3	325	1356	3707	1298	2.1
13-420	193243	1221	82883	13.5	1284	2802	11892	2532	2.9
13-445	172059	2510	72059	20.6	463	4284	12451	7353	2.0
13-470	133333	2132	49020	34.3	662	4152	10098	3500	2.1
13-495	372549	956	4824	17.2	966	2348	13284	2103	3.4
13-520	278140	2665	25535	28.8	614	3567	15116	5860	3.1
13-545	172222	1755	55093	13.0	1301	3847	26065	4120	1.7
13-570	325561	438	1857	4.0	420	552	1395	151	6.9
TRSA-1-29	243000	2850	124000	28.0	2135	3225	2400	3825	5.9
TRSA-1-44.8	24163	13846	54299	54.8	2014	6833	7919	21176	17.1
TR-SA-1-55	203182	1032	110909	30.5	1636	1523	2245	1841	0.1

Sample	Ca (ppm)	Fe (ppm)	Mg (ppm)	Mn (ppm)	Si (ppm)	S (ppm)	P (ppm)	Al (ppm)	As (ppm)
TRSA-1-80	131035	4478	25369	68.5	2360	4680	28276	6798	4.4
TRSA-1-130	191031	1175	97309	29.1	857	1511	4529	1166	2.5
TRSA-1-155	195067	1233	104484	31.4	1058	1336	4040	1390	4.8
TRSA-1-180	154751	4077	98190	50.7	1923	1670	2778	6335	4.9
TRSA-1-205	170136	3783	103620	61.1	1977	2439	900	4706	3.3
TRSA-1-213	38670	15813	46946	61.6	2207	8571	5764	20000	26.2
TRSA-1-230	133663	6485	50000	37.6	2257	4901	21386	9505	4.9
TRSA-1-255	217290	2271	113551	39.3	2093	2009	2379	3374	1.2
TR-SA-1-280	68519	9398	59259	82.9	1741	5556	1917	12037	3.5
TRSA-1-300	89604	7871	33762	36.1	2450	7475	20149	12030	7.7
TRSA-1-305	137624	5000	81188	41.6	2054	4564	8564	8465	5.3
TRSA-1-310	940	1614	124651	9.8	4837	3386	1326	3530	2.8
TRSA-1-330	158878	2136	65888	10.3	1734	2944	11729	3206	3.3
TRSA-1-355	305941	258	23119	2.0	594	916	3262	94	1.2
4-1-75	223223	2152	101422	79.6	1066	3308	11232	2204	2.7
4-1-100	241232	407	108531	78.7	886	1763	3934	1005	0.3
4-1-111	10597	19303	23731	145.3	701	18159	2338	22388	33.1
4-1-115	13860	20465	20698	118.1	2140	15349	3005	16930	18.1
4-1-125	238424	1197	125123	20.2	1345	2276	1591	1365	2.4
4-1-150	227442	879	121861	18.6	1512	2242	1940	1060	2.4
4-1-175	200472	1481	91509	48.6	1382	2028	7877	2892	3.2
4-1-200	234259	2597	93056	34.3	2250	4907	20926	1824	3.1
4-1-210	214612	1763	108676	21.9	1242	2342	1333	2128	3.2
4-1-225	177169	2575	91781	28.3	2050	1849	3438	4434	4.0
4-1-250	32277	13119	67327	35.6	2688	5198	3391	23218	10.3
4-1-275	401887	56	3783	1.4	219	410	272	<0.0009	0.8
4-1-316	257870	145	102315	16.2	291	1065	718	16	0.5
4-1-325	319118	471	37941	7.4	417	1363	3873	686	2.2

Sample	Ca (ppm)	Fe (ppm)	Mg (ppm)	Mn (ppm)	Si (ppm)	S (ppm)	P (ppm)	Al (ppm)	As (ppm)
4-1-350	159722	356	82407	11.1	829	968	2185	727	0.6
4-1-375	143981	1847	70833	19.9	1259	2051	10139	3301	0.8
4-1-400	53704	4472	7037	25.9	2356	6852	11759	4435	4.2
4-1-425	171689	1817	78539	35.2	1406	3219	5205	2530	1.3
4-1-450	243056	1569	33009	30.1	1306	2764	6111	1935	1.5
4-1-475	76617	6070	67662	60.2	701	5622	7960	13433	2.0
4-1-485	14406	12426	86634	29.2	772	10050	5644	17525	3.5
4-1-501	162439	3356	104878	53.2	486	2839	4976	5415	1.5
4-1-514	25920	20149	96517	53.2	746	13284	4776	16517	4.8
4-1-525	115423	7761	108955	46.8	647	3080	1846	14129	6.4
4-1-550	109479	5166	55450	27.0	2967	3810	8057	7488	1.3
4-1-575	193981	1972	49537	17.1	2657	1255	1949	3463	2.4
4-1-599	441176	701	2005	4.9	183	1578	359	272	7.5
5-145	205046	794	7110	2.3	537	940	1138	592	1.9
5-170	244811	689	117925	36.3	693	1792	360	774	1.1
5-195	237615	2693	31514	22.9	1023	2688	1294	2280	3.6
5-220	206132	2476	84906	31.1	797	3241	6934	3000	7.2
5-245	103153	4775	18739	60.4	1212	4270	19324	5991	4.8
5-270	299074	1269	1787	63.9	1389	2051	13056	1088	5.1
5-284	136986	7215	73516	158.0	1941	5479	2142	9224	4.4
5-295	127723	6881	7228	156.9	1807	6634	13465	9208	4.6
5-320	96396	11216	66667	78.8	3108	9595	8423	17387	23.7
5-345	310648	1139	51389	31.5	2000	2458	16898	1898	5.6
5-370	247534	1170	39283	93.3	1910	2538	21166	1471	6.1
5-395	159174	2780	41193	51.4	1972	4307	23028	6972	5.0
5-420	8565	12556	78475	48.0	2901	7713	3664	22466	25.9
5-445	252133	536	115640	41.2	455	929	1156	255	1.8
5-470	292202	165	79816	16.1	317	697	844	<0.0009	1.5

Sample	Ca (ppm)	Fe (ppm)	Mg (ppm)	Mn (ppm)	Si (ppm)	S (ppm)	P (ppm)	Al (ppm)	As (ppm)
5-495	235648	1472	104167	15.7	421	2074	6991	2926	3.6
5-570	187963	2417	78704	25.0	1079	3829	6528	3514	6.2
5-595	213426	597	96759	13.4	704	1977	5741	416	3.7
5-620	280660	632	69811	6.6	892	1835	5094	1231	2.1
5-646	292924	835	18632	10.8	1080	2047	7170	1542	4.3
5-670	294495	1257	23165	11.9	1101	2564	8761	2697	4.3
5-695	163014	1516	14338	2.3	918	1475	3795	3662	6.1
5-705	173636	809	85455	17.3	891	1318	923	1382	1.7
5-1-110	245098	451	126471	28.9	442	1691	1034	667	0.9
5-1-135	174074	2519	88889	69.9	1032	2829	8657	3912	9.4
5-1-160	199526	4787	97156	36.0	1645	4559	13744	7678	11.9
5-1-187	10139	16806	38889	53.2	258	7731	2810	22407	18.1
5-1-210	205000	2965	99000	31.0	1560	1940	8950	4735	2.4
5-1-218	14834	16872	44455	46.4	2313	7725	3910	26398	9.3
5-1-235	161000	8950	97000	48.5	2245	7350	8550	12800	17.2
5-1-260	195455	3159	99545	40.5	1845	3432	4591	5227	3.1
5-1-285	207009	172	343	3.7	194	682	2556	214	0.6
5-1-310	416500	247	2580	5.0	455	685	300	142	0.4
5-1-335	261395	329	0	1.4	902	1009	8698	160	1.9
5-1-360	206481	519	1597	1.9	630	769	2648	625	1.9
12-190	153704	6620	58333	66.7	437	6204	22361	15694	14.6
12-215	289352	1069	54167	42.1	2546	2065	9398	1648	3.2
12-240	206393	1845	73059	75.8	2269	3005	14932	5023	3.7
12-265	241509	972	18538	11.8	1858	1792	10330	2783	2.0
12-293	338389	640	68720	46.0	1313	1057	1062	431	3.3
12-315	368519	171	11111	21.8	690	843	1875	58	1.9
12-340	253554	701	85308	8.5	1687	1938	10427	1085	1.9
12-365	378199	163	12607	7.1	343	701	2218	<0.0009	0.2

Sample	Ca (ppm)	Fe (ppm)	Mg (ppm)	Mn (ppm)	Si (ppm)	S (ppm)	P (ppm)	Al (ppm)	As (ppm)
12-380	243137	362	106373	8.8	618	1721	6471	53	1.1
12-390	366667	390	3958	3.2	866	1361	8194	537	1.6
12-590	386500	324	<0.0001	0.5	241	321	865	<0.0009	0.9
12-615	308072	753	64	3.6	619	380	1009	516	1.3
12-643	314545	301	<0.0001	<0.00003	305	402	2986	75	1.1

APPENDIX F

Inductively Coupled Plasma – Optical Emission Spectrometry (ICP-OES)

Results for the Tampa Member of the Arcadia Formation

Samples sorted by well

Sample	Ca (ppm)	Fe (ppm)	Mg (ppm)	Mn (ppm)	Si (ppm)	S (ppm)	P (ppm)	Al (ppm)	As (ppm)
39-390	85392	2583	38185	21.5	460	1737	9890	8700	4.3
39-400	145421	155	<0.0001	2.5	71	244	759	<0.0009	0.3
39-425	57692	313	25440	2.7	988	319	121	1143	0.3
39-450	190118	405	1595	4.8	640	337	675	1300	0.3
39-467	374255	445	1484	10.1	584	378	2895	<0.0009	0.8
39-475	230689	497	114823	34.4	616	1083	945	435	10.4
39-500	448153	852	822	28.0	562	716	19	35	1.4
39-510	379332	117	267	8.7	135	426	23	<0.0009	0.5
22-170	104595	11729	51088	58.6	498	10190	25778	18984	14.0
22-195	32302	15038	71661	60.8	997	5865	4462	24756	12.3
22-225	208585	5429	109432	41.1	965	2165	1711	8283	3.0
22-250	261104	630	92	3.6	236	331	4382	930	0.3
22-273.5-278.5	73897	2193	<0.0001	9.5	145	232	3175	530	0.2
22-300	298292	1110	3647	5.9	213	737	2399	1938	0.9
9-230	441354	647	24244	6.0	228	741	5052	80	0.9
9-255	397124	341	8020	5.5	122	828	3568	131	0.4
9-280	403265	834	13906	9.7	259	1146	5763	<0.0009	1.5
9-305	379106	1163	5138	11.2	247	1441	5896	157	2.4
9-330	354796	1472	8476	14.5	251	1620	5016	194	2.9
9-352.5	72029	11465	7083	61.2	373	11783	13691	30732	15.2
TR-9-2-90	41337	4193	9059	9.9	563	1168	16495	7475	3.8
TR-9-2-101.5	48516	4912	6703	18.1	700	1753	10759	10879	5.2
TR-9-2-115-119	153846	10048	1644	85.1	1045	587	9815	1394	2.3
TR-9-2-140	386634	772	5990	20.8	824	530	2169	1441	0.6
TR-9-2-165	214286	241	124176	103.3	550	717	280	255	1.1
TR-9-2-190	236591	745	131704	57.8	660	900	1875	632	0.9
TR-9-2-215	174613	2652	95352	76.9	4200	1665	3326	4195	8.1
TR-9-2-240	14257	2342	18119	5.0	658	1847	4250	8069	8.3
TR-9-2-265	487745	691	931	32.4	824	956	39	382	1.4

Sample	Ca (ppm)	Fe (ppm)	Mg (ppm)	Mn (ppm)	Si (ppm)	S (ppm)	P (ppm)	Al (ppm)	As (ppm)
20-265	212425	332	368	1.5	968	551	10304	424	0.5
20-279	373063	564	2974	6.0	952	973	2773	<0.0009	0.4
20-290	282565	240	2074	0.5	863	530	2049	28	0.2
20-315	265842	369	2050	0.0	388	668	2718	363	0.3
20-340	298039	1314	4191	12.7	652	1657	6257	1789	5.5
20-365	446154	500	6779	3.4	346	1966	3289	611	2.2
20-390	697259	989	10906	13.7	1459	2569	2636	<0.0009	3.2
17-220	358823	760	3956	7.4	1529	1877	19656	515	2.1
17-245	262255	430	14902	3.4	739	1045	10044	672	0.8
17-270	232353	468	1603	2.0	1171	1213	12239	89	1.5
DV-1-100	384343	1323	13485	138.9	574	807	883	241	6.8
DV-1-106	275000	2255	1216	46.6	1241	604	264	1642	1.3
DV-1-113	302525	2475	732	66.2	756	1680	306	662	14.2
DV-1-125	393434	279	763	23.7	319	314	219	<0.0009	0.9
DV-1-139.5	204993	567	<0.0001	15.8	567	375	30	<0.0009	0.4
DV-1-150	188889	2712	2773	27.3	1878	1044	56	2126	3.9
TR-3-3-275	153806	7091	86548	38.6	470	4892	13038	10010	12.3
TR-3-3-300	392576	345	10967	1.7	199	719	4986	675	0.5
TR-3-3-309.5	414604	251	3224	3.1	79	554	1677	<0.0009	0.4
TR-3-3-325	436518	792	3821	4.2	427	1215	7281	262	1.1
TR-3-3-350	490384	837	8462	13.0	554	1548	7965	314	2.6
TR-3-3-375	358830	900	9055	17.4	325	1486	6262	799	2.3
TR-3-3-400	410011	247	6299	2.2	119	755	2795	<0.0009	0.3
TR-3-3-404	483909	703	5906	8.3	124	826	2636	<0.0009	0.4
TR-3-3-425	233516	566	115385	16.5	614	1483	2848	479	3.0
49-250	230727	471	5863	27.7	899	422	90	1243	2.7
49-275-280	106874	1966	10150	10.2	378	1309	996	5306	7.1
49-300	204410	1710	101311	98.9	882	747	2112	1335	1.8
49-325	356748	625	3252	13.3	226	822	454	1338	1.6

Sample	Ca (ppm)	Fe (ppm)	Mg (ppm)	Mn (ppm)	Si (ppm)	S (ppm)	P (ppm)	Al (ppm)	As (ppm)
49-350	415073	154	1108	7.3	288	236	40	<0.0009	0.5
49-357	19624	2463	4071	2.6	569	1409	19	8142	2.3
49-375	456731	112	505	10.6	296	731	48	<0.0009	0.7
TRSA-1-380	372093	127	1144	0.5	382	464	516	<0.0009	0.6
TRSA-1-405	378995	189	2434	4.6	401	466	303	<0.0009	0.9
TRSA-1-419	167488	990	1355	2.5	2507	1005	901	3488	1.5
TRSA-1-430	344500	414	675	6.5	1065	790	3040	1195	0.9
TRSA-1-455	297525	748	3896	16.3	1817	787	4386	3312	1.3
TRSA-1-480	396040	851	4490	10.9	220	604	530	921	2.4
TRSA-1-484	351598	735	3968	11.0	218	571	344	1059	2.5
4-1-300	250000	389	3723	1.5	302	520	3272	718	1.0
5-1-385	57727	686	1218	0.0	1332	664	3859	2527	0.4
5-1-410	206818	274	2745	4.5	389	723	3609	289	1.2
5-1-421	25682	7591	14409	21.4	2768	6364	8409	12636	10.0
5-1-436	121818	2086	52273	42.7	1168	3059	8409	6045	4.5
5-1-460	200976	2839	104878	42.4	1732	4141	1507	5268	5.6
5-1-488	384475	183	562	1.8	152	1484	53	16	2.4

APPENDIX G

Inductively Coupled Plasma – Optical Emission Spectrometry (ICP-OES)

Results for the Nocatee Member of the Arcadia Formation

Samples sorted by well

Sample	Ca (ppm)	Fe (ppm)	Mg (ppm)	Mn (ppm)	Si (ppm)	S (ppm)	P (ppm)	Al (ppm)	As (ppm)
17-295	266176	975	11667	4.9	668	1208	10044	2382	1.5
17-320	191884	1408	38627	16.0	743	2335	11183	997	6.5
17-345	289290	2293	3917	15.1	1640	3383	26072	1560	8.8
17-370	119907	4086	31665	23.3	938	3635	21495	8149	2.7
17-395	376601	319	5239	7.0	393	753	4728	308	1.0
17-412	380675	594	59953	12.8	692	1112	8227	600	2.0
17-420	399301	675	8382	8.1	550	938	6083	931	2.6
17-434	274738	2526	30675	11.6	760	1681	7880	4348	9.9
13-595	3151	16732	50732	53.2	434	6634	2444	27707	13.1
13-620	30180	8559	24054	95.5	2239	7748	2514	8243	7.1
13-627	34459	11847	12477	81.5	2275	10315	8559	10676	5.2
13-630	9318	12091	2668	37.7	2373	11500	4305	6909	13.8
13-644	40556	4815	16435	42.1	425	4611	4722	5000	3.5
13-690	384091	288	2659	3.6	258	673	923	<0.0009	0.5
13-704	479311	41	3562	3.0	118	452	140	<0.0009	0.5
5-520	311574	1093	37824	12.5	764	1944	4861	1435	3.8
5-545	323697	1464	8152	10.0	1000	2626	8152	2246	6.6
12-414-419	127602	4339	14751	33.0	525	1032	6878	2294	1.9
12-440	211111	1213	2227	13.0	1310	1421	217	2384	8.2
12-454	<0.00002	1441	<0.0001	<0.00003	1417	1607	10	1754	1.8
12-462-467	18900	555	<0.0001	<0.00003	900	227	335	650	0.5
12-490	356621	258	1269	3.2	203	321	195	<0.0009	0.9
12-517	278704	247	<0.0001	<0.00003	481	532	921	<0.0009	1.5
12-529	345320	92	<0.0001	<0.00003	194	382	1325	<0.0009	69.0
12-545	349537	161	<0.0001	<0.00003	254	284	1611	<0.0009	0.8
12-567	386500	324	0	0.5	241	321	865	<0.0009	1.6
12-590	266176	975	11667	4.9	668	1208	10044	<0.0009	0.9

APPENDIX H

Inductively Coupled Plasma – Optical Emission Spectrometry (ICP-OES)

Results for the Peace River Formation

Samples sorted by well

Sample	Ca (ppm)	Fe (ppm)	Mg (ppm)	Mn (ppm)	Si (ppm)	S (ppm)	P (ppm)	Al (ppm)	As (ppm)
39-47.5-52.5	<0.00002	264	<0.0001	2.5	133	55	326	761	0.4
39-72.5-77.5	42920	2284	<0.0001	44.8	851	1713	17667	2019	8.1
39-100	28872	12223	20962	84.6	347	4814	8117	19635	6.1
39-125	116704	4712	61947	148.8	308	3800	9277	8131	4.3
39-130	52157	15487	16759	99.6	383	11014	6760	19303	6.5
39-150	82302	14666	56559	259.9	652	10390	7504	21844	6.1
39-155	80199	8075	22954	140.5	347	6876	15143	14436	5.3
39-173-178	58628	3258	1892	55.9	623	3065	20941	3512	5.9
22-20	168057	14362	2187	85.2	2376	1825	55029	12217	11.2
22-29	22989	9004	5216	28.2	449	487	8036	11465	5.3
22-45	155462	11164	90636	184.9	416	6815	8929	14106	9.3
9-30	45277	17101	10695	30.4	242	4479	12602	23236	40.8
25-45-47	59901	1520	<0.0001	14.9	1347	1292	22199	4550	4.5
25-65-70	220330	15330	48352	97.3	1645	11597	48881	13462	37.2
25-90	268317	7178	97030	106.4	1503	7327	41624	9307	13.1
TR-9-2-40	39167	12500	44510	98.5	2892	6275	7404	18873	4.0
20-38.5	206198	5822	15018	47.1	3583	5632	60253	3033	12.2
20-48.5	16834	16283	13377	37.6	894	13379	4801	12826	9.8
20-65	250873	2509	140861	50.6	666	2466	1842	1857	1.9
17-50-56	353922	6176	27941	209.8	1407	4142	29614	4382	9.7
17-70	148529	13088	40882	455.4	859	9901	34632	13824	9.4
DV-1-6	<0.00002	8	<0.0001	<0.00003	56	103	161	1414	1.3
DV-1-25-26	66162	1889	<0.0001	27.3	954	200	50000	46212	1.1
DV-1-48.5-51	92929	10606	30455	127.3	1228	1080	22149	16061	3.0
DV-1-74.5-77	118182	8737	34899	123.7	898	1589	20778	14596	11.4
TR-3-3-56.5-61	121086	5376	13413	64.2	1986	5213	34453	2056	25.8
TR-3-3-81.5-86.5	187289	5304	61867	75.9	910	5059	23509	4235	13.9
49-77.3-82.3	85396	5365	8911	131.8	830	4292	25338	5662	14.9
13-19	12537	2605	<0.0001	1.5	507	590	5561	10634	0.4

Sample	Ca (ppm)	Fe (ppm)	Mg (ppm)	Mn (ppm)	Si (ppm)	S (ppm)	P (ppm)	Al (ppm)	As (ppm)
13-23	25248	11584	5644	18.8	2361	1629	8465	13366	0.4
13-45	180930	11395	23116	45.6	488	8465	4130	12093	8.2
13-69	180556	2778	101389	68.1	340	1421	852	4384	0.9
13-95	207407	2644	100926	19.9	1014	3556	755	1935	8.4
13-108	233659	883	118049	14.6	247	2127	737	756	3.2
13-120	171759	2898	81944	29.6	348	4106	2139	4120	3.3
13-134	25099	3040	7822	20.8	435	3327	3891	4272	1.1
13-145	167123	2904	49772	61.6	1187	5160	19909	3740	10.2
13-170	95434	9498	17991	125.6	498	9954	21781	16164	8.7
13-195	185455	6182	89545	78.2	1577	7545	12727	7636	17.7
4-1-50	46364	4441	<0.0001	21.4	1405	4291	16318	4091	5.4
5-69-74	317561	9171	16976	25.9	2180	12000	52195	8585	20.0
5-85	76852	10185	10741	24.1	3204	10324	4347	11944	5.4
5-95	82938	12559	14313	28.0	3043	14929	5782	13223	3.8
5-110	69159	7944	6168	24.8	2047	8364	14019	9533	3.2
5-120	260550	8578	10550	24.3	1904	9495	33761	10000	25.1
12-41	36864	19364	16727	40.5	3355	15364	3323	15500	5.6
12-48	206019	7593	10000	38.0	3454	5833	1755	8565	2.9
12-64.5	377251	2564	5735	3.8	468	3370	383	133	2.1
12-90	208057	1640	106635	19.4	1858	1972	1019	1649	1.8
12-115	89450	7202	45000	65.1	2271	7431	2743	8486	3.9
12-125(1)	55721	23483	40149	167.7	557	24279	4836	20149	7.7
12-125(2)	161692	104975	9254	140.8	2209	120398	52736	5970	26.7
12-125(1)dup	56098	20976	43268	173.7	416	20585	4927	20585	8.1
12-140	106849	12694	47032	206.4	3169	12192	10091	14795	11.8
12-165	119444	7963	23611	263.0	1750	6806	27778	17639	6.2

APPENDIX I

Electron –Probe Microanalysis of Pyrites

Sorted by Formation/Member of the Hawthorn Group

Sample	Hawthorn Unit	S (wt.%)	As (wt.%)	Fe (wt.%)	Pb (wt.%)	Cu (wt.%)	Zn (wt.%)	Total (wt.%)
12-125-1	Peace R.	53.134	0	45.888	0	0	0.006	99.028
12-125-2	Peace R.	53.47	0.024	46.549	0	0	0.015	100.058
12-125-3	Peace R.	53.024	0	45.456	0	0	0.011	98.491
12-125-4	Peace R.	53.694	0	46.06	0	0	0.004	99.758
12-125-2-1	Peace R.	53.775	0.005	46.183	0	0	0.01	99.973
12-125-2-2	Peace R.	53.227	0	45.851	0	0	0.002	99.08
12-125-2-3	Peace R.	53.394	0.002	46.297	0	0	0	99.693
13-195-1	Peace R.	35.866	0.027	34.764	0	0	0.145	70.802
13-195-2	Peace R.	15.111	0.048	16.268	0	0	0.132	31.559
13-195-3	Peace R.	47.443	0.063	46.297	0	0	0.034	93.837
13-195-4	Peace R.	27.88	0.137	32.178	0	0	0.172	60.367
12-48map-1	Peace R.	18.309	0	43.709	0	0	0.021	62.039
12-48map-2	Peace R.	23.855	0	40.263	0	0	0.052	64.17
12-48map-3	Peace R.	9.985	0.006	40.87	0	0	0.028	50.889
12-48map-4	Peace R.	17.89	0	36.716	0	0	0.014	54.62
9-30-1	Peace R.	50.578	0.164	45.262	0	0	0.042	96.046
9-30-2-1	Peace R.	52.51	0.163	45.018	0	0	0.002	97.693
9-30-2-2	Peace R.	51.628	0	43.07	0	0	0.031	94.729
9-30-2-3	Peace R.	46.517	0.411	43.619	0	0	0.047	90.594
9-30-2-4	Peace R.	49.517	0.078	44.921	0	0	0.012	94.528
9-30-2-5	Peace R.	27.039	0.128	42.084	0	0	0.002	69.253
9-30-2-6	Peace R.	26.388	0.06	36.802	0	0	0.044	63.294
9-30-2-7	Peace R.	46.048	0.416	44.74	0	0	0.019	91.223
9-30-2-11	Peace R.	47.727	0.099	45.704	0	0	0.026	93.556
9-30-2-12	Peace R.	48.094	0	46.465	0	0	0.008	94.567
9-30-2-13	Peace R.	52.692	0.071	45.56	0	0	0.025	98.348
9-30-2-14	Peace R.	48.036	0.2	43.442	0	0	0.014	91.692
9-30-2-15	Peace R.	41.469	0.082	48.093	0	0	0.03	89.674

Sample	Hawthorn Unit	S (wt.%)	As (wt.%)	Fe (wt.%)	Pb (wt.%)	Cu (wt.%)	Zn (wt.%)	Total (wt.%)
9-30-2-16	Peace R.	47.299	0.06	42.145	0	0	0.037	89.541
9-30-2-17	Peace R.	46.969	0.073	45.197	0	0	0.031	92.27
4-1-111-3	Arcadia F.	28.151	0.082	39.712	0	0	0.007	67.952
20-143-1	Arcadia F.	49.175	0.448	44.283	0	0	0.017	93.923
20-143-2	Arcadia F.	49.55	0.412	43.537	0	0	0.014	93.513
20-143-3	Arcadia F.	51.748	0.826	44.184	0	0	0.016	96.774
20-143-4	Arcadia F.	52.838	0.346	43.994	0	0	0.015	97.193
20-143-5	Arcadia F.	53.163	0.228	44.501	0	0	0.03	97.922
20-143-6	Arcadia F.	52.693	0.261	44.937	0	0	0	97.891
20-143-7	Arcadia F.	52.417	0.016	45.644	0	0	0.029	98.106
20-143-8	Arcadia F.	35.261	0.079	42.171	0	0	0.098	77.609
20-143-9	Arcadia F.	40.587	0.067	39.415	0	0	0.018	80.087
20-143-10	Arcadia F.	51.318	0.024	46.282	0	0	0.001	97.625
20-143-11	Arcadia F.	53.397	0.12	46.181	0	0	0.005	99.703
49-154.5-1	Arcadia F.	49.523	0.244	39.691	0	0	0.172	89.63
49-154.5-2	Arcadia F.	51.195	0.382	43.216	0	0	0.28	95.073
49-154.5-3	Arcadia F.	51.564	0.16	43.944	0	0	0.208	95.876
4-1-501-1	Arcadia F.	34.333	0.046	35.593	0	0	0.045	70.017
4-1-501-2	Arcadia F.	33.371	0	39.865	0	0	0.052	73.288
4-1-501-3	Arcadia F.	41.008	0	43.05	0	0	0.057	84.115
4-1-501-4	Arcadia F.	38.601	0.047	48.143	0	0	0.015	86.806
4-1-501-5	Arcadia F.	35.618	0	45.718	0	0	0.032	81.368
5-1-235-1	Arcadia F.	40.059	0.154	42.642	0	0	0.059	82.914
5-1-235-2	Arcadia F.	41.397	0.081	44.876	0	0	0.056	86.41
5-1-235-3	Arcadia F.	39.732	0.151	45.49	0	0	0.067	85.44
5-1-235-4	Arcadia F.	40.444	0.124	46.162	0	0	0.067	86.797
5-1-235-5	Arcadia F.	49.319	0.141	40.762	0	0	0.024	90.246
5-1-235map-1	Arcadia F.	51.21	0.026	44.568	0	0	0.029	95.833
5-1-235map-2	Arcadia F.	47.177	0.124	41.479	0	0	0.014	88.794

Sample	Hawthorn Unit	S (wt.%)	As (wt.%)	Fe (wt.%)	Pb (wt.%)	Cu (wt.%)	Zn (wt.%)	Total (wt.%)
5-1-235map-3	Arcadia F.	45.732	0.373	41.723	0	0	0.027	87.855
5-320-2	Arcadia F.	54.977	0	44.838	0	0	0.037	99.852
5-320-3	Arcadia F.	53.836	0	45.275	0	0	0.018	99.129
5-320-4	Arcadia F.	52.994	0.007	45.277	0	0	0.009	98.287
5-320-5	Arcadia F.	53.378	0.01	45.111	0	0	0.016	98.515
25-299-2	Arcadia F.	43.211	0.254	37.304	0	0	0.091	80.86
25-299-3	Arcadia F.	50.562	0.221	40.733	0	0	0.044	91.56
25-299-4	Arcadia F.	46.154	0.028	43.031	0	0	0.068	89.281
25-299-5	Arcadia F.	45.503	0.054	43.396	0	0	0.07	89.023
20-215-1	Arcadia F.	41.059	0.065	36.259	0	0	0.041	77.424
20-215-2	Arcadia F.	44.65	0.112	39.014	0	0	0.058	83.834
20-215-3	Arcadia F.	35.645	0.209	40.982	0	0	0.13	76.966
20-215-4	Arcadia F.	37.568	0.124	43.779	0	0	0.075	81.546
20-215-5	Arcadia F.	51.615	0.059	43.654	0	0	0.052	95.38
20-215-6	Arcadia F.	47.05	0.154	37.511	0	0	0.083	84.798
20-215-7	Arcadia F.	47.505	0.166	39.077	0	0	0.08	86.828
20-215-8	Arcadia F.	21.463	0.148	40.561	0	0	0.068	62.24
20-215-9	Arcadia F.	40.9	0.059	41.971	0	0	0.056	82.986
20-215-10	Arcadia F.	50.113	0	44.057	0	0	0.033	94.203
20-215-11	Arcadia F.	35.899	0.266	34.3	0	0	0.083	70.548
3-3-275-1	Tampa M.	34.098	0.17	46.564	0	0	0.194	81.026
3-3-275-2	Tampa M.	35.866	0.111	47.027	0	0	0.177	83.181
3-3-275-3	Tampa M.	35.402	0.144	46.575	0	0	0.181	82.302
3-3-275-4	Tampa M.	40.622	0.322	46.135	0	0	0.035	87.114
3-3-275-5	Tampa M.	40.697	0.271	46.528	0	0	0.035	87.531
DV-1-113-1	Tampa M.	52.879	0	45.286	0	0	0.021	98.186
DV-1-113-2	Tampa M.	52.799	0.017	45.586	0	0	0.02	98.422
DV-1-113-3	Tampa M.	51.681	0	44.432	0	0	0.019	96.132
22-170-1	Tampa M.	36.444	0.083	44.629	0	0	0.09	81.246

Sample	Hawthorn Unit	S (wt.%)	As (wt.%)	Fe (wt.%)	Pb (wt.%)	Cu (wt.%)	Zn (wt.%)	Total (wt.%)
22-170-2	Tampa M.	37.22	0.105	43.399	0	0	0.029	80.753
22-170-3	Tampa M.	48.8	0.001	43.915	0	0	0.075	92.791
22-170-5	Tampa M.	49.712	0.015	42.956	0	0	0.038	92.721
22-170-6	Tampa M.	25.307	0.207	47.414	0	0	0.117	73.045
22-170-7	Tampa M.	19.282	0.218	48.069	0	0	0.251	67.82
22-170-8	Tampa M.	32.888	0.092	45.315	0	0	0.202	78.497
22-170-9	Tampa M.	17.138	0.149	49.456	0	0	0.184	66.927
22-170-10	Tampa M.	27.52	0.135	45.406	0	0	0.218	73.279
22-170-11	Tampa M.	48.593	0.036	42.909	0	0	0.001	91.539
22-170-12	Tampa M.	49.081	0.109	39.947	0	0	0.064	89.201
22-170-13	Tampa M.	48.77	0.117	39.931	0	0	0.071	88.889
22-170-14	Tampa M.	41.516	0.054	45.434	0	0	0.034	87.038
22-170-15	Tampa M.	43.637	0.057	45.853	0	0	0.042	89.589
22-170-16	Tampa M.	51.398	0.085	41.672	0	0	0.028	93.183
22-170-17	Tampa M.	51.768	0.116	41.715	0	0	0.07	93.669
22-170-18	Tampa M.	51.977	0.002	44.852	0	0	0.082	96.913
22-170-19	Tampa M.	39.34	0.107	46.424	0	0	0.061	85.932
22-170-20	Tampa M.	39.826	0.09	45.994	0	0	0.035	85.945
22-170-21	Tampa M.	38.955	0.06	43.708	0	0	0.076	82.799
22-170-22	Tampa M.	50.903	0.018	44.354	0	0	0.047	95.322
22-170-23	Tampa M.	14.196	0.154	50.962	0	0	0.121	65.433
22-170-24	Tampa M.	47.987	0.012	44.931	0	0	0.025	92.955
22-170-25	Tampa M.	50.436	0.049	44.467	0	0	0.016	94.968
22-170-26	Tampa M.	26.583	0.136	46.548	0	0	0.094	73.361
22-170-27	Tampa M.	51.394	0.053	43.982	0	0	0.388	95.817
22-170-28	Tampa M.	50.041	0.003	43.948	0	0	0.027	94.019
22-170-29	Tampa M.	39.067	0.131	44.698	0	0	0.047	83.943
22-170-30	Tampa M.	30.558	0.139	46.681	0	0	0.146	77.524
22-170-31	Tampa M.	46.109	0.17	37.962	0	0	0.118	84.359

Sample	Hawthorn Unit	S (wt.%)	As (wt.%)	Fe (wt.%)	Pb (wt.%)	Cu (wt.%)	Zn (wt.%)	Total (wt.%)
12-529-3	Nocatee M.	38.617	0.056	34.056	-	-	-	78.055
12-529-4	Nocatee M.	33.399	0.064	36.169	-	-	-	74.56
12-529-5	Nocatee M.	53.059	0.571	45.144	0	0	0.028	98.802
12-529-7	Nocatee M.	52.98	0.42	44.963	0	0	0.036	98.399
12-529-8	Nocatee M.	51.97	0.391	44.142	0	0	0.03	96.533
12-529-9	Nocatee M.	51.523	0.102	45.126	0	0	0.019	96.77
12-529-10	Nocatee M.	52.759	0.483	44.616	0	0	0.022	97.88
12-529-11	Nocatee M.	33.705	0.273	33.781	0	0	0.023	67.782